Transfer of Railway Induced Vibrations Through Soil

A Study Owing to the Loading Characteristics And Fluctuating Water Table

Nithul Thekke Choolangot

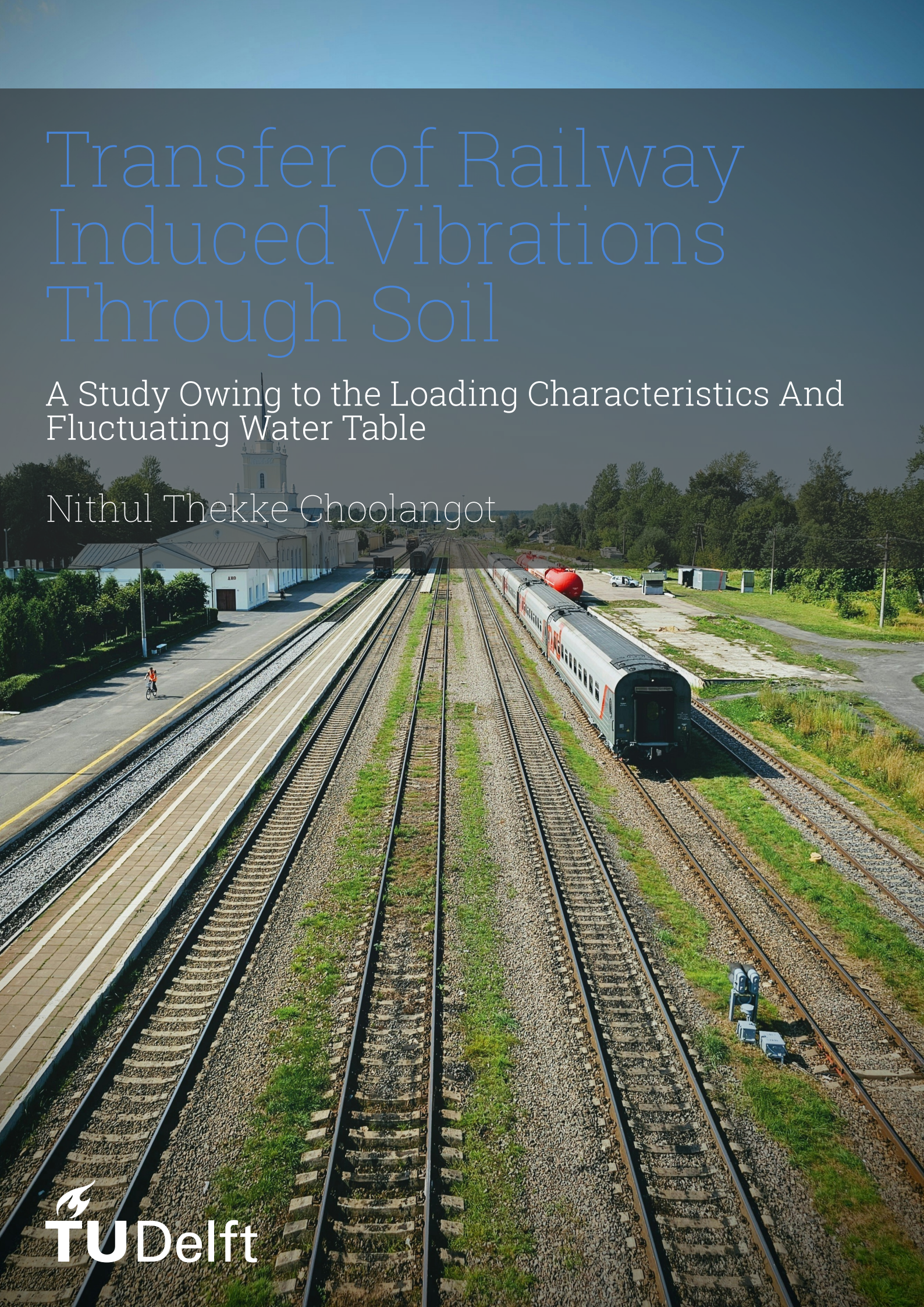

TU Delft

Transfer of Railway Induced Vibrations Through Soil

A Study Owing to the Loading Characteristics And Fluctuating Water Table

by

Nithul Thekke Choolangot

6075088

to obtain the degree Master of Science at
Delft University of Technology
to be defended publicly on August 28, 2025.

Graduation Committee

Dr. Wout Broere	Associate Professor of Underground Space Technology	TU Delft
Dr. Luca Flessati	Assistant Professor in Geotechnical Field Testing and Monitoring	TU Delft
Dr. Valéri Markine	Associate Professor at the Section of Railway Engineering	TU Delft
Ir. Saeed Hosseinzadeh	Geotechnical and Vibration Specialist	Arcadis

Project Duration: March, 2025 - August, 2025
Faculty: Faculty of Civil Engineering and Geosciences

TU Delft ARCADIS

Preface

This Master of Science thesis, titled ”**Transfer of Railway Induced Vibrations Through Soil: A Study Owing to the Loading Characteristics And Fluctuating Water Table**,” is submitted in fulfilment of the requirements to obtain the degree, Master of Science at Delft University of Technology, within the Faculty of Civil Engineering and Geosciences and in collaboration with Arcadis. The research was conducted between March 2025 and August 2025

This study aims to advance this field by investigating the implementation and effectiveness of the moving load method in Finite Element Modelling (FEM), particularly within the PLAXIS 3D software. A primary objective is to evaluate the influence of linear and non-linear material models, specifically the Hardening Soil model with small-strain stiffness (HSsmall), on vibration transfer through soil. Furthermore, the research explores the complex effects of a fluctuating water table on vibration propagation. The overarching goal is to address existing knowledge gaps and provide new insights into soil behaviour under dynamic railway loads and the effect of a changing water table on the transfer of vibrations.

I extend my sincere appreciation to my Graduation Committee: Dr. Wout Broere, Dr. Luca Flessati, and Dr. Valéri Markine of Delft University of Technology and Ir. Saeed Hosseinzadeh of Arcadis, for their invaluable guidance, expert insights, and consistent support throughout this research journey. I would also like to thank all my friends for their support throughout this academic journey. Moreover, I would like to thank my parents for their unwavering support from Day 1. You bring me joy and make sure that I am not pushing too hard. There are many things I am thankful for in my life, but you are at the top of the list.

Nithul Thekke Choolangot
Delft, August 2025

Summary

This research systematically investigated the transfer of railway-induced vibrations through soil by implementing the moving load method within finite element modelling (FEM), evaluating the efficacy of linear and non-linear material models, and assessing the impact of a varying water table. Utilising PLAXIS 3D, the advanced moving load method proved more effective than triangular pulse methods, as it realistically simulated continuous train wheel contact.

Linear elastic model (M1), despite providing patterns similar to site measurements, consistently overestimated acceleration magnitudes, particularly at greater distances from the rail. This indicated that linear models, even with Rayleigh damping, were inadequate for fully replicating complex real-life conditions due to inherent approximations and site uncertainties. Conversely, the implementation of non-linear material models, specifically the Hardening Soil model with small-strain stiffness (HSsmall), demonstrated improved agreement with field data. This finding underscores the importance of non-linear models for accurately representing soil behaviour and its intrinsic damping characteristics. Investigation into water table fluctuations using the linear-nonlinear model, M2 revealed no significant time-domain variations in acceleration magnitudes; however, a notable reduction in the intensity of higher frequencies was observed as the water table rose from 1.5 m below the ground level to 0.5 m below the ground.

The analysis of a fully non-linear model, M3 gave results closer to the site data but had variation due to the discrepancies in the input data with the site. It primarily modelled most components, except for the rails, railpads, fasteners, and sleepers, using the Hardening Soil model with small-strain stiffness (HSsmall). Additionally, in fully non-linear models (M3), external dynamic load adjustments (e.g., 5% of axle load) were found to be less critical, suggesting these models inherently capture dynamic effects. Furthermore, M3 predictions indicate that vibration amplitude increases as the water table rises, with very shallow water tables leading to much greater strains and plastic effects than linear models. Literature suggests this phenomenon involves complex interactions, often linked to changes in soil stiffness and potential for amplified vibrations near resonance.

The study acknowledges significant assumptions and simplifications within the models, such as the exclusion of surrounding buildings and the assumption of isotropic soil, which contributed to discrepancies with real-world data. Despite the higher computational demands associated with non-linear models, their incorporation is recommended for achieving results that more accurately reflect actual soil behaviour.

Contents

List of Figures

List of Tables

1

Introduction

1.1. Research Context

Railways have always been and will always be one of the main forms of transport in the world. For almost a century, it's use has only increased exponentially. Beginning with just as a method to easily transport goods to moving hundreds of people across countries, it has become an essential part of our everyday lives. Railways are one of the best solutions to congestion in traffic and to reduce pollution, but they are not without drawbacks, noise, and vibration. In recent years, there has been extensive expansion of railways throughout the world to compete with other forms of transportation [29]. This increase has boosted the efficient movement of people and goods throughout different landscapes but has also increased the vibrations felt in its surroundings. In modern societies, this has been considered an important problem due to their tangible impacts on human comfort and well-being, potential (though often exaggerated) impacts on structural integrity, and measurable effects on performance in rail infrastructure [48]. The study of ground-borne vibrations from railways began in the early twentieth century and has progressed a lot since then. Studying railway-induced ground-borne vibrations is crucial because they pose significant challenges to human comfort and well-being, sensitive equipment, and the structural integrity and performance of both buildings and railway infrastructure. These challenges are further amplified by increasing train demands and urban development, making a comprehensive understanding of the topic increasingly necessary. Previous studies have explored various methods for modelling train-induced ground vibrations, each with its own capabilities and limitations in simulating train loads. These approaches can generally be categorised into empirical, analytical/semi-analytical, and numerical methods, often incorporating different levels of detail for the train itself. Numerical modelling, which offers greater versatility, has been in wide use due to its ability to model complex geometries of the track-ground system in detail. Loads are often simulated as moving point loads that are applied directly to the rails by incorporating dynamic multipliers [25]. Some studies also use triangular pulses to represent loads [1] [20]. However, simple point/axle load models show poor agreement with the experimental data in situations where dynamic effects are significant [54]. Past studies have extensively explored material models for simulating train-induced ground vibrations, primarily employing numerical methods like the Finite Element Method (FEM). Linear Elastic (LE) models were widely used in 2D and 3D FEM analyses, often with Rayleigh viscous damping due to their lower computational demands [20]. However, LE models are limited as they inaccurately represent soils at large strains or near critical train speeds, fail to capture plasticity and hysteretic damping, can overestimate vibrations in 2D models lacking

geometric damping, and struggle with water table fluctuations affecting soil stiffness and wave propagation. More advanced non-linear material models were implemented in time-domain FEM analyses to account for the complex soil behaviour [20] [3].

This study will focus on the ground-borne vibrations from railways investigating the loading characteristics focussing on the latest moving load method in finite element modelling (FEM), exploring the effect of linear and non-linear material models as well as the effect of a changing water table.

1.2. Research Problem

With the increase in demands for better transportation, a trend observed in this context is the increase in the speed and loads of railway trains, which in turn imparts heavier loads on the tracks. This movement of the train on the rails causes significant dynamic forces between the rails and wheels, generating vibrations that propagate to the nearby regions [33]. But the transfer of vibrations depends on quite a lot of factors such as the speed of the train, the type of soil on which it is laid, the type of sleepers, the length of continuous rails, to name a few [17][35][20].

In recent years, researchers have been trying to reduce these environmental effects while improving passenger comfort. Over time, they have been attempting to study this complicated relationship between train-induced vibrations and its effects on the surroundings, but are yet to dive deep into it. The loading of the tracks by the wheels of a moving train occurs at varying speeds because of its acceleration, deceleration, and varying loads, making it difficult to compute. This brings in a combination of multiple speeds and loads at a single point on the track in a very short period of time. Therefore, it is essential to make sure that the loads from the trains are modelled in a manner that it represents reality to the closest for better understanding. Majority of the research conducted has been shown to load the rails using point loads with the addition of dynamic multipliers to simulate the dynamic movement of trains [28][25]. Since 2018, the commercial finite element software for geotechnical analysis, PLAXIS has come up with updates which allow the user to incorporate a moving load function to simulate movements of vehicles, like trains. The implementation of this is seldom seen in academic literature. Furthermore, from the review of literature, it was seen that the soil behaves differently under saturated and unsaturated conditions [24], and with nonlinearity in its behaviour [26] [13], making the problem even more complex. With heavier loads and trains passing through densely populated regions, vibration transfer from railways needs to be studied on a deeper scale to understand its behaviour through the soil. The nonlinear behaviour through the material model and the effect of a varying water table on the transfer of vibrations will be explored, but the partial saturation conditions of the soil will not be the main focus in this work, as it brings more complexity to the problem at hand. The main points of focus will be discussed in the following subsection.

1.3. Research Objective

This master thesis aims to investigate the implementation of the moving load method function to study the transfer of vibrations through the soil due to the movement of trains and the effectiveness of the aforementioned function in the finite element software in loading the model. This work will dive into how the vibrations are transferred when using a linear material model and a non-linear material model, specifically the Hardening Soil model with small strain stiffness. The nonlinear behaviour of soil is a critical aspect when studying ground-borne vibrations, especially as it significantly influences the dynamic response of the soil under train loading and also provides a much more accurate, realistic and safer representation of soil

behaviour. This phenomenon becomes particularly relevant when large shear strains are calculated, which can occur in the embankment and soft soil layers beneath the rail. Additionally, the effects that the varying water table on the transfer of vibrations will also be investigated with the implementation of a non-linear material model. The objective is to fill this knowledge gap and provide new perspectives to the field of soil behaviours under dynamic loads.

1.4. Research Questions

This master thesis will focus on the modelling of moving loads in finite element (FE), studying the effects of the material model on the transfer of vibrations and varying water tables on the vibration propagation. Multiple methods have been explored in the past [58] [2] [25] [12]. The questions this master thesis intend to focus on are:

1. How should train loads be modelled?
    - How did past loading methods differ and which of them fits best?
    - How effective is simulation of train movement with the moving load function in Finite Element Modelling?
2. How does the material model and/or a fluctuating water table influence the transfer of ground borne vibrations?

1.5. Reference work

For this work, the master thesis research conducted by Ewa Anna Kunicka [30] at Delft University of Technology in collaboration with Arcadis is taken as a starting point. The mentioned work is highly relevant as it addresses the mitigation of railway-induced vibrations to people in buildings near railway tracks. This is particularly important in soft soils, where the Rayleigh wave velocity is low and vibration amplification is more likely to occur. The study specifically assesses the effectiveness of a concrete slab beneath the ballast bed as an abatement measure with the numerical model validated through field measurements conducted in the Netherlands. In the work, the author examines a conventional passenger railway line in the Netherlands, focussing on routes where VIRM (Verlengd InterRegio Materieel) trains operate as this is a standard intercity passenger service rather than a high speed or freight railway along the study area. Train speeds of 110-150 km/h, with the validated model using 130 km/h is being analysed, which falls within the conventional passenger rail category rather than high-speed rail (which typically operates above 200 km/h). The thesis uses the intermediate carriages of the VIRM train with documented axle loads of approximately 21.3 tonnes (105.5 kN per wheel), as well as the moving load module to simulate the movement of trains, but does not dive deep into the moving load module. The study is taken as a reference, as it represents a common scenario in countries with soft soil conditions or sandy soil conditions, especially The Netherlands, where conventional passenger railways must address the ground-borne vibrations without reducing operational speeds below commercially viable levels.

The current study focusses on understanding and implementing the moving load module in PLAXIS, representing a substantial advancement over the approach of the earlier study which focused on investigating the effectiveness of a concrete slab as a vibration abatement measure. A dedicated moving load module is expected to provide a more realistic simulation of the train-track-ground interaction compared to simulating train movement using point loads with dynamic multipliers such as triangular pulses.

2

Literature Review

2.1. Theoretical Background

Wave propagation through soil is a complex phenomenon which is influenced by numerous factors like the soil properties, soil stratification and layering, water table, distance from the source, reflections and refractions and the loading, to name a few. Understanding wave propagation is fundamental to analysing the environmental effects of train-induced ground vibrations, which has acquired considerable attention due to their potential to damage buildings and affect people. The following subsections will discuss in depth the types of waves, damping, and the effect of various factors influencing the vibration through the soil.

2.1.1. Waves

In the context of railway-induced ground vibrations, the energy that causes movement is transmitted through the soil by elastic displacement waves [1]. These waves are generally referred to as seismic waves and are classified into two main categories, body waves and surface waves.

Body waves propagate primarily beneath the soil surface and can travel through soil and fluids. They are divided into two, compression waves or P- waves and shear waves or S-waves. Compression waves (P-waves), also known as primary, longitudinal, or irrotational waves [30]. In these waves, the movement of a single particle is in the direction, parallel to the direction of propagation. They travel through the compression and expansion of the material and have the highest wave speed compared to the other wave types. They propagate mainly downward into the medium or radially in case of underground tunnels [57] and their velocity of propagation depends on many factors, a few of them being stiffness, Poisson's ratio, and density of the medium, with higher velocity for mediums with higher densities. Based on studies across seven European sites that included very soft soils, the measured compression wave (P-wave) velocity ranged from 280 m/s to 1760 m/s [57], but is not restricted to this range. The range of velocity varies quite a lot and it is important to note that the P-wave speed increases dramatically in saturated soils, where the wave speed becomes more representative of the water component [42].The presence of pore water significantly affects soil compressibility, leading to higher P-wave velocities [42] [36]. Shear waves (S-waves), are also known as secondary, transverse, rotational, or equivoluminal waves where the movement of a single particle is perpendicular to the direction of propagation. These waves cannot propagate in fluids, only in ground and are usually directed obliquely into the medium with shorter wavelengths than P-waves, and with velocities ranging from 30 m/s to 500 m/s. In an infinite elastic homogeneous

and isotropic medium, shear waves propagate at a constant speed without mentioning the frequency dependence [54]. However, when the ground is stratified or layered, its structure significantly affects wave propagation. In such a layered ground medium, surface waves (often called P-SV waves or Rayleigh waves of different orders) are dispersive, meaning that their phase velocity varies with frequency. This means that in real-world scenarios where soil is rarely homogeneous, S-wave components within the surface waves would exhibit dispersion [29].

Surface waves are the result of interaction between compression and shear waves but not merely a general interaction of P and S waves, but rather a specific phenomenon that arises from the interaction of these body waves at a boundary condition, such as a free surface or interface between soil layers [54]. They travel along the surface and their amplitude decays exponentially with depth [25], but despite the high attenuation rate, they are generally more damaging than body waves due to their occurrence at the surface. They are divided into two, Rayleigh waves or R-waves or P-SV waves and Love waves or SH waves.

Rayleigh waves are the most relevant for building excitation because they are not subject to the same geometrical spread because they are surface waves, but it is also crucial to understand that all waves attenuate with distance due to both geometrical spreading (or damping) and material damping. [57] [6]. Rayleigh wave particle motion is elliptical, meaning that the particles move both in the direction of propagation and perpendicular to it, with the amplitude generally growing towards the surface. The particles follow an elliptical path, often described as counter-clockwise to the direction of wave propagation. Rayleigh wave usually carries the largest part of the wave energy transmitted, particularly to larger distances along the surface and their velocity is usually 10% lower than that of shear waves [54].

Love waves are another type of surface waves and only involve horizontally polarised shear deformation [54]. They can occur when the top soil layer has a noticeably smaller Young's modulus than the underlying layer, causing the wave to be trapped in the top layer due to multiple reflections. Since vertical forces dominate the excitation of vibration in case of railways, these are usually ignored in the calculations.

2.1.2. Damping

Damping is a measure of the rate at which energy is reduced as the wave disperses and passes through a material. Geometrical damping and material damping comprise the total damping, and it has a nonlinear relationship with frequency. The dependence of damping on frequency makes it challenging to model in time domain.

Geometrical damping is where the amplitude of the vibration waves decreases as they propagate farther from the source. In this type of damping, the amplitude of waves is the highest at the point of contact. The major difference between geometrical damping and material damping is that geometric damping is generally considered frequency-independent, rather than merely "less dependent" on the frequency of vibrations, while material damping is inherently frequency-dependent. In mathematical formulations, geometrical damping is often represented by a "power of geometric attenuation" (denoted as 'n'), which indicates how rapidly the wave amplitude decays with distance, rather than a dimensionless ratio. For example, the power 'n' is given as 0.5 for shear waves, compression waves, and Rayleigh waves from a point source, and can be 0 for Rayleigh waves from a line source in some idealised scenarios [6].

Material damping is an important factor influencing the propagation of vibrations through the ground. It is the component of total damping that causes the attenuation of wave energy as it

passes through the material. It is commonly expressed as a damping ratio (ξ). In addition to this, geometrical damping also contributes to attenuation, but material damping refers to the dissipation of energy within the soil medium itself due to inelasticity and other internal friction mechanisms. Due to it's frequency dependency, different frequency components lose energy at a different rate. It is stated that material damping is highest in the high-frequency range and in the upper layers, since the soil particles are less compacted. It was also observed that damping decreases with depth, and saturated soils can exhibit elevated viscous damping at high frequencies [42]. Due to the combination of the two types of damping, low frequencies tend to dominate at larger distances from the source. Material damping is generally higher in soft soils. However, the concept of "vibration absorption capacity" provides a more nuanced view, suggesting that gravel soils and dry sand have the highest capacity, while peat and soft clay have the lowest, implying varying damping characteristics across different material types. In contrast, stiff or hard soils are noted to attenuate ground vibration much more rapidly with distance compared to soft soils [31]. In conclusion, while material damping tends to be higher at high frequencies and in less compacted upper layers, its magnitude and behaviour are also significantly governed by the specific soil type and its inherent properties, including those related to plasticity.

2.1.3. Rayleigh Damping

Rayleigh damping, also known as proportional damping, is often used in numerical simulations in the time domain to represent material damping, where the damping matrix (C) is defined as a function of mass (M) and stiffness (K) matrices represented as

$$C = \alpha M + \beta K \tag{2.1}$$

The coefficients α and β, are carefully selected to provide an "almost constant damping" or a damping ratio that "can be treated as constant" within a specific "range of frequencies of interest" or "main expected frequencies". Outside of this designated frequency range, the damping ratio tends to be significantly higher [20]. This formulation is particularly efficient for time domain analyses because it allows the equations of motion to remain decoupled in modal analysis, provided that the modal damping matrix is assumed to be diagonal. For instance, in studies concerning train-induced ground vibrations, a frequency range of 10 to 50 Hz has been commonly chosen for soils and track elements [20]. Despite its practicality and widespread use in software like PLAXIS, Rayleigh damping presents notable limitations. Its frequency-dependent nature inherently leads to a loss of accuracy outside the chosen "constant damping" frequency band. This can cause the model to underestimate the influence of low frequencies (e.g., 2 Hz dynamic components) and potentially over-attenuate high-frequency vibrations (e.g., above 100 Hz, where numerical results might show almost zero magnitude). The influence of damping ratio is significant and non-linear, for points of consideration. Although changes in the damping ratio affect primarily the amplitude, they do not alter the overall pattern of vibrations. Given its sensitivity, Rayleigh damping parameters often require careful calibration through an iterative procedure to achieve the best fit with real measurements, particularly when the response at distant points is of interest. Some advanced soil constitutive models, such as the Hardening Soil model with small-strain stiffness (HSsmall), can inherently account for hysteretic damping in cyclic loading, potentially reducing the need for an additional Rayleigh damping model, although HSsmall may show small damping at very small strains [39]. However, applying Rayleigh damping can still be used to compensate for the lack of damping consideration in simpler models. Consequently, relying on Rayleigh damping can lead to a "loss of accuracy in certain frequency bands", particularly outside the chosen optimal

range (e.g., 5–80 Hz), where the ”numerical response fits worst due to high damping induced outside these limits” [20].

2.2. Railway Induced Vibrations

Understanding railway-induced vibrations has been a topic of interest for railway and geotechnical engineers since the mid-1900s. The prediction of railway-induced vibrations, especially ground-borne vibrations, has been a daunting task involving numerous uncertainties and variables. The three main components, the source, the propagation path, and the receiver, must be studied in depth for the prediction and mitigation of vibrations. In this thesis, the propagation path will be focussed in detail.

2.2.1. Generation Mechanisms

The primary source of railway-induced vibrations is the dynamic interaction between the train wheel and the rail [54] [59]. This interaction generates forces that propagate through the track system to the ground. These forces can be broadly categorised into two main components:

1. **Quasi-static Excitation (Moving Load Effect):** This component arises from the static weight and the effect of it under the movement of the static load at a speed, but independent of time. The quasi-static loading is constant throughout the passage of the train and mainly depends on the axle loads and the axle separation distances of the train [54]. It primarily dominates the track response and near-field vibration at very low frequencies [29].
2. **Dynamic Excitation:** This component of vibrations results from several more complex excitation mechanisms. Some of the mechanisms are,
    - **Parametric Excitation:** This is caused by iterative track variations like the sleeper spacing or spatial variations in soil impedance [44] [57].
    - **Rail Unevenness/Roughness:** Wavelengths between 0.1 to 10 meters can be caused by variations in track alignment or track bed undulations [13].
    - **Rail Corrugation:** The periodic wear of the running surface on the rail head can cause wavelength generation between 0.01 and 0.05 meters [57].
    - **Wheel Out-of-Roundness/Flats:** These are responsible for the generation of high-frequency impact forces at every wheel rotation, caused by repeated high-frequency loading or manufacturing defects.
    - **Discrete Discontinuities:** Localised impact excitations can be caused by the presence of rail joints, welds, switches, and turnouts.

Factors influencing the level and characteristics of train-induced ground vibrations also include the axle weight, speed of the train, track configuration, ground conditions, and damping characteristics of the materials. [59] [1]. The mechanism of generation of these vibrations at the wheel/rail interface as depicted in the figure 2.1.

However, models for predicting ground-borne vibration are usually developed on the basis of simplifying assumptions. These may depend on engineering insight to replicate the operational conditions of interest, or may be necessary due to a lack of complete data for the simulations or limitations in the available computational power and time.

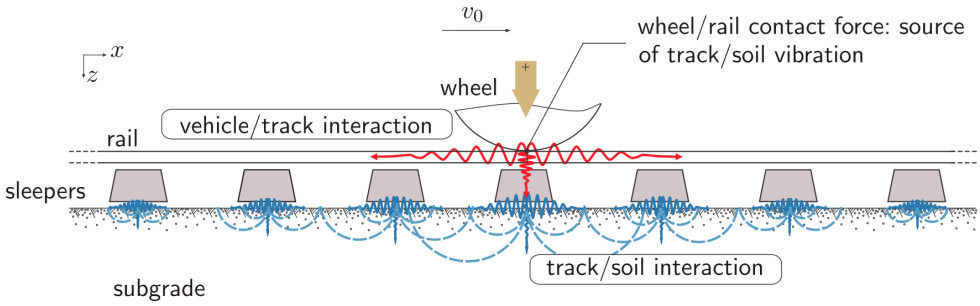

Figure 2.1: Generation of vibrations due to wheel-rail interaction [55]

2.2.2. Transmission Path (Propagation)

Once generated, vibrations propagate from the track, through the ground, and potentially into nearby building foundations. The transmission of vibrations is a complex process involving different types of wave, mainly body waves and surface waves. The properties of the ground significantly influence wave propagation, including density and stiffness. The ground is inherently an inhomogeneous medium, with considerable differences between layers (e.g., sand, clay, rock, groundwater), making detailed soil surveys necessary for accurate modelling [57] [54]. Damping is crucial in reducing vibration energy as it disperses through the material. Another critical phenomenon during transmission is the Critical Velocity Effect. This occurs when the speed of the train approaches the Rayleigh wave speed of the supporting soil, leading to significant increases in track vibration and potential ground movement amplifications. If the train exceeds this critical velocity, a ”Mach cone” wave propagation pattern can develop at the tail of the train. Railway designers typically aim to ensure that the train speed does not exceed 0.7 times the Rayleigh wave velocity to mitigate this risk [13] [25] [56]. It should be noted that while the 0.7 factor is a widely adopted practical guideline in railway design to manage the risks associated with critical train speeds, it is important to understand that the phenomenon itself is complex and still an active area of research. Therefore, it should be regarded as a design assumption or recommendation rather than a strict, immutable physical law [13].

2.3. Effect on Receivers

Railway-induced vibrations manifest in various ways at the receiver, primarily affecting humans and structures.

- **Human Response:**
  - **Feelable Vibration:** This perceived as whole-body vibrations, usually in the 1-80 Hz frequency range [57]
  - **Ground borne Noise (Re-radiated or Structure borne Noise):** This occurs when vibrations transmit into a building’s structure, which causes the walls, windows and ceilings to vibrate and radiate low frequency sound which resembles a rumble, usually in the 20-250 Hz range.
  - **Secondary effects:** Rattling of loose doors and objects inside buildings.
  - **Annoyance and Sleep Disturbance:** These are major concerns of residents living close to railway lines. The responses of humans to these are subjective and are also influenced by psychological factors, and combined exposure to noise and vibrations

can significantly increase annoyance [44] [54].

- **Impact on Buildings/Structures:**
  - **Structural Damage:** The vibrations from railways are rarely strong enough to cause structural or even cosmetic damages to buildings. These vibrations are usually on average between 0.1-0.6 mm/s, and to cause damage, they should be above 5.0 mm/s in the context of minor cosmetic damage to buildings, often associated with sources such as pile driving or in extreme cases very close to tracks, rather than typical railway operations [**17**]. Although 5.0 mm/s is a reference for cosmetic damage, it is not a universal threshold, and standards account for the specific characteristics of the building, its age, and the nature of the vibration when setting damage limits. For railway-induced vibrations, the levels are typically well below these damage thresholds, with the primary impact usually being human discomfort. However, old historical buildings may need more detailed consideration.
  - **Resonance:** Buildings usually have its natural frequency below 10 Hz, and if the frequency content of incoming ground vibration aligns with these natural frequencies, structural resonances can amplify vibration levels within the building [57]. Although frequency ”below 10 Hz” figure is a general guideline for the fundamental (whole-body) resonance, the actual frequency content of vibrations within a building and its various components is complex and influenced by a multitude of design and material choices.
  - **Settlement:** These vibrations also have the potential to contribute to the settlement of railway tracks and surrounding structures, especially in soft soils. In the case of regions with loose sandy layers under the tracks, increased pore pressure due to cyclic loading can also cause liquefaction and significant settlements [56] [66].
- **Sensitive Equipment:** The working of sophisticated instruments like electron microscopes or sensitive weighing machines can be disrupted by train-induced vibrations and need to be assessed critically.

2.4. Existing Prediction Models

A model is fundamentally defined as a description of some properties of a system suitable for a certain purpose. It is important to note that a model does not necessarily need to be a true and accurate description of the system to serve its intended purpose [6]. In the context of railway-induced ground vibrations and geotechnical analysis, models serve as powerful tools for prediction, assessment, and design. They allow engineers and designers to:

- Study problems and propose mitigation methods during different phases of railway design processes.
- Predict future ground-borne vibrations based on factors such as increased train speed and axle load.
- Determine the amplitude of vibrations and assess their effects on the surrounding infrastructure and ground.
- Evaluate the effectiveness of different countermeasures and adopt the best.

Compared with airborne noise, ground vibration is much more complex, as the medium through which the vibration propagates is anisotropic, with its properties varying significantly from one place to another. The reason why airborne noise is used as the reference point here is to

highlight the inherent simplicity and predictability of its propagation medium (air) compared to the highly variable and complex nature of the ground. In recent decades, the approach to predicting railway vibrations has evolved from experimental and empirical methods to advanced numerical techniques, due to increased computational capacity. This change has been largely driven by the availability of more powerful computational resources. Numerical models, particularly those based on the Finite Element Method (FEM), have become more widely adopted in engineering practice due to their versatility in handling complex geometries and material non-linearity. Until now, there has been no common assessment criterion or quantity of measurement for ground-borne vibrations, other than the guidelines established by various institutions that are being followed.

2.4.1. Empirical Model

The empirical model is a research-based approach where observations and measurements of the phenomena are used to derive conclusions or models. They are one of the earliest approaches to studying railway vibrations. It relies on real-world data to validate or develop predictive models. Empirical models, like those developed by Kurzweil and others, use measurements to estimate ground borne vibrations and re-radiated noise in buildings near railway tracks. These models consider factors such as train speed, track type, and soil characteristics [20][44]. Such methods are commonly applied during the initial or early stages of similar projects to identify potential problematic areas or to select new track locations without a high computational effort [29][44]. Although a simple method, the major drawback of this method is its reliability with accurate field data, which may not always be available. In addition, these models are unable to account for complex interactions between vehicles, tracks, and soil or non-linear behaviour that advanced methods are easily able to incorporate [20][44].

The Federal Railroad Administration (FRA) [26] and the Federal Transit Administration (FTA) [27] of the U.S. Department of Transportation have developed a methodology that predicts vertical vibration velocity levels L_v using [62]:

$$L_v = L_F + T_{ML} + C_{build} \tag{2.2}$$

Where:

- L_F represents force density which is a measure for the power per unit length radiated by the source.
- T_{ML} is line transfer mobility determined experimentally via impact hammer tests along tracks, averaging transfer functions between impact points and receivers
- C_{build} accounts for building coupling losses (dB) which is a is a measure for the modification of vibration spectrum due to the dynamic interaction between the foundation and the soil

The Peak Particle Velocity (PPV) predictors for freight lines were derived by Malaysian studies through multivariate regression:

$$\text{PPV} = 0.67 \cdot \left(\frac{v}{40}\right)^{0.48} \cdot \left(\frac{10}{r}\right)^{0.33} \tag{2.3}$$

Where:

- v in km/hr

- r in meters
- $(R)^2$ is 0.89

Table 2.1 gives a summary of a few of the empirical and semi-empirical models created in the past decades [31]. In a study[31], a regression-based empirical model was developed to predict ground-borne vibration velocity caused by freight trains. The authors used a multiple linear regression model to predict the Peak Particle Velocity (PPV) of ground-borne vibrations. The two main parameters used were the train speed (km/h) and the distance between the vibration source and the receiver in meters. The final regression equation of the PPV is

$$\text{PPV} = 0.554 + 0.0555 \cdot \text{Speed} - 0.100 \cdot \text{Distance} \tag{2.4}$$

This model simplifies previous approaches by focussing on easily measurable parameters, reducing the dependency on advanced equipment [31]. The study focused on soft soil types, particularly silty clay and alluvial deposits, which are common in the study area (Klang and Shah Alam, Malaysia). Measurements were taken at nine sites along the railway track, and these sites were chosen due to their proximity to residential areas. Ground-borne vibration velocities were measured using a Mini-Seis digital seismograph. The correlation analysis identified significant relationships between PPV and independent variables (speed and distance). A regression model was then developed and validated through residual analysis, normality tests, and scatter plots. From the study the authors concluded that the PPV increases linearly with train speed but decreases with greater distance from the railway track. The model effectively predicts ground borne vibrations using minimal tools or data inputs. Unlike other models that required complex parameters such as wheel forces or building amplification factors, this model simplifies prediction by focusing only on train speed and distance. However, it is tailored for local Malaysian conditions and provides a practical alternative for practitioners without access to advanced equipment.

2.4.2. Analytical Model

The analytical method involves the use of mathematical models and theoretical formulations to predict the behaviour of vibrations from railways.These methods are grounded in physics-based principles unlike empirical models, which heavily rely on observed data. It uses simplified representations, such as Euler-Bernoulli beams for rails on an elastic foundation (e.g., Winkler models) [29]. Analytical methods are particularly useful during preliminary assessments, as they are computationally efficient. They provide quick estimates of vibrations based on axle loads, track stiffness, and soil properties [29]. A major drawback of this method is that these models often assume linear behaviour and may not capture the complex interactions or non-linearities in the soil. And the need of a simplified geometry for these models may not help in accurate prediction of complex situations [20].

2.4.3. Numerical Model

The numerical methods use computational models to simulate and predict the dynamic behaviour of railway systems. These methods are based on solving mathematical equations numerically using techniques like Finite Element Method (FEM), Finite Difference Method (FDM) or Boundary Element Method (BEM). FEM is widely used for its versatility in modelling complex geometries and material behaviours. It is particularly effective in time domain simulations and can even model non-linear material behaviour. 2D, 2.5D and 3D are the most used modelling techniques in FEM.

Author / Year	Study origin	Model	Description
Madshus et al. (1996)	Norway	$V = V_T F_S F_D F_R F_B$	V is the peak particle velocity in mm/s. V_T is the specific vibration level for specific train types. F_s is the speed factor. F_D is the distance factor. F_R is the track quality factor. F_B is the building amplification factor.
Jones and Block (1996)	England	$V_{Dk} = F_D(f)X_{Dk}$, $X_{Dk} = (\sum_{j=-\infty}^{\infty} x_{jk}^2(f))\frac{1}{2}$, $x_{jk}(f) = \sum_{l=0}^{N} a_{jl}P_l(\cos\theta_j)$	The models are only applicable for freight train. V_{Dk} is the vertical vibration prediction. X_{Dk} is the total transfer function. $F_D(f)$ is the vertical vibration for sleeper. x_{jk} is the energy sum of the transfer function. k=0 is the vertical response function and k=1 is the lateral. θ is the angle between the normal to the track at the response position and the excitation point on the track
Suhairy (2000)	Southern Sweden	$V = V_T(\frac{D}{D_0})^B(\frac{S}{S_O})^A F_R F_B$	This equation is used to find the vibration rates at different distances for different types of train. V is vibration velocity in mm/s. V_T is the measure of vibration levels for the trains. D is distance from the centre of track. D_0 is reference distance. S is train speed. S_o is the reference speed. B is distance dependent A is speed dependent exponential. F_R is the track quality factor. F_B is the building amplification factor.
Jiang and Zhang (2004)	Shanghai	$VL = 70 - 13.6\log(r/10)$	VL is vibration level. r is the distance from the viaduct centre line in m.
Bahrekazemi (2004)	Sweden	$V = (a\text{speed} + b)\left(\frac{r}{r_0}\right)^{-n}$	V is the particle velocity on the track. a and b are parameters of the model. R is the source distance from the receiver. n is the attenuation power. r_0 is the reference distance.
With et al. (2006)	Sweden	$v_{rms} = (a_1 F_{rms} + a_2)V + b_1 F_{rms}$	V_{rms} is the r.m.s. particle velocity. F_{rms} is the r.m.s wheel force applied. V is the speed of the train. a is the gradient. b is the intercept.
Hanson et al. (2006)	USA	$VL(\text{in dB}) = 20\log_{10}(v_m/v_{ref})$	v_m is the measured velocity. v_{ref} is the reference velocity. VL is the vibration level
Paneiro et al. (2015)	Lisbon	$PVS = 0.191(V) - 0.208log(D)$	PVS is the peak vector sum in mm/s. D is the distance in m. V is the speed of train in km/h.

Table 2.1: Previous models of ground-borne vibration induced by trains

2D methods

Two-dimensional numerical models are simpler and require less computational effort. They are often used for tunnels or surface lines where a uniform section or plane-strain assumption is acceptable. They are often implemented using numerical techniques such as FEM or FDM. One of the key assumptions of this method is the plain strain assumption, meaning that deformation in the direction perpendicular to the analysed cross-section is negligible or uniform. Despite the simplification, 2D models are widely used due to the following advantages:

- Significantly lower computational effort and time compared to 3D models.
- 2D models are often used in the preliminary stage to identify potential problematic areas for ground-borne vibration, especially for large areas.
- They are well-suited for geometries with uniform cross-section.
- 2D models are commonly used for calculations related to tunnels and underground lines and have shown acceptable agreement with real measurements [20][39].
- In some cases, a 2D plain strain soil response can represent an upper bound for the actual response, thus providing a conservative estimate.

Despite their utility, 2D methods have significant limitations due to their inherent simplifications. Some of them are:

- They cannot fully capture or accurately model three-dimensional wave propagation. This is a major drawback, as wave propagation in the ground is fundamentally a 3D phenomenon [39][1].
- It has been noticed by various researchers that 2D model tend to overestimate displacements and vibration levels compared to 3D models due to smaller geometric damping.
- Models formulated in 2D are often in frequency domain, which restricts the model to linear elastic behaviour of materials. This may be insufficient to simulate the dynamic responses from railways.
- 2D models are unable to account for geometric inhomogeneity and thus inhibiting the consideration of complex geometries.
-

Hall [25] concluded that two-dimensional models could be used to study certain effects of train-induced ground vibrations, but that three-dimensional analyses are necessary to achieve a better simulation of the response for practical purposes and to analyse requirements for simulating train-induced ground vibrations. The author utilised stationary loading in two-dimensional perpendicular and axisymmetric models. These models were designed to generate stress waves only from the main source, the track structure response, and did not consider other sources like rail defects or unsteady vehicle riding. However, it was stated that for a detailed simulation of the problem, a 3D model should be used.

Ruiz [20] [39] investigated the influence of soil constitutive models, comparing an advanced model (Hardening Soil model with small-strain stiffness (HSsmall)) with the Mohr-Coulomb (MC) model, and the influence of soil stiffness (considered in the range of small strains (E50) or very small strains (E0)) using a 2D finite element model formulated in the time domain for railway vibrations in tunnels. It was concluded that both soil stiffness and the amplitude of the maximum tangential strain are the most important geotechnical parameters for estimating deformational parameters and selecting appropriate constitutive models for studying railway

vibrations in tunnels. The authors found that the HSsmall model showed a better fit with real data than the Mohr-Coulomb model with E50 stiffness. However, when the Mohr-Coulomb model was considered with E0 stiffness, the HSsmall model offered little advantage, as the results were quite similar in the two cases studied, particularly for non-soft soils.

Researchers [56] aimed to model soil settlement caused by train vibration using the 2D finite element programme. The work demonstrated how their model could numerically simulate track-subgrade systems with dynamic train load and analyse soil dynamic performance under different situations. It evaluated the impact of soil responses from different design solutions by introducing various protective layers with different stiffnesses, confirming that this led to track vibration reduction and enhanced dynamic behaviour. The modelling and comparison of soil dynamic responses, including soil stresses, pore water pressure, and soil displacement, at design conditions with the water table at different soil layers were performed. It discussed the determination of the critical zone of influence due to dynamic train vibration by examining the relationship between the distance from the source and the attenuation of dynamic soil stresses along the depth of the subgrade. It was concluded that deformation of soil increased with the rise in water level, which in turn induced a higher pore water pressure in the soil.

Authors [25] [44] highlighted the drawbacks of 2D FE models, noting that they cannot consider the movement of a train or wave propagation in the direction of the track and often overestimate ground vibration levels. They concluded from comparisons between 3D FE-BE models and 2D models that 2D models can predict correct trends, but 3D models are required to predict absolute levels, although at a significantly higher computational cost.

2.5D methods

2.5D models are numerical approaches that offer a compromise between the high computational cost of a 3D model and the limitations of a 2D model. The basic assumption here is that the geometry in the longitudinal direction of the track is invariant. To achieve this, 2.5D models utilise a Fourier transform in the longitudinal direction. This transforms the problem into the frequency-wavenumber domain. Instead of solving a single complex 3D problem, it solves a series of 2D problems, one for each wave number. This approach typically only necessitates the discretization of the cross section. Some of the advantages of the method are as follows:

- A primary advantage is the reduced computational effort compared to full-scale 3D models. This makes them a more practical choice for many 3D problems.
- Despite using a 2D mesh, the Fourier transformation allows 2.5D models to include three-dimensional wave propagation effects.
- They are well suited for studying sections of railway tracks with invariant geometries.
- Tey can be combined with other analytical or empirical methods in hybrid prediction models, leveraging the strength of each approach [61][44][13].

Despite having a god number of advantages, this method has its own disadvantages, some of them are:

- The assumption of an invariant geometry limits modelling of features like complex geometries, changes in track stiffness, and other non-uniform structures.
- Models in 2.5D domain are formulated in frequency domain, which are limited to linear elastic material behaviour. Including non-linearity in longitudinal direction is not possible.
- The model's dependence of Green's functions and the difficulty to calculate the functions, especially in complex layered soils, make it unattractive.

- The potential of a 2D plane strain model to overestimate the displacements and vibrations are also present in 2.5D models.
- Although generally good, dispersion within complex track geometries can be a challenge in 2.5D models.

Sheng et al. [45]are recognised for developing 2.5D FE-BE models and applying them to trains in tunnels and embankments. They noted that these models allow for more complicated geometry and material properties in the cross section of the track-tunnel-ground system and are flexible for parametric studies compared to full 3D models. They found the 2.5D approach to be computationally more efficient than full 3D Finite Element (FE) models. Their work also led to the development of a relationship between wheel/rail roughness power spectral density and ground vibration power spectral density using the 2.5D FE-BE approach. While 2.5D models can predict the correct trends, they concluded that 3D models are still required to predict absolute levels of ground vibration [54].

3D methods

Three dimensional models are developed either in time domain or frequency domain, while 3D models formulated in the time domain are often preferred for capturing nonlinear behaviour and complex geometries. The major drawback of models in the time domain is the computation effort for analysis [20][29][25].

A summary of previous studies are given in table 2.2 and the loading methods are further explained. Multiple studies have been conducted on the development of FEM models to study the transfer of vibrations, the settlement of ballasted tracks, and the railway embankment performance [24] [56] [2]. For the analysis of similar problems, [24] developed a three-dimensional FEM of two adjacent moving trains. In this work, the author investigates the impact of the coarseness of the mesh, the depth of subgrade layer, model width, and time step on the settlement of the track. They modelled the sleepers to have a linear elastic response to the dynamic load and the subgrade soil, ballast, and sub-ballast to behave following the elastic perfectly plastic soil constitutive model with Mohr-Coulomb failure criterion. The movement of the train in their work was simulated in real time employing the load movement function in PLAXIS. The depth of the subgrade layer was found to have little impact when it was greater than 20 m. They also concluded that the model width had little to no effects on the amount of settlement, concluding that a model width four times the spacing between adjacent trains captured the behaviour well. A time step of 0.05 was found to be enough for a robust analysis when considering train speeds between 25 and 450 km/h.

The paper published by [1] evaluates the impact of vibrations from railways with respect to the variation in the embankment, the ballast stiffness, and the speed of the train. The author carried out an FEM analysis using PLAXIS 3D, version 21. For the analysis, the material model used for soil was Mohr-Coulomb model. The rails were modelled as a beam section with properties of of UIC60 beam and a spacing of 1.6 m was adopted between the rails. The sleepers were had a length of 2.4 m and a spacing of 0.6 m between them and were modelled as a beam section with the B70 sleeper properties. Rail pads of 0.1 m thick were used to connect sleepers and rails, modelled as two node-to-node anchors in each sleeper. The ballast and embankment were modelled using a drained linear elastic material model. An axle load of 25 tonne (250 kN) was assumed and suggested that 40% to 60% of the load is distributed among the adjacent sleepers. In their work, it was assumed that 60% of the load was only taken up by the point directly underneath the point load.

The passage of the train was simulated by a pair of point loads that were activated and de-

Study	Methodology	Soil Type	Track Type	Train Type	Key Findings	Limitations
Jens Fernández Ruiz et al. (2017)	Plaxis 3D FEM (Time Domain)	Soft soils	Ballasted track	High-speed train	Validated numerical results with experimental data; effective for soft soils and transitions.	High computational cost; limited to specific geometries and linear damping.
Swati Acharya et al. (2025)	Plaxis 3D FEM	Sandy soil	Ballasted track	Standard gauge train	Embankment height significantly reduces vibrations; ballast stiffness has minimal effect.	Ignored groundwater effects; limited to single soil type and embankment configurations.
Fatou Samb et al. (2019)	Plaxis Dynamic FEM	Sandy and clayey soils	Ballasted track	Regional train	Dynamic loads caused lower track settlement compared to static loads; useful for sandy contexts.	Did not account for permanent deformation over multiple load cycles.
Kouroussis et al. (2014)	BEM/FEM Hybrid	Layered soils	Various	Multiple train types	BEM effective for infinite domains; FEM suitable for complex geometries in finite domain simulations.	BEM limited to linear problems; FEM requires careful boundary condition treatment.
Connolly et al. (2013)	2.5D FEM-BEM	Soft soils	Embankments	High-speed train	Efficient modeling of embankments; generalized less accurate for nonlinear soil behavior compared to full 3D models.	Limited to longitudinally invariant geometries; less accurate for nonlinear soil behavior.

Table 2.2: Summary of studies on soil-track interaction methodologies and findings.

activated in turn. A load multiplier was given for each point, and the dynamic representation of load was done using Winkler beam approach. [41] mentions in their work the effect of railway-induced vibrations on the stability of nearby structures. The analysis was conducted in PLAXIS dynamic and a comparison between static and dynamic load was also performed. In their work, the ballast, under ballast and form layer was given to have linear elastic be-

haviour, the backfill, sand dune, and silty clay to have Mohr-Coulomb behaviour and the track to have a linear behaviour. It has also been mentioned that the majority of the settlement arose from the contribution of rail traffic.

The study conducted by Lars Hall [25] looked at actual vibration measurements and compared it with results from mathematical and numerical models performed both in frequency and time domains. A two-dimensional FEM perpendicular to the track was used to study the train-induced ground vibrations, and an FEM model along the track was used for studying the track response due to moving loads. The author performed all the analysis in time domain using direct time integration with implicit time schemes. The time step for the analysis was set to 0.001 s. Beam elements were used to model the rails and were given properties of regular railway rails (UIC60). The model had a length of 65 m and only half of the model was modelled due to symmetry. Moving point loads were applied on the nodes in the beam elements simulating the rail. Another loading model where the beam elements were removed in order to improve the simulation time, and the load was directly applied to the sleepers. The loads were considered as triangular pulses moving from one node to the next by a time step equal to the node spacing of loading nodes. Figure 2.2 below shows the load distribution of the moving point load on the beam travelling at a fixed speed. The material models used in the analysis were all linear elastic since they had less computational effort. The conclusion of that experiment was that 2D models were helpful in studying certain effects, but a 3D analysis was necessary to achieve better simulation results.

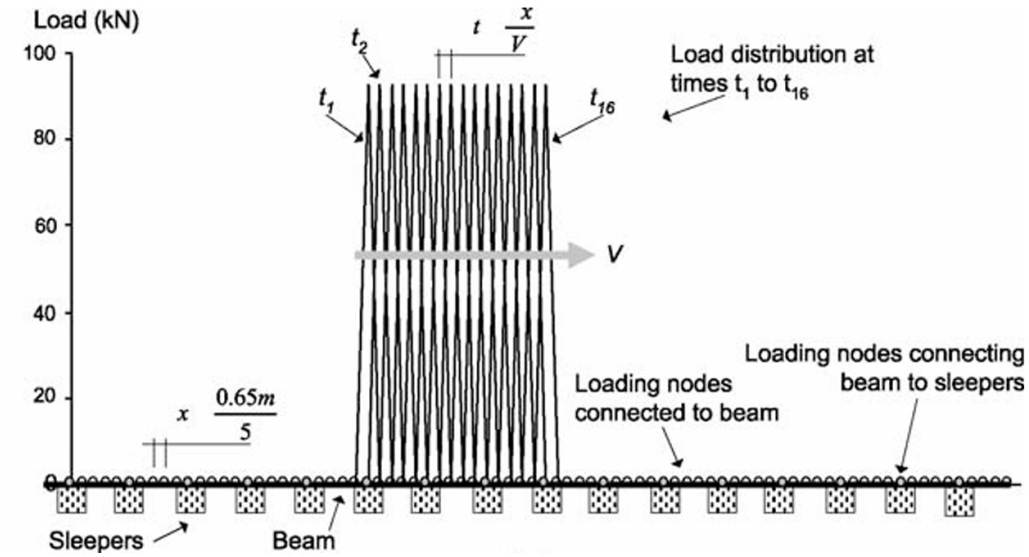

Figure 2.2: Load distribution of a moving point load on a beam travelling at a fixed speed [25].

In another study on ground response analysis for train-induced vibrations [1], the authors discuss about the influence of the height of embankment to the intensity of vibrations. The effect is attributed to the increased distance from the vibration source to the receptor and the longer, stiffer path through which the vibrations must travel. Numerical simulations conducted using PLAXIS 3D show that an increase in embankment height from 1 m to 3 m results in a reduction of the vertical velocity and the vertical acceleration at the edge of the embankment by approximately 58% and 67%, respectively. A higher embankment acts as a buffer, dissipating vibration energy over a greater distance and reducing its intensity before it reaches nearby structures or receptors. While increasing embankment height is effective in reducing vibrations, it requires more land area to maintain slope stability, which may not always be feasible

in urban or constrained environments.The study suggests increasing embankment height as a practical mitigation measure for reducing railway-induced vibrations, especially in areas where vibration impacts are a concern.

A study focussing on the environmental aspects of vibrations from railways [58] mentions the effect of the unevenness of the track and the presence of pipelines in the vicinity on the importance in the generation of vibrations. The study used field measurement data to calibrate the model. The results obtained from the numerical analysis were compared with the allowable threshold values to determine the effects. The loading plan employed for a train moving at a fixed speed is represented in figure 2.3. Viscous boundary conditions were used to absorb the waves at the boundaries. The authors considered cohesive soils to have an undrained behaviour and non cohesive soils to have drained behaviour in the analysis. They found that the numerical analysis for the considered location underestimated the vibration levels at short distances from the track, which the authors suspect might be due to the simplifications in the FEM analysis. It was also observed that comparable results were seen at distances of 20m and 30m from the track. The authors also highlighted FEM's application in designing mitigation measures like wave barriers but also noted its time-intensive nature. Recommendations for further research opportunities were also mentioned in the paper which will be discussed in detail later.

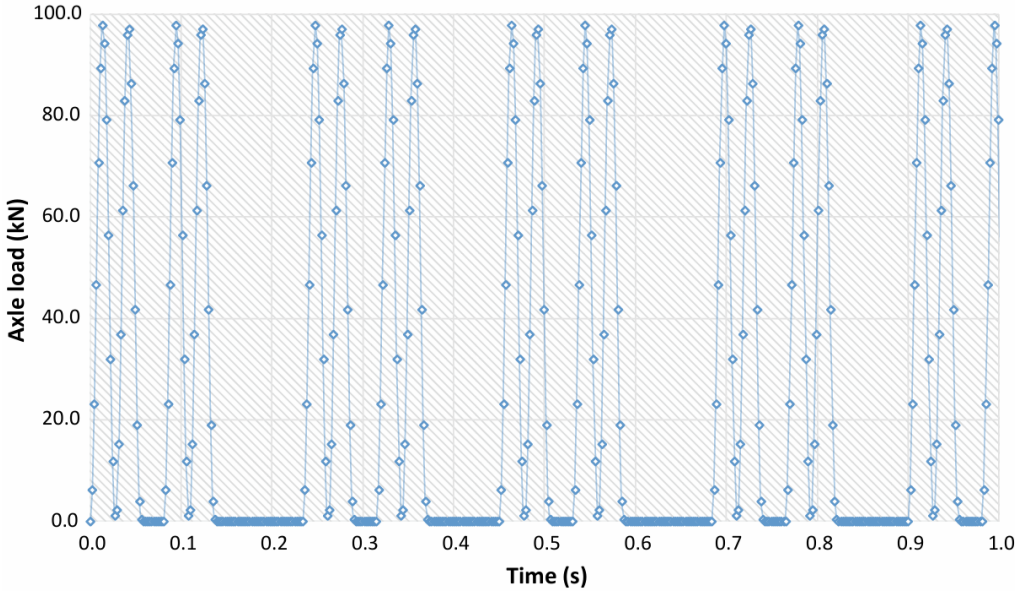

Figure 2.3: loading plan employed for a train moving at constant speed[58]

In case of loading the rails, [20] has represented them in the numerical model as triangular pulses to avoid transient responses. The same analysis was simulated in a 2.5D FEM-BEM approach to validate the results from the FEM analysis. It has been observed that several authors have worked on studying the vibration transfer from railways and related topics with respect to static and dynamic loading. Most of these studies have used finite model methods for the analysis as it makes it possible to model complex geometries, incorporating non-linear behaviour and dynamic forces.

Various sizes of models have been used by the authors to model and analyse vibrations, one of them [20] had a refined region of the finite element mesh of 30 m x 45 m (length x width). To ensure accurate wave propagation, the global dimensions of the model were extended to 65 m x 70 m x 30 m (length x width x depth). The study emphasized using a fine mesh near critical

areas such as the track and embankment to accurately capture dynamic responses. Coarser meshes were applied at greater distances to optimize computational efficiency. Shahraki et al, [43] had model of dimensions, 35 m x 35 m x 9.5 m (length x width x depth) using PLAXIS 3D. The UIC Railway Vibration Report [57] suggested that models should extend sufficiently beyond the area of interest to prevent boundary reflections from interfering with results. The authors advised using absorbing boundary conditions to minimise wave reflections at model edges. The recommendation was to refine the meshes in areas where high-frequency vibrations or steep gradients are expected. In a large case study [58] involving a 40-km-long railway track, measurements were performed at more than 25 reference locations, with each section spanning approximately 200 meters. Numerical modelling was validated with measurement data to ensure accuracy, particularly for dominant frequencies ranging from 16 to 31.5 Hz. The study highlighted the use of viscous boundary conditions to absorb seismic waves and avoid wave reflections. These recommendations provide a balance between computational efficiency and accuracy for railway-induced vibration analyses. The thesis [30] used a model with specific dimensions of 70 m length x 55 m width x 30 m depth, which was carefully chosen based on several considerations.

2.4.4. Analysing vibrations in frequency and time domain

The analysis of vibrations in either the frequency or time domains presents distinct advantages and disadvantages, particularly when applied to complex railway-induced ground vibration problems.

Frequency domain models generally require less computational effort compared to time domain models. For example, solving an eigenvalue problem for each frequency of interest in the frequency domain can significantly reduce computational requirements. It is well suited for systems that can be assumed to behave linearly and elastically. This is often considered valid for vibrations from railways, where soil particle deformation is typically very small. Damping can be modelled in a straightforward manner in the frequency domain using a complex-valued shear modulus, which effectively represents hysteretic material damping. Viscous or viscoelastic damping can also be included. When coupled with the Boundary Element Method (BEM), frequency domain analysis efficiently handles unbounded domains, such as the surrounding soil, because BEM only requires the boundary of the domain to be meshed and automatically includes the radiation of waves towards infinity. For structures with longitudinal invariance (i.e. properties remain constant along the track direction), 2.5D models formulated in the frequency-wavenumber domain are highly efficient. These models only require cross-section discretisation, significantly reducing computational demand while still capturing 3D wave propagation effects. They are also computationally faster and require less memory than conventional 3D finite- or boundary element models. Semi-analytical approaches, which often operate in the frequency-wavenumber domain, are plausible in the early stage of design as they allow rational decisions regarding track design for vibration reduction without looking into structural details, and computations are faster than periodic models.

A major limitation is that frequency domain models are primarily restricted to linear elastic behaviour. This means they struggle to account for non linear soil behaviour, such as stiffness degradation at large shear strains, generation of excess pore pressure, or complex dynamic responses that occur when train speeds approach critical velocities. These models are generally not flexible enough to handle complex geometrical variations along the track, such as transitions from slab to ballast track, embankments, cuttings, or local defects. The basic assumption of 2.5D models is that geometry in the longitudinal direction of the track must be invariant. While some numerical methods like FDTD (Finite Difference Time Domain) have easily imple-

mented high-performance absorbing boundary conditions, implementing these in frequency domain FEM can be difficult. In 2.5D approaches, accurately modelling the stress distribution associated with discrete sleeper or ballast tracks is more challenging compared to continuous slab tracks. While generally more efficient than time-domain 3D models, accurately resolving higher frequencies still requires smaller element dimensions, which can rapidly increase computational requirements and thus computational cost and time. Two-dimensional plane strain models formulated in the frequency domain may overestimate vibrations compared to more realistic 3D models. While hysteretic damping can be introduced, certain approximations for viscous damping (e.g., Rayleigh damping with fixed alpha and beta parameters) can lead to a loss of accuracy in certain frequency bands, especially at very low or very high frequencies [54] [29] [13] [45] [20]..

Time domain models formulated with FEM can account for non-linear soil behaviour, such as stiffness degradation at large shear strains and generation of excess pore pressure, which is crucial when train speeds approach critical velocities or in specific cases like soft soils. 3D models developed in the time domain can overcome issues with complex geometrical variations along the track, such as transitions from slab to ballast track, embankments, cuttings, or local defects, and can handle geometric inhomogeneity or changes in track stiffness. Time domain analysis allows for direct simulation of continuously moving loads and dynamic train loads, making it suitable for capturing transient effects. Complex problems can be broken down into sub-problems, with the vehicle-track interaction solved in the time domain, and resultant forces then applied to a ground model (which can also be in the time domain).

A significant limitation is the high computational effort required to compute solutions at every time step, especially for 3D wave propagation models. This can result in run times of hours or days. For example, one study reported 36 hours per second for simulating wave propagation in a 3D FEM model. Although viscous damping is used, accurately modelling frequency-dependent material damping in the time domain can be more challenging than in the frequency domain. Rayleigh damping, commonly used, has limitations and can lead to a loss of accuracy in certain frequency bands if parameters are not carefully chosen. The accuracy of time-domain simulations is highly dependent on element size (which needs to be small enough to represent wave phenomena) and the time step of the analysis. Higher frequencies require smaller element dimensions, rapidly increasing computational requirements. While direct measurements in the time domain are possible, they can be challenging to conduct over long periods and distances due to factors like extraneous noise and the need for sufficient train pass-bys for reliable data. Despite numerical advancements, differences between numerical responses and experimental results can arise due to limitations such as finite model distances and frequency-dependent damping, highlighting the complexity of validation. Modelling often assumes idealised material properties, and uncertainties exist regarding the material parameters used as input. Obtaining detailed soil properties for numerical models often requires in situ geophysical tests, and optimisation during post-processing can lead to non-unique solutions [20] [57] [36] [13] [62].

2.5. PLAXIS 3D

PLAXIS 3D is a powerful three-dimensional finite element software specifically chosen and used to simulate complex geotechnical problems, particularly railway-induced ground vibrations and the dynamic response of track-ground systems. It is a versatile commercial code that is often employed by engineers. It is based on the finite element method formulated in the time domain. It typically employs an implicit time integration scheme, such as the Newmark method, for solving dynamic equilibrium equations. This approach is crucial for simulating the

complex dynamic response of the track-ground system and handling real-world scenarios.

2.5.1. Material Model

Linear Elastic

The Linear Elastic model is based on Hooke's law of isotropic elasticity involving two basic elastic parameters, i.e. Young's modulus E and Poisson's ratio ν. It is the simplest material model available and is based on Hooke's law of isotropic elasticity, which assumes a linear relationship between stress and strain. It is often considered too crude for simulating complex soil behaviour due to its limited number of input parameters. The stress states in the linear elastic model are not limited in any way, causing the model to show infinite strength. The linear elastic material model is primarily used to simulate the behaviour of stiff structures, where their strength properties are typically high compared to soil [52].

The linear elastic material model for soil is an assumption often employed in the study of railway-induced vibrations, mainly due to the relatively low strain levels typically experienced by soil during the passage of trains [54]. It is particularly chosen for its computational efficiency compared to non-linear models, which are much more computationally expensive. Multiple studies on railway-induced ground vibrations assume that ballast, sub-ballast and subgrade soils behave as an elastic material.

But the model has its own drawbacks. The assumption of linear elastic behaviour is not acceptable when train speeds approach the propagation velocity of Rayleigh waves in the ground, as strains can be strongly amplified [20]. Simplified linear elastic models often treat saturated soil as incompressible (Poisson's ratio 0.5) and dry above the water table, which can introduce a sharp contrast in stiffness and acoustic impedance, potentially amplifying numerical estimates of vibrations [36]. For soft soils, where the stiffness degradation by rail traffic might be more pronounced, advanced constitutive models like the Hardening Soil with small-strain stiffness (HSsmall) model may offer more accurate results, though at a higher computational cost. However, for medium-stiff and stiff soils, if soil stiffness is considered in the range of very small strains (E0), the linear elastic model (Mohr-Coulomb with E0) can provide results comparable to more advanced models like HSsmall, with significantly lower computational effort [39]. Even at relatively small strains, frictional materials can exhibit nonlinear behaviour with loss of shear stiffness, which may not be fully captured by a pure linear elastic model[25].

Hardening Soil model with small-strain stiffness

The Hardening Soil model with small-strain stiffness (HS small) is an advanced constitutive model for soils used in numerical simulations, by incorporating the complete stress-strain curve, including the range of very small strains (shear strains, γ), less than 10^{-6}. This is particularly relevant for railway-induced vibrations where soil deformations are typically very small [39].

HS small model accounts for the decay of soil stiffness with increasing shear strain. A fundamental aspect of the Hardening Soil model, and thus HSsmall, is that stiffness is dependent on the effective stress level. It considers two types of hardening: shear hardening, which models irreversible plastic strains from primary deviatoric loading, and compression hardening, which models irreversible plastic strains from primary compression. Unlike simpler models like Mohr-Coulomb (MC) which have fixed yield surfaces, the HSsmall model's yield surface can expand due to plastic straining. It features two plastic yield surfaces: a cone and a spherical cap, formed by increasing plastic shear strains. The model intrinsically includes hysteretic damping in cyclic loading, with the amount of damping being dependent on the amplitude of the applied load and corresponding strain amplitudes. This can reduce the need for additional

Rayleigh damping (which is frequency-dependent). However, at very small strains, the model exhibits a small damping because the hysteresis loops of cyclic shear strain cover a very small area [12]. The influence of soil stiffness is very important on the ground surface, and HSsmall provides more accurate results compared to simpler material models. This material model is also necessary for studying the effect of changing water tables on the transfer of vibrations. It has been utilised in fully coupled dynamic FEM analyses to model the cyclic behaviour of loose soil and predict the generation of excess pore water pressures under train vibrations. Increasing water levels lead to greater excess pore water pressure and reduced soil stiffness, resulting in larger dynamic responses and soil deformation when subjected to dynamic train loads. This is because pore water may not have sufficient time to drain under high-speed impact loading, and reduced stiffness allows the Rayleigh wave velocity to be reached more easily [56].

Despite its advantages in capturing complex soil behaviour, the HSsmall model has several limitations, particularly regarding computational demands and specific material conditions. The HSsmall model is computationally much more expensive than simpler models. While it offers hysteretic damping, at very small strains, which are typical for ground vibrations induced by railway traffic, the model exhibits limited damping because the hysteresis loops of cyclic shear strain cover a very small area. This might necessitate the introduction of additional Rayleigh damping to control high-frequency noise [66]. The model requires a high number of input variables (e.g., oedometric parameters, tangent parameters, unloading and reloading shear modulus, reference shear modulus, shear strain). Obtaining all these parameters from geotechnical investigations can be challenging, and their absence might necessitate using a simpler model.

2.5.2. Impedance and Reflection coefficient in soil

Impedance in geotechnical terms refers to the resistance a material offers to wave propagation and is a key property in determining how much of a wave is being transmitted or reflected at the interface between soil layers. The equation for impedance is as follows:

$$Z = \rho \times V \tag{2.5}$$

where Z is the impedance, ρ is the density of the material kg/m^3 and V is the propagation velocity in the material. For normal incidence on a planar boundary, the reflection coefficient (R), which is the ratio of the amplitude of the reflected wave to the incident wave, which is:

$$R = \frac{Z_2 - Z_1}{Z_2 + Z_1} \tag{2.6}$$

where Z_1 is the impedance of the first (incident) layer and Z_2 is the impedance of the second (target) layer. These coefficients quantify how much of the shear wave is reflected at each boundary due to changes in impedance between the soil layers. A positive R value means that the reflected wave does not invert in phase, and a negative R means that the reflected wave inverts in phase. A value close to zero indicates little reflection and values closer to +1 or -1 indicates strong reflection.

2.5.3. Finite element discretisation

In PLAXIS 3D, various finite elements are used to model the components of a geotechnical project, enabling the analysis of deformation, stability, and flow.

Elements in modelling

In this section, various elements used in the modelling process will be briefly explained [8].

- **10-node tetrahedral element:** It is a fundamental component of the 3D finite element mesh, primarily used to model behaviour of the soil. They are defined by 10 nodes and operate using three local coordinates, has three degrees of freedom: translational displacements in the global x, y, and z directions. They are designed to provide a second-order interpolation of displacements to accurately represent nonlinear displacement fields within the element. The quality and refinement of this mesh, composed of 10-node tetrahedral elements, are critical for achieving accurate numerical results without leading to excessive computation times. The local numbering and integration points of a 10-node tetrahedral element is shown in Figure 2.4.

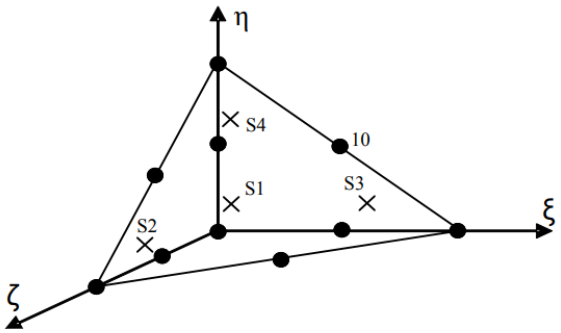

Figure 2.4: Local numbering and positioning of nodes (•) and integration points (x) of a 10-node tetrahedral element

- **Beam:** Beam elements are a type of structural object specifically designed to model slender (one-dimensional) structures that possess significant flexural rigidity (bending stiffness) as well as axial stiffness. They are made up of 3-node line elements. These 3-node line elements are compatible with the sides of 6-node triangular elements or 10-node volume elements (the standard soil elements in PLAXIS 3D), as they also have three nodes on a side. Each node of a beam element has six degrees of freedom, displacement in the global x, y, and z directions, and rotation about the global x, y, and z axes. Beam elements in PLAXIS 3D are formulated based on Mindlin's beam theory. This theory is more advanced than simpler beam theories (like Euler-Bernoulli) because it accounts for beam deflections due to shearing as well as bending. Additionally, the element can change length when an axial force is applied.
- **Plates:** Plate elements are structural objects specifically designed to model thin two-dimensional structures within the ground that possess significant flexural rigidity (bending stiffness). Plates are composed of 6-node triangular plate elements. These elements are compatible with the sides of 6-node triangular elements or 10-node volume (soil) elements. The 6-node triangular elements provide a second-order interpolation of displacements, allowing for accurate representation of displacement fields within the element. Each node of a plate element has six degrees of freedom in the global coordinate system: three translational displacements and three rotational displacements. Plate elements in PLAXIS 3D are based on Mindlin's plate theory. This theory is more comprehensive than simpler plate theories as it accounts for plate deflections due to

both shearing and bending. Plates are often used in conjunction with interface elements to accurately model the soil-structure interaction. These interfaces are represented by pairs of nodes that allow for differential displacements (slipping and gapping). The local numbering and integration points of a 6-node plate element is shown in Figure 2.5.

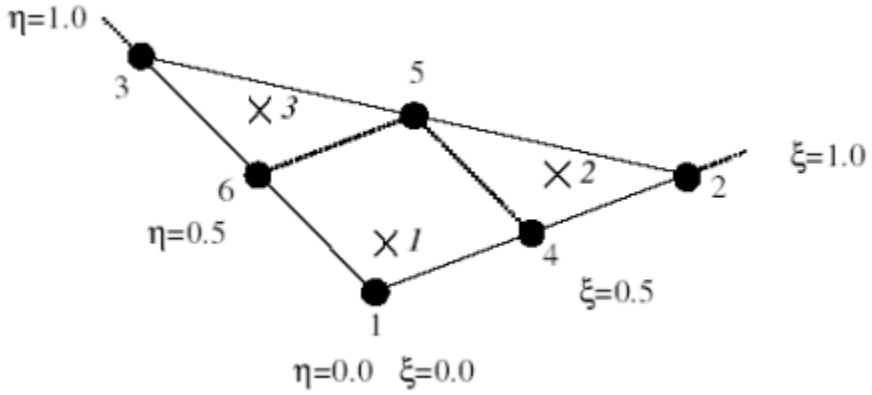

Figure 2.5: : Local numbering and positioning of nodes (•) and integration points (x) of a 6-node plate triangle.•) and integration points (x) of a 6-node plate triangle.

- **Interface Elements:** Interface elements are specialised joint elements designed to accurately model soil-structure interaction by simulating the thin zone of intensely shearing material at the contact between a structure and the surrounding soil. They are typically added to plates or geogrids, or placed between two soil volumes. Interface elements are crucial for simulating the behaviour where a structure interacts with the soil, such as along a diaphragm wall, a foundation, or a tunnel lining. They allow for differential displacements between the structure and the soil, meaning they can model slipping (relative movement parallel to the interface) and gapping or overlapping (relative displacements perpendicular to the interface). They are distinguished as either positive or negative interfaces, which merely serves to differentiate between interfaces on either side of a surface and has no physical meaning regarding their behaviour. After meshing, interfaces are composed of 12-node interface elements. These elements consist of pairs of nodes, which are compatible with the 6-node triangular sides of a soil element or plate element. Each node of an interface element has three translational degrees of freedom.

2.5.4. Advantages in using PLAXIS 3D

A significant advantage of PLAXIS 3D is its ability to handle complex geometries and non-linear soil behaviour. But with its versatility, it comes with its pros and cons, and a few of them are as follows [20][25][12][47]:

- PLAXIS 3D excels at handling complex geometries and non-linear soil behaviour, including the generation of excess pore pressure. This capability makes it a useful tool for specific cases, such as soft soils, inhomogeneous geometries along the track, and transition zones. Advanced material models like the Hardening Soil model with small-strain stiffness (HSsmall) can account for small-strain stiffness and hysteretic damping, capturing non-linear soil effects like stiffness degradation at large shear strains.
- The program is based on the finite element method formulated in the time domain, typically employing an implicit time integration scheme, such as the Newmark method, for solving dynamic equilibrium equations. This formulation is crucial for simulating the complex and time-variant dynamic response of track-ground systems.

- PLAXIS 3D supports various material models to simulate soil behaviour, including the Linear Elastic model, Mohr-Coulomb model, Hardening Soil model (HSsmall), and NGI-ADP model. This range allows for flexibility depending on the problem's complexity and available data.
- The soil is typically modelled using 10-noded tetrahedral elements, which is the only element available for soil volume in PLAXIS 3D.
- While older methods involved manually assigning dynamic multipliers as triangular pulses to static point loads to simulate movement, newer versions of PLAXIS 3D introduced a dedicated moving load function. This feature allows the software to interpret the load's location based on its velocity and time, simplifying the implementation of oscillatory components of the load. Train excitation can include both quasi-static (due to weight) and dynamic (due to rail unevenness, etc.) components.
- To simulate unbounded domains like the ground and minimise spurious wave reflections, viscous boundaries (dashpots) are typically applied at the sides and bottom of the model during dynamic analysis. For static phases, standard fixed boundaries are used.
- The direct output from PLAXIS 3D simulations is in the time domain, including particle displacements, velocities, accelerations, strains, stresses, and pore water pressures. These time domain results can then be converted into the frequency domain using the Fourier Transform for vibration assessment and comparison with established criteria. The model can also predict critical speed and dynamic settlement and analyse the effect of various parameters such as ballast modulus, fill modulus, axle load, and speed.

2.5.5. Disadvantages in using PLAXIS 3D

Just like any advanced commercially available software, it has its own disadvantages as well, a few of them are as follows [13][3][1][12] [39]:

- A significant limitation of time-domain models in PLAXIS 3D is the high computational effort required, which makes simulations very time-consuming. For instance, simulating wave propagation in a 3D FEM model can take approximately 36 hours per second of real-time simulation. While coarser meshes can reduce the time for some analyses like settlement, accurate wave propagation still demands a dense mesh, increasing computational burden and memory usage.
- In some earlier versions, PLAXIS software did not have adequate features to simulate the moving vehicle along the track directly. This necessitated a sub-structuring approach where train loads were first calculated by a 2D vehicle-track model and then directly imposed as force-time signals on sleepers in the 3D model. Furthermore, manually assigning dynamic multipliers to each point load could be laborious. Time-domain models also have the limitation that the domain must be truncated, as the train load cannot be considered from negative to positive infinity. The triangular pulses method, used for moving loads, can also generate frequencies associated with rail discretisation distance.
- For specific geotechnical calculations, such as slope stability, PLAXIS 2D has been shown to be a more accurate modelling program than PLAXIS 3D. The 10-node tetrahedral elements used in PLAXIS 3D are simpler and require less memory, but may not yield results as accurate as the 15-noded triangular elements in PLAXIS 2D for certain applications. This can lead to 3D calculations potentially overestimating total stability.
- Using more advanced, non-linear material models, while more realistic, is more demand-

ing on computer resources. There may be uncertainties with respect to the material properties used as input to the model. For instance, selecting appropriate Rayleigh damping parameters (alpha and beta) can be complex, and even the HSsmall model, while superior, may exhibit small damping at very small strains. Obtaining all necessary input parameters for advanced models can be challenging, often requiring specific laboratory or geophysical tests, and if unavailable, simpler models must be used.

- While mesh density may have little influence on track settlement with PLAXIS 3D's automatic meshing, the time step has a pronounced influence for train speeds above 100 km/h. This necessitates remarkably smaller time steps (e.g., 0.01 s for speeds between 150 to 350 km/h). This directly increases the computational time.

2.6. Representation of load

The representation of train loads by authors in the sources varies depending on the complexity of the model, the specific focus of the study, and the software used. Generally, train loads are considered as dynamic forces induced by the interaction between the train and the track structure.

2.6.1. Triangular pulses

The triangular pulses method is a common approach used by authors to represent train loads, particularly in three-dimensional (3D) finite element models (FEM) and coupled FEM-Boundary Element Method (BEM). This method is often employed when commercial software, such as PLAXIS or ABAQUS, does not natively support the direct application of a continuously moving load along a specified path [20]. Point loads are applied at these loading nodes. These loads are conceptualised as triangular pulses distributed between three nodes. The load distribution is linear. To simulate the movement of the train, these triangular pulses are moved from node to node over time. This movement is achieved by activating and deactivating the point loads at successive nodes. The triangular pulses method primarily incorporates the quasi-static component of the train load [25]. For each point load, a dynamic multiplier is assigned as a time-shear force signal. These multipliers represent the shear forces in the beam due to the static load along the rail at specific times. These shear forces are often calculated using static analysis based on the theory of a beam on an elastic foundation, sometimes with auxiliary software like PROKON [43] [37].

The triangular pulses method primarily models the quasi-static component of the train load, which is associated with the movement of the train's weight distributed by its wheel sets. If the dynamic components (arising from rail unevenness, welds, or wheel flats) are not explicitly included, the generated waves may not propagate significantly away from the track, making the method suitable mainly for studying the direct vicinity of the rail. The discretisation of the load in triangular pulse representation is highly important as it significantly influences the frequency spectrum. A finer discretisation of the distance between sleepers (e.g., dividing the distance between sleepers into more parts, like four or even eight) can yield more detailed and accurate results. Assigning the dynamic multipliers to each point load can be a computationally intensive process if done manually for high accuracy. This method may generate frequencies associated with the rail discretisation distance, but it does not accurately capture the sleeper passing frequency in the results.

2.6.2. Moving load method

The load in the numerical model, specifically concerning the ”moving load,” is primarily represented using the Oscillatory Moving Load feature available in PLAXIS 3D software since late

2018. This method allows for the direct application of a moving point load along a specified path, which in this case is the rail. This approach is crucial because it facilitates the inclusion of both the quasi-static (train's weight) and dynamic (oscillatory) parts of the load. To accurately simulate a train passage, individual loads are applied to separate nodes along the rail and are activated with a specific time offset. This time offset is determined by the train's geometry and speed, ensuring that the loads do not merge and correctly simulate the movement of the wheels. For instance, 12 separate point loads are arranged and applied to 12 different nodes to overcome the software's tendency to merge loads applied to the same node. PLAXIS employs the finite element method (FEM) for its calculations, which involves distributing applied loads to the nodes of the finite elements rather than applying them directly to the soil or structure. When simulating a moving load, PLAXIS does not treat the load as a single, continuous entity; instead, the software discretizes the movement into a series of finite time steps. At each time step, the position of the load is updated according to the user-defined velocity and acceleration, and the software calculates the equivalent nodal forces at the nodes of the elements that the load is currently traversing. Typically, the load does not coincide exactly with a node and instead is located between two nodes; in such cases, PLAXIS distributes the load across the adjacent elements and nodes, creating the effect of a smoothly moving load. The apparent ”jumping” of the load between discrete positions is governed by both the movement function and the chosen time step. At each increment, the previously applied nodal forces are removed and new forces corresponding to the updated load position are applied. This process allows PLAXIS to realistically simulate the dynamic effects of a moving load, such as that of a train wheel travelling along a track, particularly when sufficiently small time steps are used. As is typical in finite element analyses, a finer mesh generally enhances accuracy, but it must be balanced against computational demands, as excessively fine meshes can result in substantially longer calculation times without a commensurate increase in precision. Therefore, both element size and time step are critical factors influencing simulation accuracy, and conducting a sensitivity analysis is recommended to determine optimal model settings.

2.7. Vibration transfer and Water table fluctuation.

The impact of an increase in the water table on ground-borne vibrations and surface waves in sandy soils is complex and can lead to attenuation or amplification, depending on specific conditions and the nature of the dynamic loading. Several studies have reported that fluctuations in the groundwater table can significantly alter the dynamic response of the structure–soil system. The principal mechanism underlying this influence is the variation in soil stiffness and shear wave velocity (Vs) with changes in the water table. A rising water table reduces both the Vs and the initial shear modulus (G0), leading to lower overall stiffness of the soil. This degradation in stiffness is largely attributed to the generation of excess pore water pressures under dynamic loading, particularly at higher excitation frequencies, where the capacity of saturated soils to dissipate pore pressures is limited. Rising groundwater levels typically reduce surface displacement amplitudes and increase natural frequencies for general seismic ground motion. This implies an attenuation of vibrations [65]. This phenomenon depends on the situation, the type of soil and how the vibration is generated.

In saturated soil, metro-induced vibrations can be as much as 35% less than in dry soil. As the water table level increases, the intensity of ground motion caused by railways generally decreases [19]. Vibration along the free surface in saturated soil is generally smaller than in dry soil because the compressibility of saturated soil is lower. For machine-foundation systems, the rise of the water table in sand may amplify the vibrations induced by the machine. When the sand is fully saturated and the system operates near resonant conditions, vibration levels have been observed to increase. This amplification is produced by a decrease in the stiffness

of the sand when it is dynamically loaded under a fully saturated state, exacerbated by excessive pore water pressures and impeded drainage. The rise in water table also generates a decrease in the fundamental natural frequency of the system [33].

Literature shows that dry soils exhibit the highest values of Vs and G0, while fully saturated soils show the lowest. Under dynamic excitation, saturation tends to accentuate non-linear soil behaviour, lowering effective stiffness and increasing the potential for amplified vibrations. Experimental investigations confirm that, as the water table rises from dry to saturated conditions, the fundamental natural frequency of a foundation–soil system decreases in both horizontal and vertical directions. Reported reductions are on the order of 30–35% in the horizontal and about 20% in the vertical direction when comparing dry and fully saturated cases. This trend aligns with theoretical expectations, as the natural frequency of the system is directly linked to the soil stiffness and shear wave velocity [33] [7]. With reduced natural frequency under saturated conditions, frequencies of the vibration may coincide with or approach resonance zones. This study showed that when operating near 50 Hz in fully saturated soils, vibration responses can sharply increase due to resonance effects caused by reduced soil stiffness. Taken together, the literature highlights that groundwater levels play a critical role in dynamic soil–foundation interaction. A rising water table not only reduces the stiffness of the supporting soil and shifts the system's resonant characteristics but also markedly amplifies vibration response when excitation frequencies approach resonance.

In the context of train-induced ground-borne vibrations, when the water table reaches the ground surface (Dw/B = 0), the ground-borne vibration velocity can increase to approximately 1.36 times its maximum value in dry soil conditions [7]. In dynamic compaction of high-groundwater-level (HGL) foundations, water-soil interaction under high groundwater levels (HGL) can lead to a decrease in the damping ratio within the soil, causing it to oscillate more. This suggests that vibrations may be less attenuated or even amplified under these specific conditions, as energy is consumed by free water before being transferred to the sand [51]. The presence of the gaseous phase (air) in unsaturated soil significantly affects its dynamic properties. Even small changes in saturation in the unsaturated layer above the water table can drastically alter wave velocities and substantially influence seismic response. The damping ratio of sandy soils is generally low (below 0.05). When damping decreases, the system tends to oscillate more [51].

In summary, while rising groundwater levels often lead to the attenuation of ground-borne vibrations and surface waves due to increased damping and lower compressibility in a general seismic or metro-induced vibration context, specific scenarios involving machine foundations operating near resonance, the water table reaching the ground surface, critical water table conditions causing resonance, or liquefaction susceptibility in loose saturated sands can lead to the amplification of these vibrations or their destructive effects.

3

Site Investigation

This chapter presents a comprehensive summary of the site investigation activities focussing on soil and its properties at the site along with soil profile layering, cross-section of the embankment, sleepers and rails. The objective is to establish a robust dataset for subsequent numerical modelling and validation of railway-induced ground vibrations.

3.1. Ground Conditions

The chosen location is towards the South-East of Utrecht, The Netherlands. The properties of the soil layers up to 9 m are presented in table 3.1, derived through Cone Penetration Test (CPT) conducted near the location. Along with this the CPT results from DINOLoket are also presented below in figure 3.1. The soil is predominantly composed of loose to medium-density sand layers.

Parameter E_{oed}^{ref}, will initially be obtained using mathematical correlations [9] according to equation 3.1 from the CPT data obtained from a test site close to the location. The modulus of elasticity (E) will then be automatically calculated by PLAXIS for the linear elastic material model,based on user-defined inputs of E_{oed}^{ref}. The relative density of the soil at the site will be calculated with the help of multiple equations [38] and an average of them will be used in the calculations. The correlations used for calculating the rest of the parameters are explained in Appendix B. The groundwater table is located at approximately 1 m below ground surface at the site. The RD in Equation 3.1 is the relative density of the material.

$$E_{oed}^{\text{ref}} = 60000\frac{RD}{100}kN/m^2 \tag{3.1}$$

3.2. Measurement

The measurements at the location were carried out in accordance with guideline SBR A 2017 'Damage to buildings' in which the measurement system is formulated. Semi-continuous vibration measurements were carried out at the designated points with piezoelectric accelerometers. The sensors measure vibrations, which are transmitted via an amplifier to a computer where the signals are made visible and stored for future analysis. For each of the measurement points, measurements are taken in three orthogonally opposing directions (Z-vertical, Y-horizontal, parallel to the direction of motion and X- horizontal, perpendicular to the direction of movement).

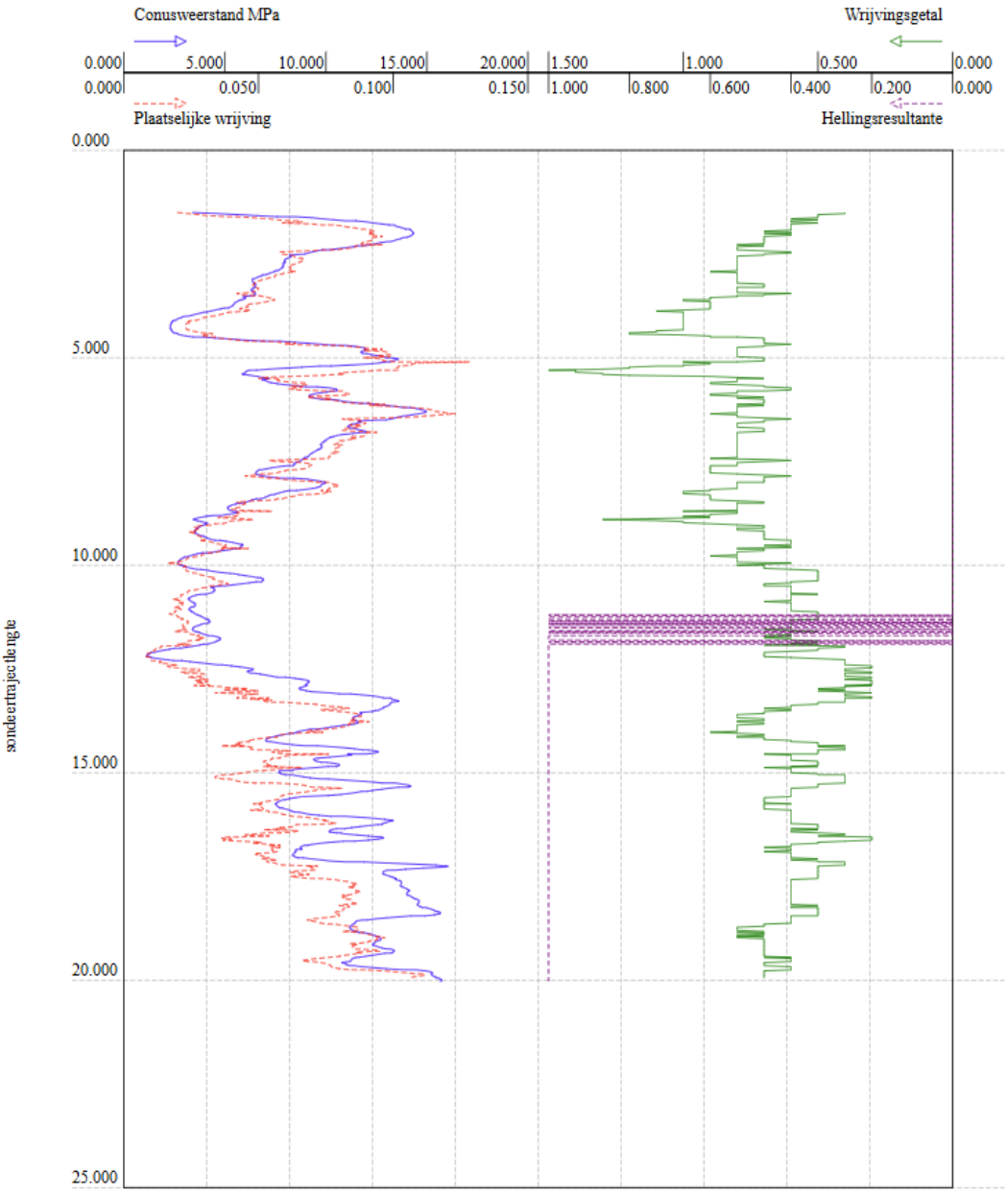

Figure 3.1: CPT from DINOloket

From the report of the conducted measurements, a selected set of points at a particular location will be considered in this work. The set of points lie in line, perpendicular to the rails. Three measurement points (MP) along the line are taken initially for the analysis. Each of them were assigned with names MP1, MP2, and MP3 . Detailed representation of the layout is shown in figure 3.2 below. Buildings and other structures near the location will not be considered in this work to avoid further uncertainties and complications in the model.

3.3. Embankment

The embankment supporting the railway was characterised based on available design documentation in reference with the embankment at the site. It consists of three layers with the compacted sand at the base, then a layer of sub ballast and ballast above it. The cross section

No.	Layer Description	$\gamma_{uns}\ \left[\frac{kN}{m^3}\right]$	$\gamma_{sat}\ \left[\frac{kN}{m^3}\right]$	$\rho\ \left[\frac{kg}{m^3}\right]$	Poisson's Ratio	E_{oed}^{ref} $[MPa]$	Thickness $[m]$
1	Loosely packed sand upper layer	17	19	1732.93	0.22	67.8	1
2	Sand, loosely or moderately packed, upper layer	18	20	1834.86	0.22	49.9	2.5
3	Sand, very loosely packed, weak to extremely silent	17	19	1732.93	0.22	39	2
4	Sand, loosely or moderately packed, lower layer	18	20	1834.86	0.22	34.2	3.5

Table 3.1: Soil Properties at the site

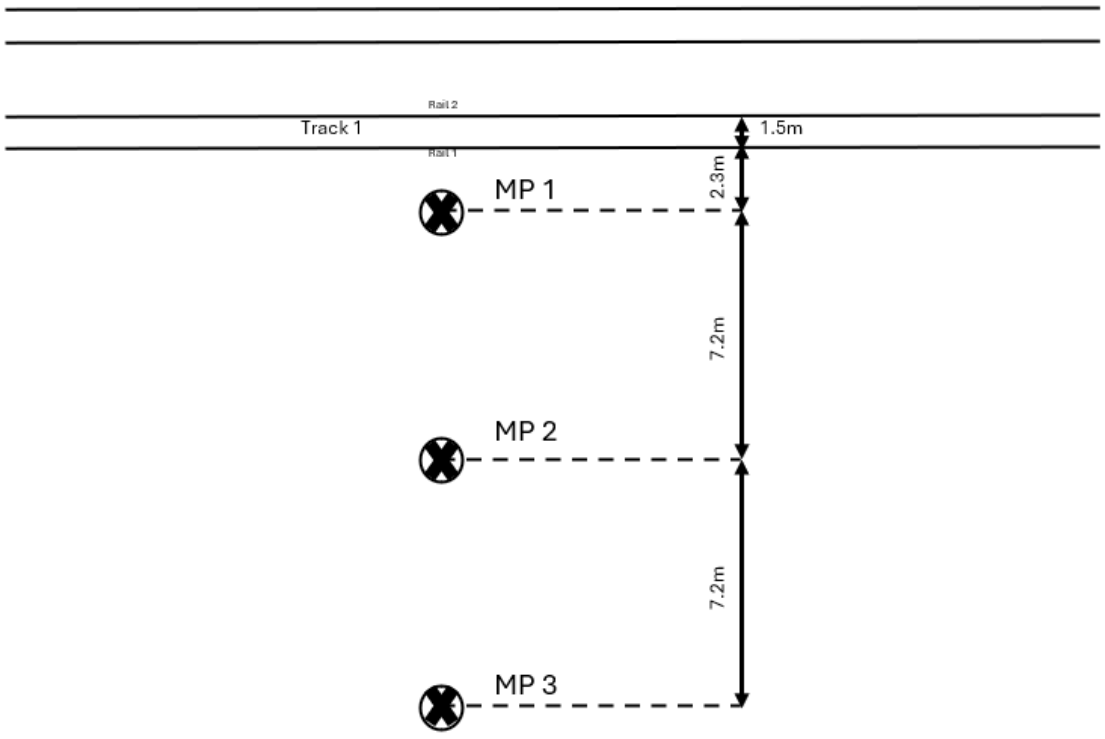

Figure 3.2: Layout of measurement points [30]

of the embankment is depicted in the figure 3.3 is the same as from [30]. Due to the possibility of slight variation in the measurements between the design and implementation, engineering approximations are taken where necessary to establish the geometry and parameters of the

embankment for the numerical analysis. The properties of the materials of the embankment are presented in table 3.2 were adapted from another validated model[30].

	$\gamma \left[\frac{\text{kN}}{\text{m}^3}\right]$	$\gamma_{sat} \left[\frac{\text{kN}}{\text{m}^3}\right]$	$\rho \left[\frac{\text{kg}}{\text{m}^3}\right]$	Poisson's ratio	E [MPa]	G [MPa]	$V_s \left[\frac{\text{m}}{\text{s}}\right]$	$V_p \left[\frac{\text{m}}{\text{s}}\right]$
ballast	16	17	1733	0.15	130	56.52	186.2	290.1
subballast – crushed stone	22	23	2243	0.22	180	73.77	181.4	302.7
compacted sand	20	22	2038	0.3	74.3	28.57	118.4	221.5

Table 3.2: Embankment layers material properties

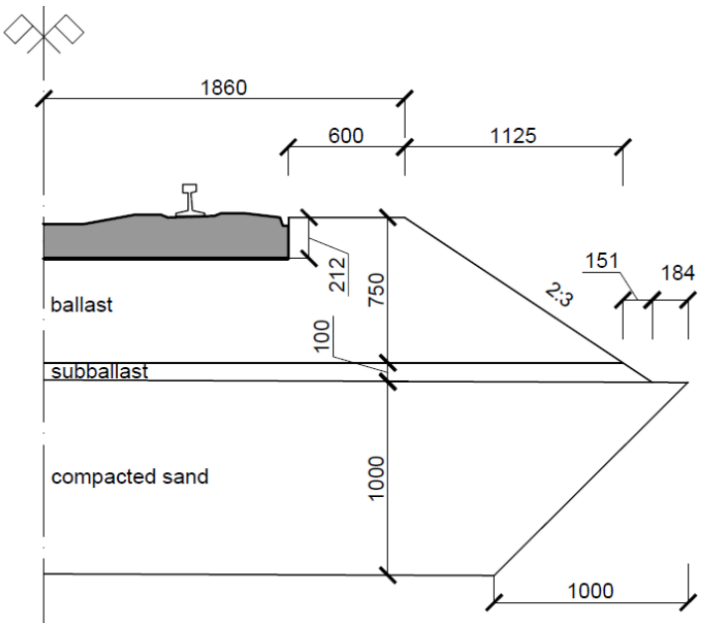

Figure 3.3: Embankment cross section [30]

3.4. Sleeper

A distance of 35 meters to either side of the line of measurement is taken for modelling and analysing. Two types of concrete sleepers are present along the investigated section: NS90 and 14-002, each with distinct mass and geometric properties. Their spatial distribution is non-uniform, with the layout mapped over a 70-meter section. Along the investigated section, to the left of the line of measurement, 12 sleepers of 14-002 and then 47 of NS90 are present. To the right of the line of measurement, there are 22 sleepers of 14-002 and thereafter 36 of NS90.

For modelling purposes, the 14-002 sleeper dimensions are used as a reference, while density variations account for the mass differences between sleeper types. The layout of sleepers in the region of focus is shown in figure 3.4. The properties of the mentioned sleepers are given in table 3.3. Dimensions of 2500 mm x 300 mm 220 mm were chosen to be a standard, having a volume of 0.15 m^3.

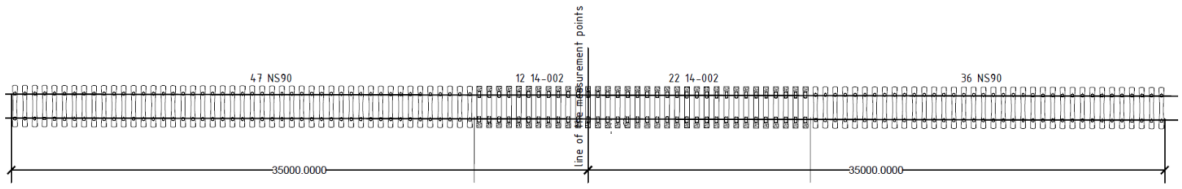

Figure 3.4: Sleeper distribution with the line of measurement

	Length (mm)	Width(mm)	Height (mm)	Weight (kg)
NS90	2520	300	214/175	276
14-002	2500	300	200	369

Table 3.3: Properties of sleeper NS90 and 14-002

3.5. Rails

The rail present at the site has a 54E1 profile, which is equivalent to UIC54 available in PLAXIS. The specifications for UIC54 was taken from the details available in the market. The input parameters for the rail will be discussed in the further sections. The cross section of the rail is represented in Figure A.1 in Appendix A.

3.6. Railpad and Fasteners

Through model calibration, stiffness of the railpad was obtained and is set to 1560 MN/m. As the rule of thumb, in the Dutch train network the stiffness of the railpad should be around 1300 MN/m which is in line with the value obtained by the referenced article [35]. However, if one would decide for modelling the fastener-railpad pair as volume, Equation 3.2 can be used. By proper selection of the parameters, stiffness k can be recreated during numerical modelling process, which will be described in detail in further sections. The approach introduced in the referenced articles cannot be applied to this research because the type and properties of the fasteners are unknown in this case. As a result, accurately adapting the real system into the numerical model is not feasible.

$$k = \frac{EA}{L} \tag{3.2}$$

where L is the height of the railpad and A is the area of the railpad.

3.7. Trains

During vibration measurements, different types of trains passed through the location. The majority of them were passenger trains, and the one that will be focused on in this work will be the loading and vibrations from VIRM (Verlengd interregiomaterieel) trains. They are a series of electric double-deck trains having multiple units and are operated by the Nederlandse Spoorwegen (NS). The loads, configuration and other considered properties will be discussed in the following sections.

4

Numerical Modelling

Numerical modelling is a computational approach that is used to simulate complex physical phenomena by solving mathematical equations that describe system behaviour. Unlike experimental methods, it allows for cost-effective parametric studies and scenario testing without physical constraints. In geotechnical engineering, numerical models predict soil-structure interactions, stress distributions, and wave propagation dynamics. For railway vibrations, these models simulate how dynamic loads from trains propagate through the track, embankment, and subsoil, enabling the assessment of environmental impacts and mitigation strategies [43] [54].

This chapter focusses on the numerical modelling strategy adopted to simulate railway-induced ground vibrations, focussing on the translation of field and material data into a computational framework. Detailed explanation for the choice of the software, the material models, size of the model, mesh, time step, and the loading mechanisms will be provided. Initially, the model is considered to be elastic, which is borrowed from the reference work [30] to build a validated model and study the loading mechanisms. In the next step, the model will be adapted to have non-linear material behaviour to explore the effect of water table fluctuations on the transfer of vibrations.

4.1. Size of the model

The size of the model was implemented in accordance with works done by [20] and [30] and incorporating the necessary modifications to suit the objectives of this work. The major reason for using this reference is that the authors employed the same numerical modelling tool, namely PLAXIS 3D, in their work. In the work published by [20], author investigated distances up to 45 meters away from the track, and to avoid spurious reflections of waves from the model boundaries, they were extended beyond the region of interest by 20 meters in the X direction and by 20 meters in the Y direction.

In this work, the region of interest is up to 20 m away from the track. Considering the methodology implemented by [20], the dimensions of the model approximates to 70 m x 40 m x 9 m, but it was extended in the Y direction by 15 m to further take into account the chances of spurious reflections from the boundaries. The depth considered in this work was 9 meters. The soil layers were cut at a depth of 9 m considering two of the following reasons. Firstly, it was the base of one of the soil layers and secondly, the reflection coefficient was calculated for the bottom layers 3 and 4 and the value of R came out to 0.044. Thus, showing very little

to no reflection. The calculation is shown in Appendix B. Thus, the soil layer can be safely cut at the mentioned depth. The model employed for this research work is presented in figure 4.1. The top view and the side view of the model is represented in Figure 4.3 and Figure 4.2 respectively.

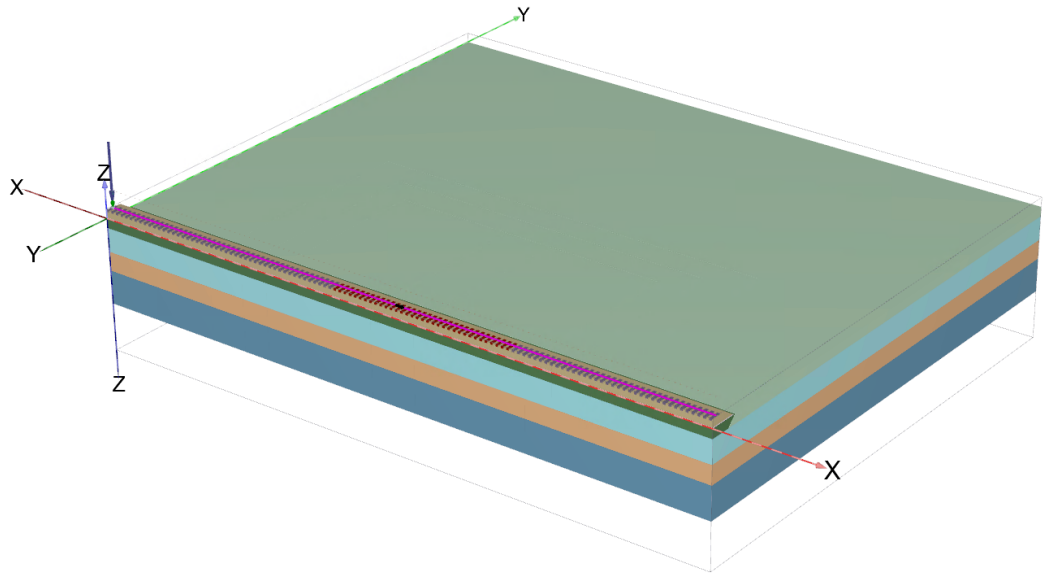

Figure 4.1: Overview of the implemented model-70m x 55m x 9m

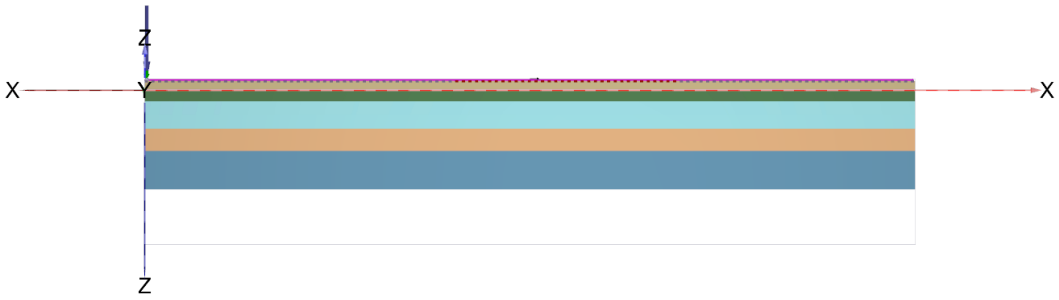

Figure 4.2: Side view of the model

4.2. Boundary Conditions

The goal when setting boundary conditions is to ensure that the model is sufficiently large to prevent any artificial influence from the model boundaries on the simulation results. However, balancing accuracy with computational efficiency is crucial, as larger models lead to longer calculation times and increased memory usage. PLAXIS 3D automatically applies a set of standard fixities to the boundaries of the geometry model, but they can be modified as per the user's need. Static boundary conditions apply to both deformations (displacements) and hydraulic (groundwater flow) aspects of the model. Water conditions can be defined via bore-holes, which specify information on soil layer positions and water table.

For dynamic calculations, special boundary conditions are required because the real soil medium is semi-infinite, and standard fixities would cause artificial wave reflections at the boundaries. These dynamic boundaries are designed to absorb or account for outgoing wave energy.

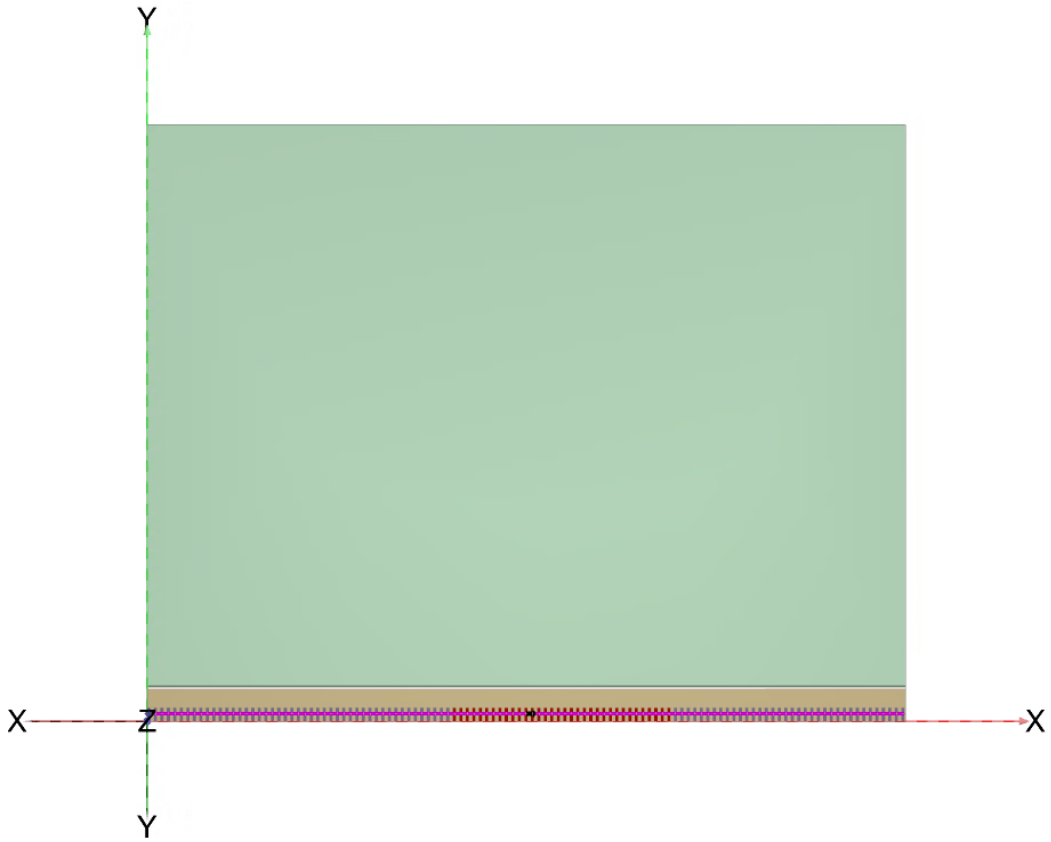

Figure 4.3: Top view of the model

To replicate realistic wave propagation and avoid artificial reflections, a combination of boundary conditions was implemented:

- **XMin/XMax** (sides): Viscous boundaries to absorb outgoing wave energy by simulating viscous dampers (dashpots).
- **YMin** (front): Fixed, exploiting symmetry to reduce computational cost by modelling only one half of the system. This boundary leads to a full reflection of downward-propagating waves.
- **YMax** (rear): Viscous, to prevent wave reflection from the far edge of the domain.
- **ZMax** (top): Free, simulating the ground surface.
- **ZMin** (bottom): Viscous, justified by the continuation of similar soil properties below the model depth.

This setup allows for the correct simulation of both the symmetry of the problem and the dynamic behaviour of the soil-structure system.

4.3. Embankment and Soil layers

The embankment and soil layers were defined through the use of boreholes within the drawing area where information about the position of soil layers and water table is provided. The soil is modelled using 10-noded tetrahedral elements. PLAXIS 3D can automatically interpolate between multiple boreholes to derive the positions of non-horizontal soil layers, even if they

are discontinuous or have varying thicknesses. To simulate soil behaviour, a suitable material model and parameters are assigned to the geometry. Water conditions are crucial, as PLAXIS 3D is based on effective stress principles. They are defined within the borehole information. The head value set in a borehole defines the phreatic level (water table), which is then used to calculate initial effective stress states.

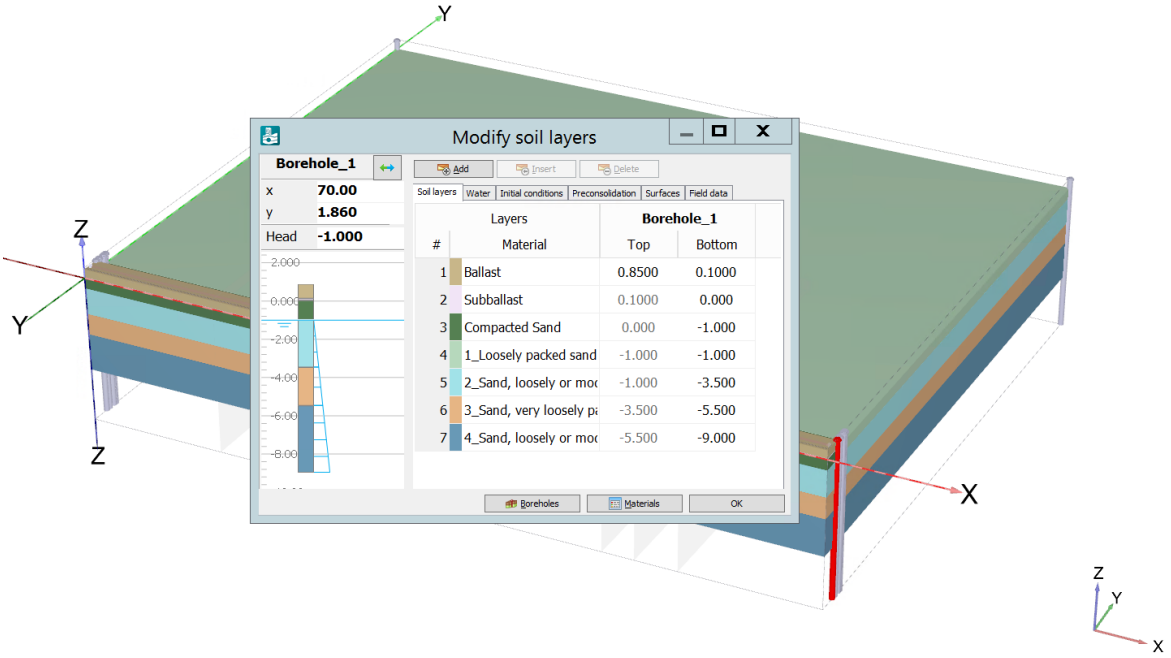

Figure 4.4: Borehole input for modelling (Selected borehole in red).

4.4. Sleepers

The sleepers in this model were modelled with the same geometry, but varying densities to account for the variation at the site. The dimensions of the modelled sleepers were 2500 mm x 300 mm x 200 mm. The centre to centre distance between them is 0.6 m. The sleeper is raised by 5 cm from the embankment to mimic site conditions and also to make sure that the rails are not in contact with the embankment directly. This would help to ensure that the rails are discretely supported and the transmission of loads occurs only though the sleepers. It was chosen to model the sleeper using 10-node tetrahedral elements, to ensure the sleeper to be a volumetric object.The interface interaction between the concrete sleeper and the embankment is reduced to 80% to incorporate real-world conditions. The properties of sleepers are presented in Table 4.1.

	γ_{unsat} [kN/m^3]	Rayleigh α [-]	Rayleigh β [-]	R_{inter} [-]	E' [kN/m^2]	ν [-]
NS90	18.30	1.67	0.000053	0.8	30 000 000	0.2
14-002	24.20	1.67	0.000053	0.8	30 000 000	0.2

Table 4.1: Properties of sleepers NS90 and 14-002 for modelling

4.5. Railpad and Fictitious plate

The railpad is a crucial component in the system, particularly concerning the connection between the rail and the sleepers. The railpad was modelled as a volume element to incorporate the rotational degree of freedom which is not present in the plate element in the software. This

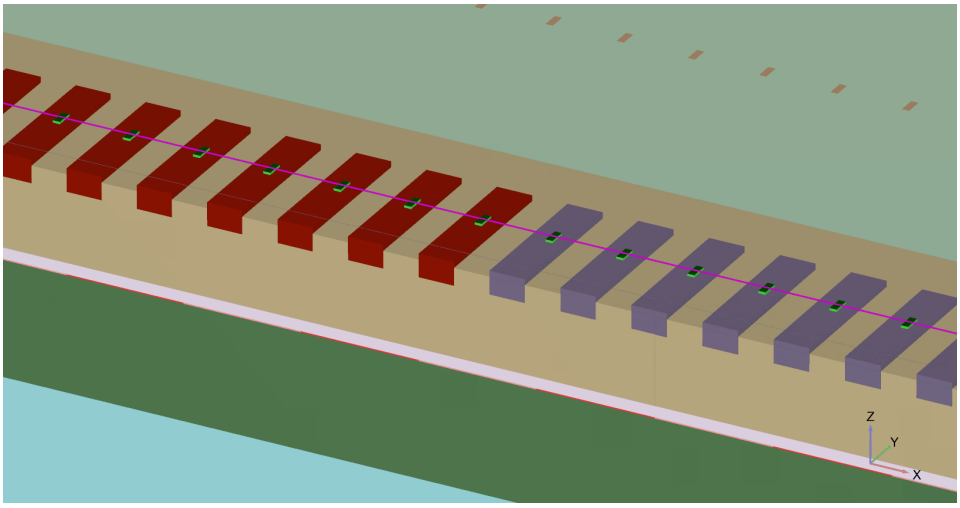

Figure 4.5: Schematic view at the sleeper and railpad in the 3D model

Figure 4.6: Side view for the sleeper and railpad

approach aimed to simulate a hinge mechanism as closely as possible by significantly reducing the railpad's area to approximate a discrete spring-dashpot representation. The modelled railpad has dimensions of 15 cm x 6 cm x 2 cm. It is considered massless [30]. An average stiffness value for the Dutch railway network, 1300 MN/m, was assumed for the railpad. Using the formula 4.1

$$K = \frac{E \cdot A}{L} = \frac{1300000kN/m \cdot 0.02m}{0.06 \cdot 0.15m^2} = 2.89 \cdot 10^6 kN/m^2 \tag{4.1}$$

$$E = 2.89 \cdot 10^6 kN/m^2 \tag{4.2}$$

where L is the height and A is the area, the Young's modulus (E) was calculated to be $2.89 \cdot 10^6 kN/m$.

A "fictitious plate" (also referred to as a plate element) is placed on top of the railpad. Its primary function is to distribute the load from moving point load evenly to the railpad, preventing loads from being applied only locally to the railpad. This ensures that the rail, modelled as a beam, is discretely supported by the railpad. The fictitious plate has a thickness of 0.03 m, a width of 0.06 m, and a length of 0.15 m. It has a very high Young's modulus of 400,000,000 kN/m², which is 138 times stiffer than the railpad and twice as stiff as steel. This high stiffness ensures

that the plate does not bend, but effectively transfers the entire load to the railpad in a more evenly distributed manner.

	d [m]	w [m]	l [m]	γ [kN/m^3]	E [kN/m^2]
Fictitious plate	0.03	0.06	0.15	1.00	400 000 000

Table 4.2: Properties of fictitious plate

4.6. Rail

The rail is primarily modelled as a 3-noded beam element. This type of element is selected for its capability to represent slender objects that possess significant flexural and axial rigidity. Each node of the beam element is assigned six degrees of freedom, which include three translational movements (ux, uy, uz) and three rotational movements (φx, φy, φz). The local axes of this 3D beam are defined to indicate the directions of its cross-section properties. A schematic view of the rail in the 3D model typically shows it as a pink line. The rail profile implemented in the model is 54E1, which is equivalent to UIC54. These specifications are based on the information available from the site and the manufacturer data. The rail is designed to be discretely supported by the railpad. The input for the rail is as mentioned in Table 4.3.

	A [m^2]	I_2 [m^4]	I_3 [m^4]	γ [$\mathrm{kN/m}^3$]	E [$\mathrm{kN/m}^2$]
UIC54	$6.877 \cdot 10^{-3}$	$4.190 \cdot 10^{-6}$	$0.0234 \cdot 10^{-3}$	78.5	200000000

Table 4.3: Properties of the rail used in modelling

4.7. Train model and Load

The considered section of rail has multiple types of trains passing through it. The type of train focused on in this study will be the VIRM (Verlengd InterRegio Materieel), the intercity passenger trains in The Netherlands. This was because the majority of trains that passed through the section was the VIRM. Train specification were taken from literature and the loads were found to be approximately 21.3 tonnes. Considering the symmetry of the model, half of the load was used, which amounted to 105.5 kN on individual wheels of the trains at maximum. During modelling, only intermediate carriages were considered as their exact configuration changed with different trains. An exemplary image of the train is represented in Figure 4.7 and the schematic sketch of the wheel distances is presented in Figure 4.8. One of the objectives of this work is to understand how the moving load method is implemented in the software and its suitability to simulate the movement of trains. The loads from the train can be broadly divided into two:

Quasi-static Load Component: This component represents the train's weight. For the symmetric model used in this research, the axle load is assumed to be 105.5 kN, derived from the VIRM train type which has a maximum load of 21.3 tonnes. This component accounts for the static part of the train's weight.

Dynamic Load Component (Sleeper Passing Frequency): This oscillatory part of the load is related to the sleeper passing frequency, which is calculated as the train velocity (V) divided by the distance between sleepers (a). For a train running at 130 km/h, with a sleeper spacing of 0.6 m, the frequency of oscillations is approximately 60 Hz.

The quasi-static load amounted to 105.5 kN on individual wheels of the trains at maximum and the dynamic oscillatory loads are set to be 5% of the axle load. This value was chosen as an educated guess, aiming not to exceed approximately 10% of the dead load.

Figure 4.7: Exemplary image VIRM train type [50].

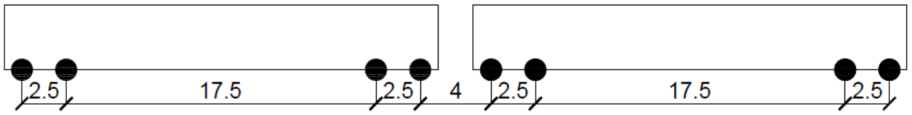

Figure 4.8: Wheel distances in VIRM train implemented in the numerical model.

4.8. Mesh and Time step

To effectively simulate train-induced ground vibrations using finite element models, careful consideration must be given to both the mesh design and the time step of the analysis. These parameters significantly influence the accuracy of the results and the computational effort required [3] [12]. A refined mesh with smaller elements generally leads to more accurate solutions. However, excessively small elements or a very dense mesh can lead to high computational demand, requiring significant computer memory and extending calculation times, sometimes by hours or even days for 3D models. For 3D analyses, computational effort is a primary disadvantage, directly related to the size of the model and the number of elements and nodes [13].

The dominant frequency from the site data was shown to be near 60 Hz and to capture it, the mesh and time step should be calculated accordingly.

$$\Delta l = \frac{V_s}{f} \tag{4.3}$$

where Δl is the wavelength, V_s is the shear wave velocity and f is the upper frequency limit. Based on equation 4.3 the wavelength cam out as:

$$\Delta l = \frac{180 m/s}{60 Hz} = 3m \tag{4.4}$$

Elements must be small enough to accurately represent wave phenomena. A common guideline is to have at least six points per wavelength, with some researchers suggesting 9-10 points or more for higher accuracy [54]. The maximum element size is often determined by the slowest shear wave velocity in the soil and the upper frequency limit of interest for the vibrations. The time step is chosen to ensure that a wave front does not travel a distance larger than the

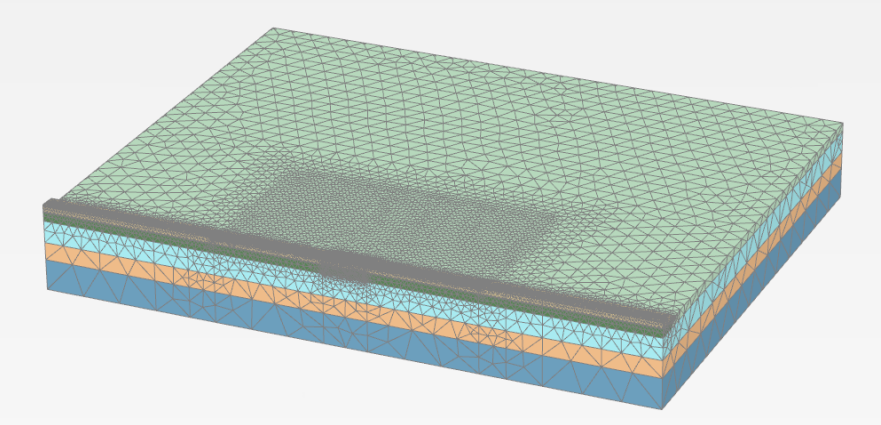

Figure 4.9: Mesh in PLAXIS 3D

minimum dimension of an element within a single step. A smaller time step generally yields more accurate results, but significantly increases computational effort. PLAXIS has 10-node tetrahedral elements, which have 3 modes at the edges. Considering 4 elements to capture the wave properly, the element size should not be larger than $3m \div 4 = 0.75m$. With the help of the mesh function, and specifying it to use 'very fine' as the coarseness and additionally adding a coarseness factor of 0.3 to the input, the wave can be sufficiently captured. The calculation is as follows:

$$2.356 \cdot 0.3 = 0.706m \tag{4.5}$$

This makes sure that the frequency range up to 60 Hz is captured with sufficient accuracy and higher frequencies with less accuracy, taking into account the computational effort and time needed. The region of interest is located in the middle of the model and has dimensions of 30 m x 20 m and this section is meshed in such a way to capture the frequency of interest and the rest to be with a larger mesh size.

In addition to the mesh size, the time sampling must also be appropriately adjusted. For this, approximately 9 to 10 points are necessary; therefore, to capture a 60 Hz frequency wave, the time step should be as per 4.6. An exemplary representation of the meshing performed in PLAXIS is shown in Figure 4.9.

$$Timestep = \frac{1}{600} = 0.001667 \tag{4.6}$$

4.9. Stages of Simulation

The simulation of railway-induced ground vibrations is typically performed through a series of sequential calculation phases. This staged approach allows for realistic modelling of construction processes and the subsequent application of dynamic loads, ensuring numerical stability and accuracy.

- **Initial Phase:** This is the first and fundamental phase in any PLAXIS 3D model. Its primary purpose is to generate the initial stresses within the soil layers, typically under gravity loading. The K0 procedure is often preferred for defining initial stresses, especially when the ground surface is horizontal and the soil layers are parallel to the surface, as it accounts for the soil's loading history. During this phase, all soil strata are defined

and active. For some analyses, an elastic material model is assigned to establish initial stresses and hydrostatic pore pressures before switching to more advanced constitutive models in later stages. [12][66].

- **Subsequent Static Phases:** Following the initial phase, non-dynamic parts of the model are activated sequentially in various static phases, replicating real-life construction stages. The general rule is to activate one element or a specific group of elements at a time. Examples of elements activated in these static phases include embankment layers,railway track components, and structural elements. These phases typically use a ”Plastic” calculation type for deformation analysis, performed according to the small deformation theory. Sometimes, excavations of stabilised soil are also modelled sequentially in these static phases. Displacements are often reset to zero before the dynamic loading phase to isolate the effects of the train passage.
- **Dynamic Phase(s):** This is the stage in which the loadings of the moving train are applied and the dynamic response of the system is analysed. The calculation type is set to ”Dynamic”. Moving loads are simulated using a dedicated function in PLAXIS 3D, where the software interprets the load’s location over time based on its velocity. Previously, moving loads were simulated using methods like ”triangular pulses,” where static point loads were activated and deactivated with a time offset, or by using auxiliary software like PROKON to calculate shear forces as dynamic multipliers. The simulation duration typically ranges from a few seconds (e.g., 2.75 to 3 seconds) for model calibration, as longer durations might increase the calculation time significantly (around three times) without substantial improvement for the primary area of interest. Simulations are sometimes divided into smaller time intervals to prevent data loss due to unforeseen software errors.

4.10. Results from Simulations

PLAXIS 3D primarily outputs data in time domain, but for many practical applications, particularly in vibration analysis, time-domain data are converted into the frequency domain using mathematical tools such as the Fourier Transform. Frequency domain analysis helps identify the dominant frequencies of the vibrations generated by railway traffic. This is critical for understanding the source mechanisms and for assessing the potential for resonance in nearby structures or building components. Different wave types (P-waves, S-waves, Rayleigh waves) have distinct propagation characteristics and energy content across frequencies. Analysing data in the frequency domain provides insight into how these waves propagate, attenuate with distance, and how their energetic content shifts towards lower frequencies further away from the source. Field measurements of ground vibrations are frequently processed and presented in the frequency domain (e.g. power spectral density, Fourier amplitude spectra). Converting numerical results from PLAXIS 3D to the frequency domain allows a direct and meaningful comparison with experimental data, which is essential for validating the accuracy and reliability of the numerical model.

4.10.1. Time to frequency domain transformation

This research utilizes a standardised signal processing , implemented in Python, to automate the post-processing of ground vibration data collected from field accelerometer measurements and the simulations. The developed script is specifically tailored for engineering applications, where understanding the frequency content and intensity of ground motions is essential for vibration assessment. The methodology provides a robust and repeatable framework for extracting engineering insights from large datasets, ensuring data integrity and efficiency throughout

the analysis process. The main steps are as follows:

- **Data Acquisition and Preprocessing:** Raw acceleration-time data files are automatically imported from a specified directory. The import routine supports both period and comma decimal separators to ensure international compatibility and precise conversion to floating-point values.
- **Digital Filtering and Signal Conditioning:** A fourth-order low-pass Butterworth filter (cutoff at 100 Hz) is applied in a zero-phase manner to remove high-frequency noise and preserve the temporal accuracy of the measured signals. This process, implemented in the lowpass filter function, serves to eliminate high-frequency noise and non-physical artifacts, thereby maintaining fidelity to the actual vibrational phenomena of interest while avoiding aliasing in subsequent calculations. The use of zero-phase filtering ensures that no phase distortion is introduced, preserving the temporal alignment of key waveform features.
- **Time-to-Velocity Transformation:** The filtered acceleration data are numerically integrated to obtain the velocity time history, with the initial velocity set to zero, reflecting typical conditions in ground motion monitoring. This transformation is foundational in vibration analysis, as velocity spectra offer complementary insights into energy transmission and soil-structure interaction dynamics beyond those achievable from acceleration alone.
- **Frequency-Domain Analysis:** Both acceleration and derived velocity signals are transformed into the frequency domain using the Fast Fourier Transform (FFT), producing normalised amplitude spectra within the 0–100 Hz range relevant to geotechnical applications in the case of ground-borne vibrations from railways.

5

Calibration and Validation

This chapter will focus on calibration, validation, and the results obtained from the simulations. It begins with the presentation of the measurement signals that will be used for calibration and validation of the linear model.In addition, the validated model and its associated simulation results will be presented and discussed. The results from measurement points 1 (MP1),2(MP2) and 3(MP3) are presented, but the points MP2 and MP3 will only be discussed in detail. The reason for the focus on measurement points 2 and 3 is due to the uniformity of the mesh in the region. MP1 is present at a location where the ballast, subballast, and compacted sand layer meet; thus having a complicated system of meshes at the location which makes the interpretation of results complicated, and additionally the interface region brings in additional complexity and variation in the obtained results.

5.1. Measurement Data

The measurement data for this research are a set of acceleration-time history data measured from the location of interest during the passage of trains. The measurement signals were filtered to include only the signals acquired during the passage of the VIRM trains. Two of the measurement signals from the location is presented in the Figure 5.1 below.The graph shows the zoomed-in version of the raw data, between -2m/s^2 and 2m/s^2 The raw measurement data from the site had unusual peaks at measurement point 1, and the acceleration in time domain graphs are in Appendix C

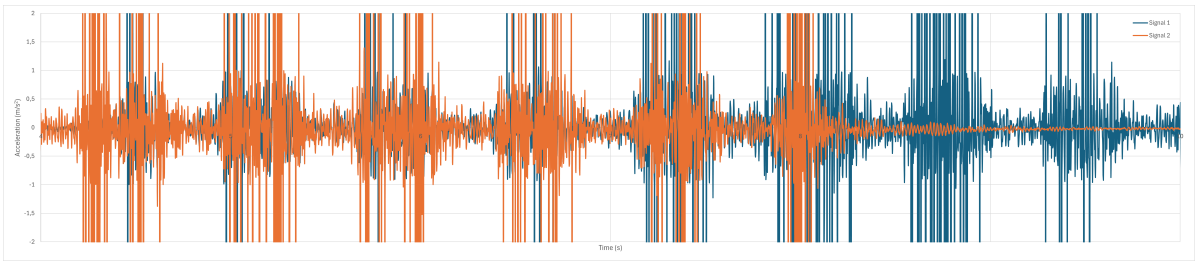

Figure 5.1: Measured acceleration at MP1 for two recorded train passages

From the acceleration-time graph, excessive peaks were observed and they are usually due to vehicular effects, like flat wheel or other site-specific irregularities. By comparing such excessive high peaks, abnormalities related to the train can be observed and limited. The measurement result from the nearest point to the rail is presented in figure 5.1. From figure 5.1

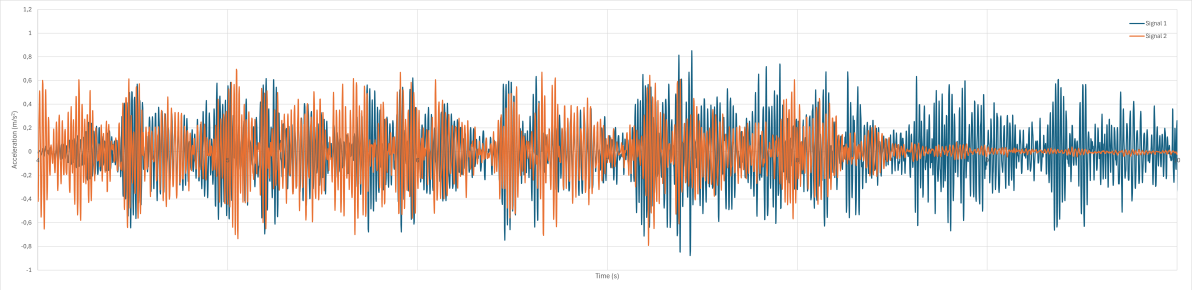

Figure 5.2: Measured acceleration at MP2 for two recorded train passages

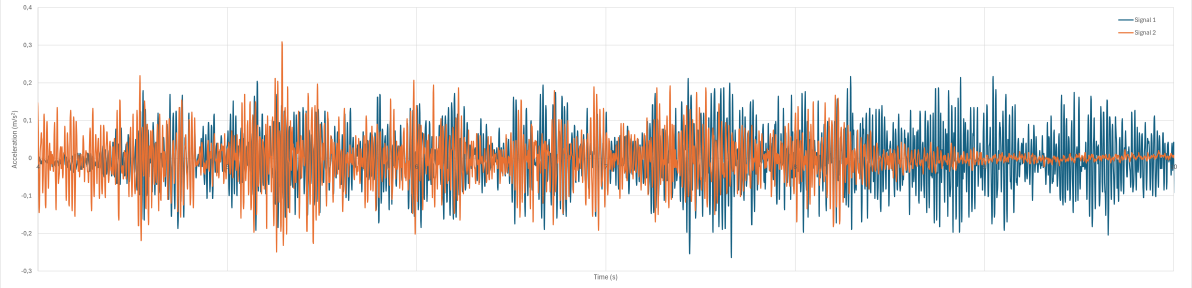

Figure 5.3: Measured acceleration at MP3 for two recorded train passages

and comparison of it with the rest of the measurement results of acceleration in time domain, the high peaks of values greater 2m/s^2 and lesser than -2m/s^2 can be disregarded. This can be done since it was observed that such high peaks were not visible in the signals when other trains passed through the same location. This can be attributed, the proximity of the sensors to the rail, to local effects and/or with particular non-repetitive axle load. It is also known that wheel irregularities enhance higher frequencies in the near-field region and can cause very high acceleration peaks in the measurement data. Thus it is concluded that the high peaks were due to irregularities from the wheel or other site effects. Additionally the measurement point 1 (MP1), closest to the rail is of less importance in this study and the measurement points 2 (MP2)and 3 (MP3) are investigated in detail to learn about the transfer of vibrations through the soil from railways.

A Fast Fourier Transform analysis was performed on the acceleration-time data from the site to obtain the frequency distribution of the data. The graphs of those are shown below.

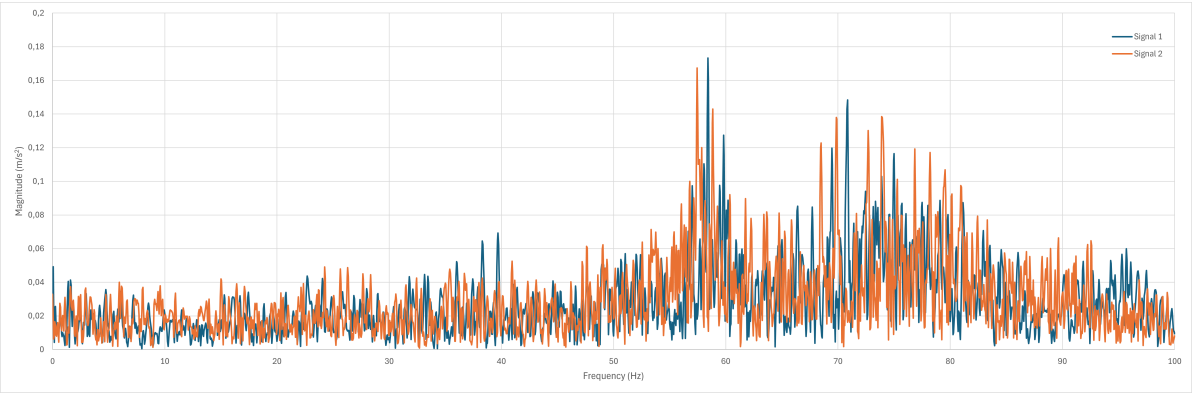

Figure 5.4: Frequency spectrum at MP1 for 2 train passages

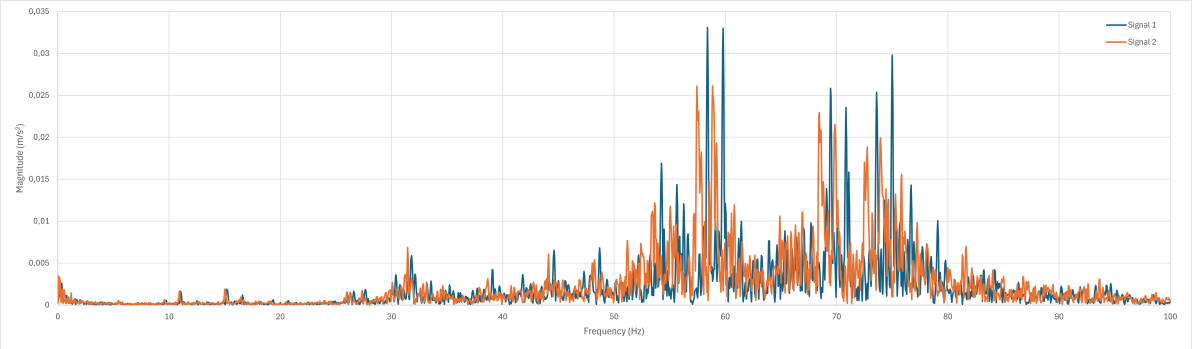

Figure 5.5: Frequency spectrum at MP2 for 2 train passages

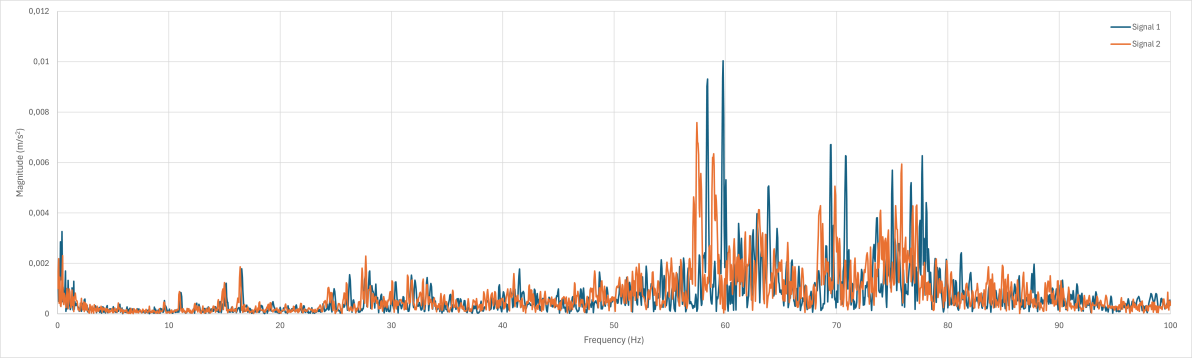

Figure 5.6: Frequency spectrum at MP3 for 2 train passages

	MP1	MP2	MP3
Acceleration a_z [m/s^2]	1.6 - 2	0.6 - 0.8	0.2 - 0.25
Frequency range (the highest magnitude) [Hz]	55 - 100	55 - 80	55 - 80

Table 5.1: Range of expected values from the numerical simulations based on available signals

5.2. Model Input and Results

In this work, the initial step is to prepare a similar model with parameters calculated from a CPT measurement nearby and to calibrate and validate it against the data obtained from the site. The whole process is split into three steps:

1. At first, the model with the linear elastic material model was analysed and the results are interpreted in time domain and frequency domain.
2. The second step involves the modification of the model such that the embankment has linear elastic material model and the soil layers have a non-linear, Hardening Soil with small strain stiffness material model (HSsmall).
3. Finally, all the materials except the sleepers, railpad and fasteners and the rail are modelled with HSsmall material model and calibrated and validated with the site data.

The parameters used as input for various soil layers is as given in Table 5.2 below:

5.2.1. Linear Model (M1)

A model similar to the reference model was created with linear elastic material model and analysed with three dimensional FEM and the results will be compared with the data obtained from the site. The parameters for the linear model was as mentioned in table 3.1. A maximum

	E_{oed}^{ref} (MPa)	E_{50}^{ref} (MPa)	E_{ur}^{ref} (MPa)	G_{o}^{ref} (MPa)	$\gamma_{0.7}$
Compacted Sand	40.2	40.2	203.3	136.8	8.71E-5
Layer 1	67.8	67.8	149.6	116.5	1.17E-4
Layer 2	49.9	49.9	116.9	104.2	1.35E-4
Layer 3	39	39	102.1	98.6	1.43E-4
Layer 4	34	34	120.6	105.6	1.33E-4

Table 5.2: PLAXIS 3D Input Parameters

damping percentage of 10% was taken and cross-referenced with the reference model and used in the model. The damping parameters used for the model is represented in Table 5.3 The acceleration time graph is compared first and is shown in figure 5.7 to figure 5.9.

	α	β
Sleeper	1.257	3.2E-4
Ballast	8.93	5.0E-3
Subballast	7.74	8.0E-3
Compacted Sand	0.980	7E-6
Layer 1	0.98	7E-6
Layer 2	0.98	5E-5
Layer 3	1.20	5E-5
Layer 4	1.20	5E-5

Table 5.3: Damping parameters for the Linear model (M1)

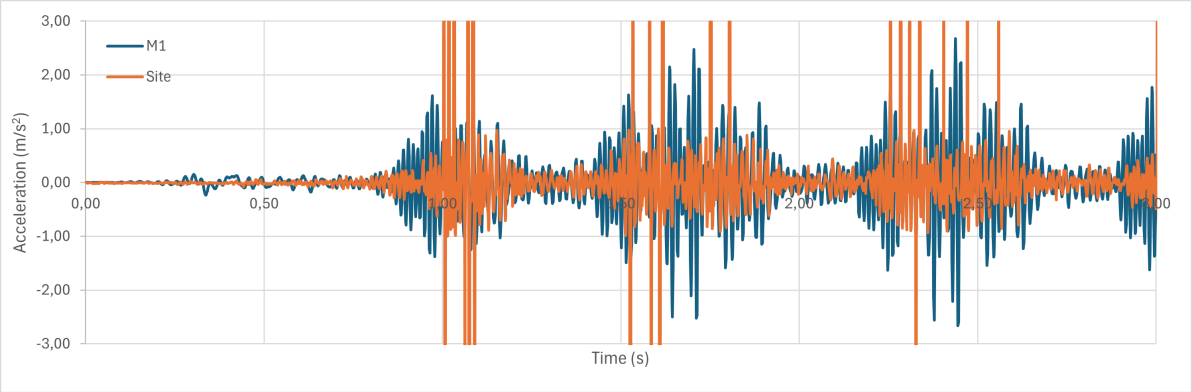

Figure 5.7: Comparison of site and M1 simulation data at MP1 in time domain

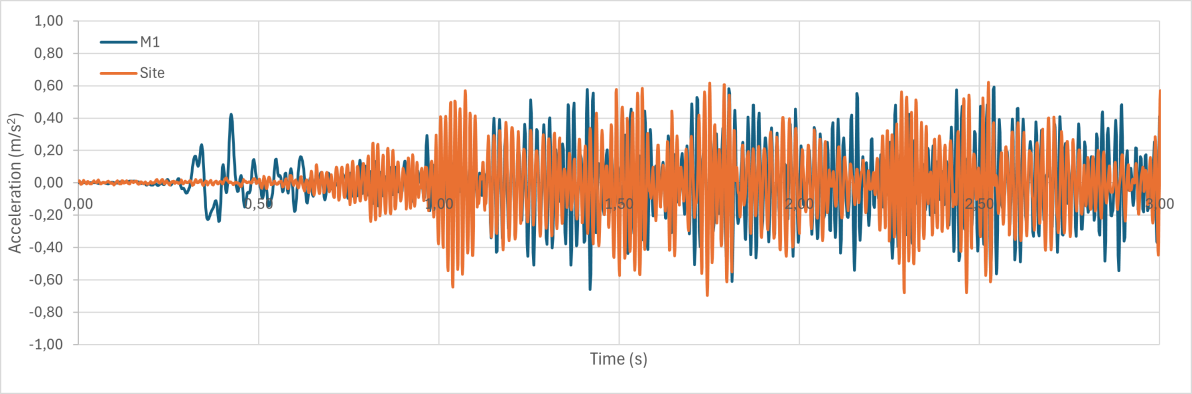

Figure 5.8: Comparison of site and M1 simulation data at MP2 in time domain

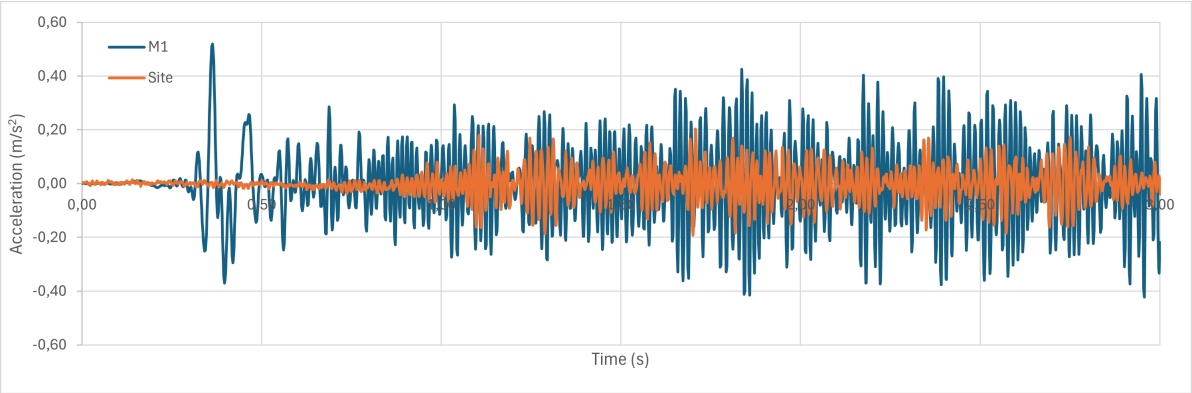

Figure 5.9: Comparison of site and M1 simulation data at MP1 in time domain

From the graphs, it is observed that the model M1 resembles with the pattern of acceleration. It must be noted in the results that the magnitudes are higher than that of the site. This is due to the approximations and assumptions used in modelling which resulted in the variation. The acceleration values are in the same range of expected values at the distance 9.5 m from the rail. The acceleration data in time domain for the simulation resembled the pattern which clearly showed the loading due to the movement of the wheels of the train. The range of magnitudes of acceleration was closer to the site data at 9.5 m from the rail and overestimated at 16.7 m. The variation in results in the simulations are attributed to the unknowns at the site, the exact travel path length, the utilities underneath, etc. to name a few. But, these results provide a representation as to how the vibrations travel through the soil.

For an in-depth understanding and the functioning of the model (M1), an FFT was performed, and the data in the frequency domain is also compared. It was observed that the magnitudes showed similarity in pattern but higher than those observed from the site, except near 50 Hz where a higher peak was seen, which was absent in the site data. The magnitudes in frequency domain are higher and are attributed to the assumptions made during the modelling and the presence of uncertainties at the site. The uncertainties at the location were not included and the soil was also considered isotropic, thus leading to higher peaks.

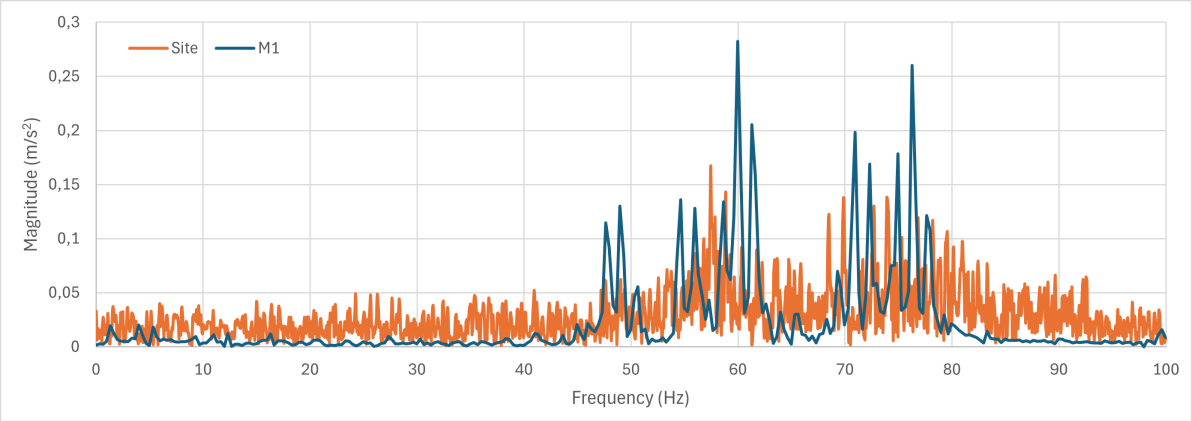

Figure 5.10: Comparison of site and M1 simulation data at MP1 in Frequency domain

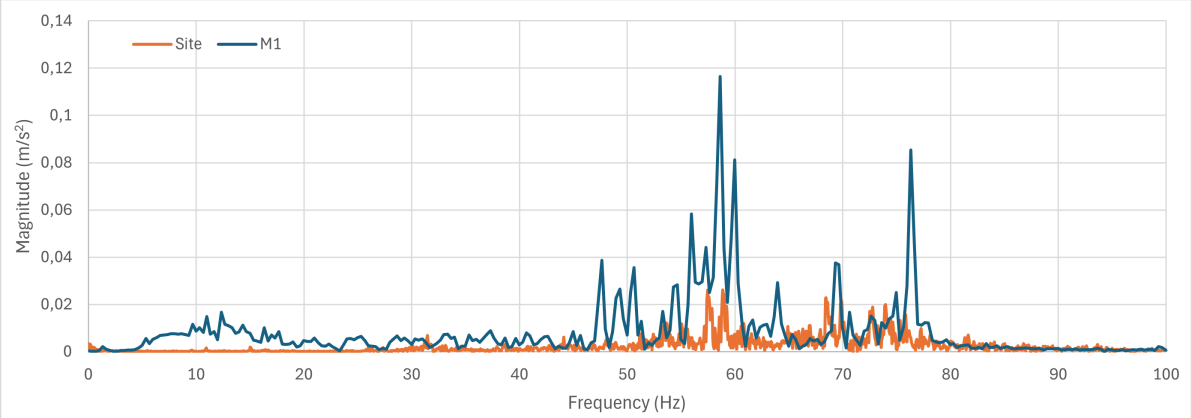

Figure 5.11: Comparison of site and M1 simulation data at MP2 in Frequency domain

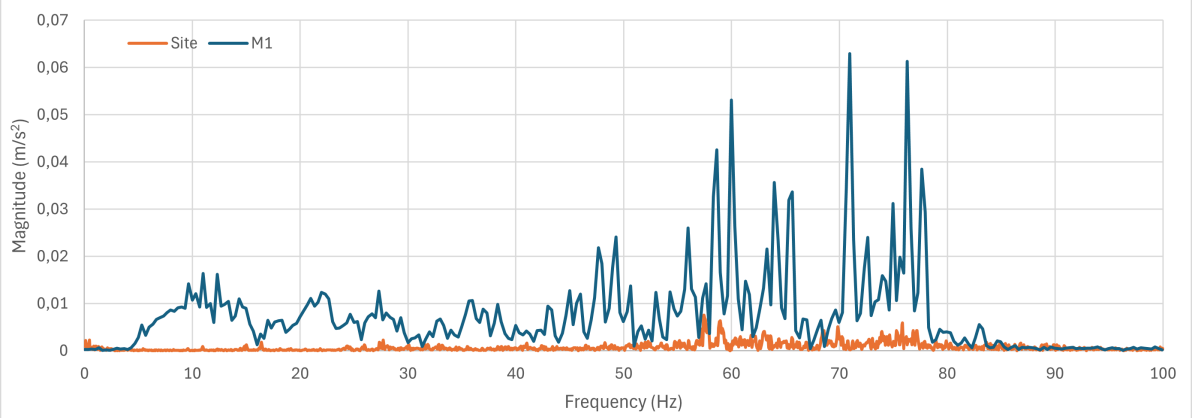

Figure 5.12: Comparison of site and M1 simulation data at MP3 in Frequency domain

Variation in Train Velocity

After the initial linear model was studied, a few simulations were performed where the velocity of the train was varied from 110 kmph to 150 kmph to investigate its effect in the dominant frequency range and the magnitude of acceleration. The acceleration measured at the measurement points 1, 2 and 3 which are 2.3 m, 9.5 m, and 16.7 m respectively from the rail in time domain is presented in figures 5.13 to 5.15.

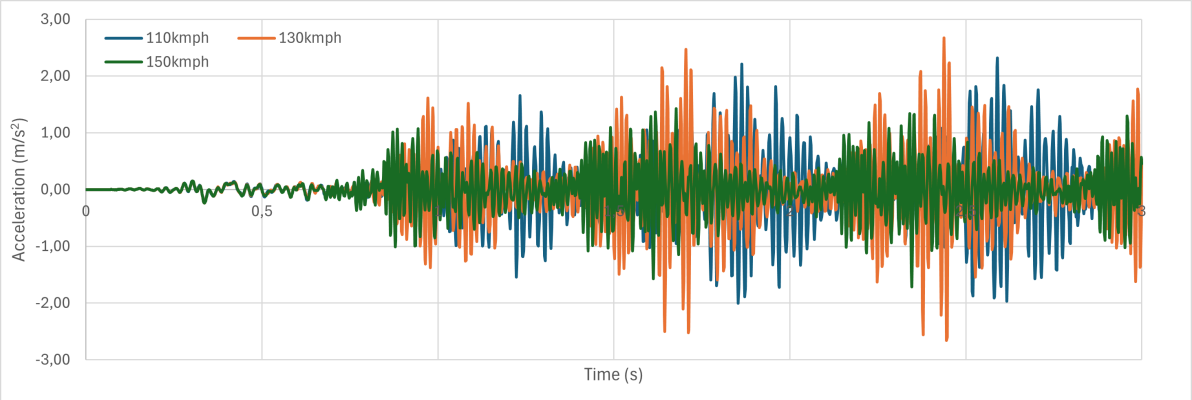

Figure 5.13: Comparison of acceleration at MP1 in time domain for varying velocity

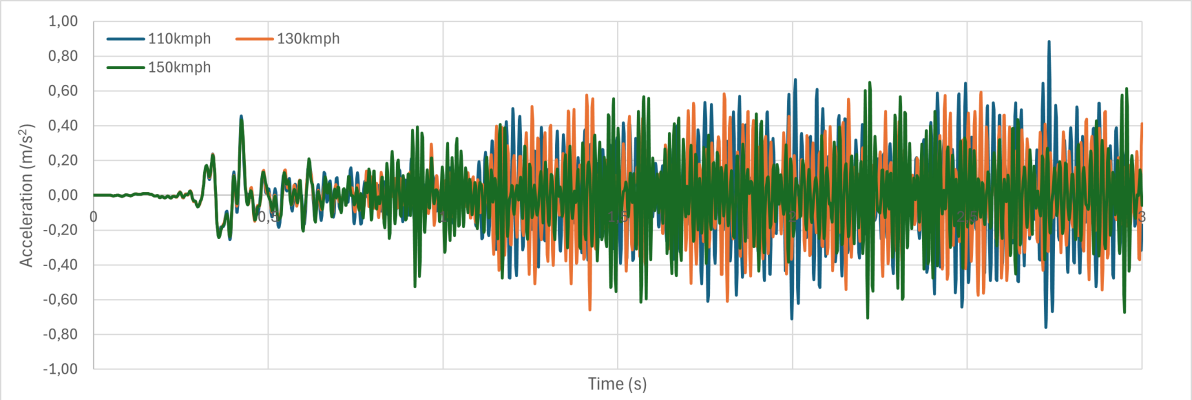

Figure 5.14: Comparison of acceleration at MP2 in time domain for varying velocity

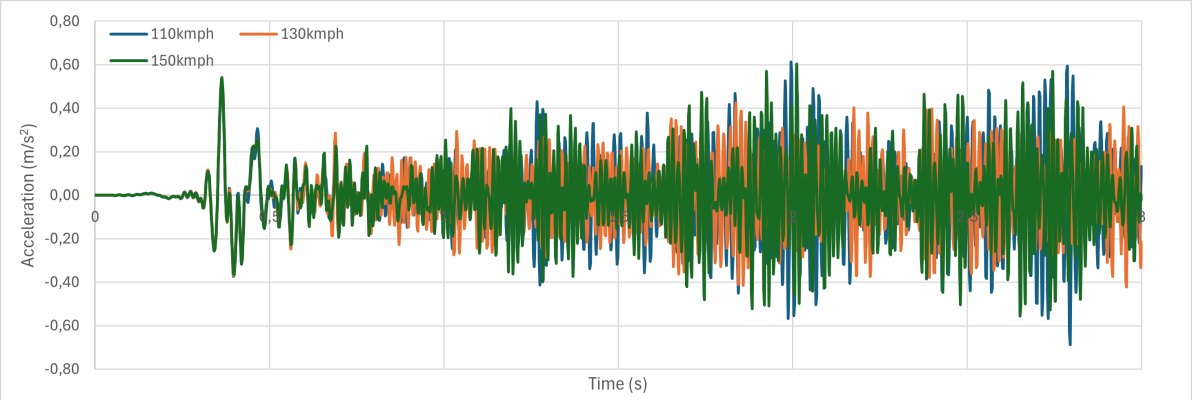

Figure 5.15: Comparison of acceleration at MP3 in time domain for varying velocity

The acceleration data is presented in pairs of time, acceleration value. By examining the range and patterns of these values, the dynamic response characteristics at each point can be observed. This point, being closest to the rail, exhibits the highest acceleration amplitudes among all measurement points for this speed. The signal demonstrates a clear dynamic response with multiple high-amplitude events occurring over the observation period, reflecting the train's passage. At this intermediate distance, the acceleration amplitudes are noticeably reduced compared to MP1. The oscillatory pattern is still evident, but the magnitude of vibrations is significantly attenuated due to distance from the rail. At MP3, the vibrations are

considerably damped, indicating that ground motions attenuate significantly with increasing distance from the rail. The overall shape of the signal is similar to MP2, but with reduced intensity. Surprisingly, the peak accelerations observed in the provided excerpts for MP1 at 150 kmph are lower than those at 110 kmph and 130 kmph. This observation suggests that either the peak events for the 150 kmph simulation occur outside the provided data excerpts, or there are specific simulation parameters or real-world phenomena (e.g., resonance, track conditions, train characteristics) that lead to lower peak accelerations at this specific speed compared to the other two for this measurement point. The effect of different ”energy releases” (train speeds) would typically correlate with stronger or weaker ”shaking,” but sometimes environmental factors or the nature of the ground can lead to unexpected dampening.

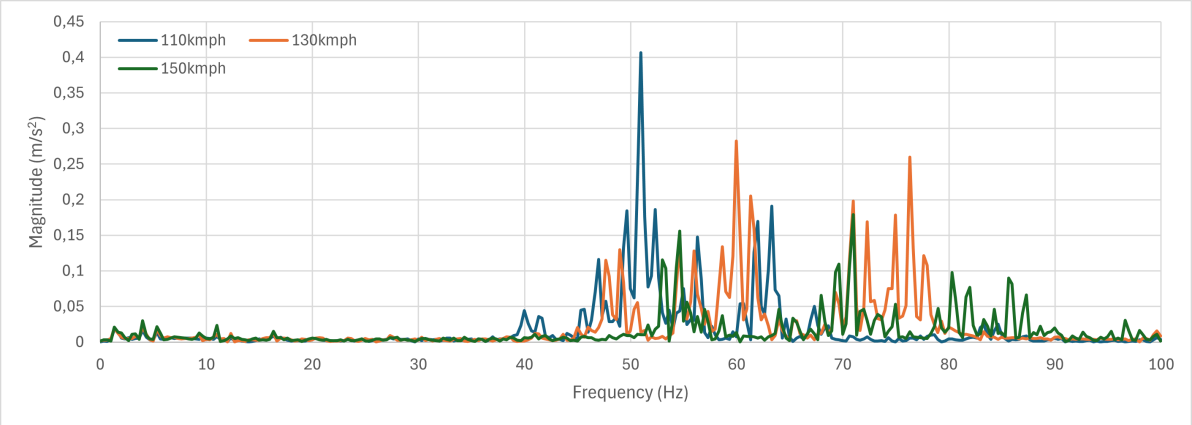

Figure 5.16: Comparison of acceleration at MP1 in frequency domain for varying velocity

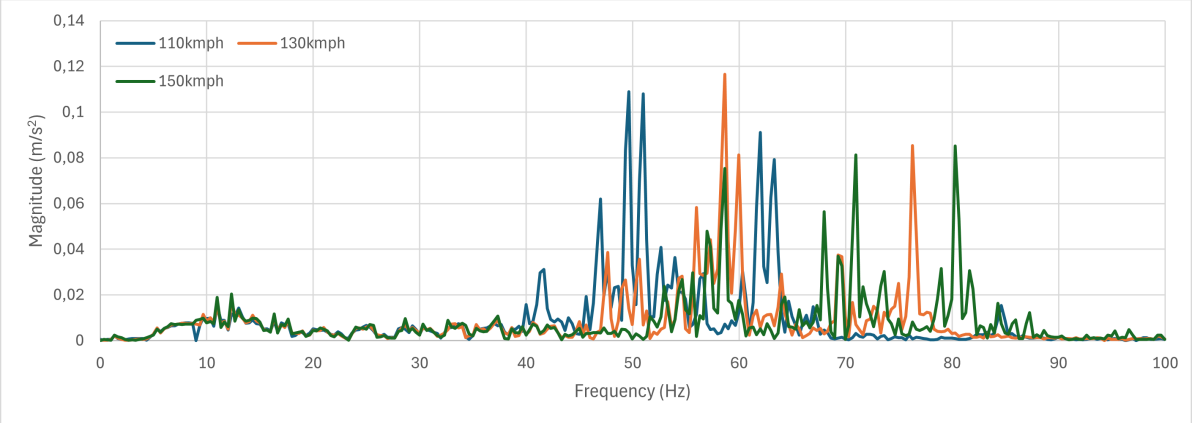

Figure 5.17: Comparison of acceleration at MP2 in frequency domain for varying velocity

In the frequency domain, it was observed that as the velocity of the train increased, the dominant frequency moved to higher values. For a velocity of 110 kmph, a peak was seen close to 51 Hz. When the velocity increased to 130 kmph, the peak shifted close to 60 Hz and for 150 kmph, the peak was closer to 71 Hz. This indicates a complex interaction between train speed, vehicle characteristics, track irregularities, and ground response, where energy may be excited at different resonant frequencies of the system. Surprisingly, the highest absolute acceleration magnitude observed at MP1 is for the 110 kmph train. This is notably higher than the peak for 130 kmph and 150 kmph. This counter-intuitive observation suggests that the ground-vibration response is not simply proportional to train speed. It likely points to a resonance phenomenon where the excitation frequencies produced by the 110 kmph train align

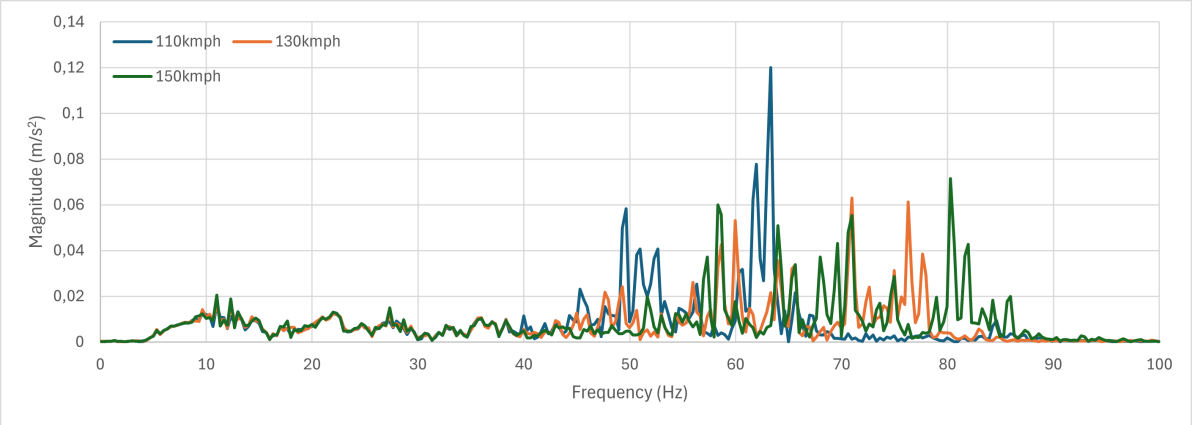

Figure 5.18: Comparison of acceleration at MP3 in frequency domain for varying velocity

more critically with the natural frequencies of the track-ground system at MP1, leading to amplified vibrations. Although overall magnitudes decrease with distance, for the 110 kmph case, the maximum magnitude at MP3 is higher than that for 130 kmph and 150 kmph . This further supports the idea that the initial excitation spectrum at the source, driven by factors beyond just speed, plays a crucial role in the propagated vibration levels.

5.2.2. Linear-Non Linear Model (M2)

The reference model was 30 meters deep, but for this work, the model was modified to 9 meters deep. This was also done considering the computational efficiency and the time consumption. The parameters of the location were cross referenced with the available CPT data from DINOloket, at a point close to the site.

A dynamic analysis was performed on the 9m deep model with 4 soil layers, a compacted sand layer below the embankment, subballast and ballast under the sleeper-rail configuration. Multiple simulation were run in order to find the most suitable model that fit the site data. In these simulations, only the moving load method was considered as it was the focus of this work. The stiffness of the ballast and subballast along with their damping parameters were varied to find the best match. It was inferred from the reference work [30] that exact cross-section of the embankment was unknown and the validated cross section from the reference work [30] was chosen. Damping parameters similar to the linear elastic model was given for the embankment consisting of the rail, railpad and fasteners, sleepers, ballast and subballast. The soil layers beneath the embankment were not given any input for Rayleigh damping as HS small material model was chosen for the soil layers.

The results of acceleration in time domain are presented in Figure 5.19 for MP1, Figure 5.20 for MP2 and Figure 5.21 for MP3 comparing it with the site results. The results of acceleration in frequency domain are presented in Figure5.22 for MP1, Figure 5.23 for MP2 and Figure 5.24 for MP3 comparing it with the site results.

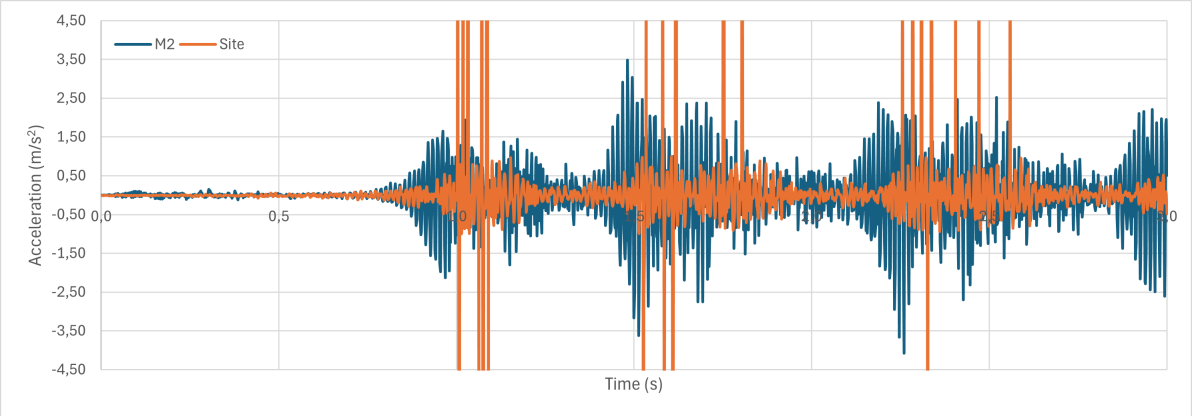

Figure 5.19: Comparison of site and M2 simulation data at MP1 in time domain

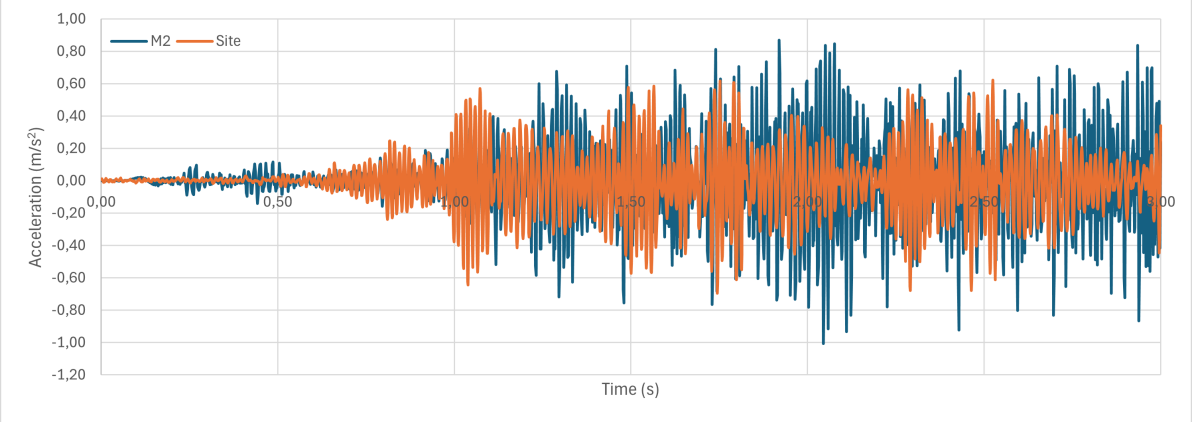

Figure 5.20: Comparison of site and M2 simulation data at MP2 in time domain

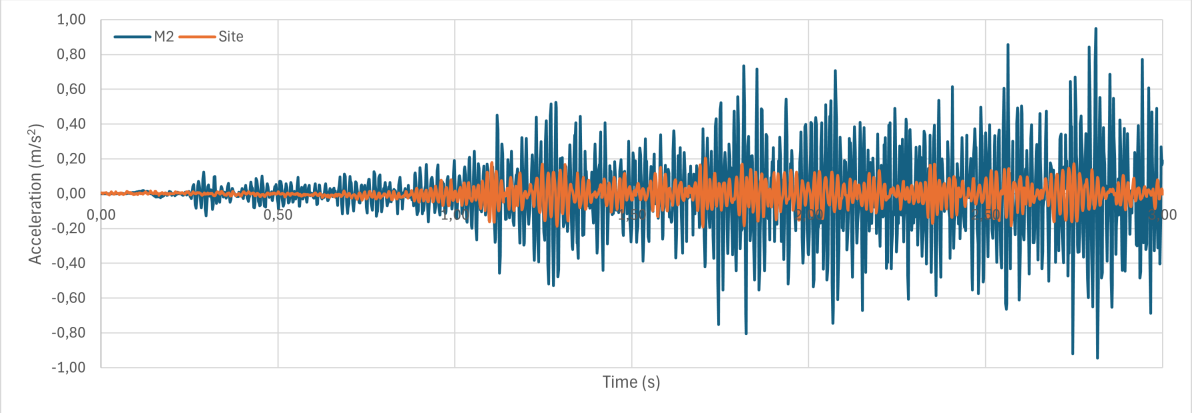

Figure 5.21: Comparison of site and M2 simulation data at MP3 in time domain

When the linear model was updated to a combination of linear and non-linear material models, clear differences were visible. The magnitude of acceleration at MP1 was higher than the site; however, it must be noted that this may be due to the presence of various materials and meshes at the point where MP1 is located. But the acceleration magnitude at MP2 was closer to the range of expectation. The acceleration magnitudes at MP3 was higher than measured at site. This was also seen in the linear model. This can be due to assumptions, the uncertainties and the simplification of the model compared to real-world situation.

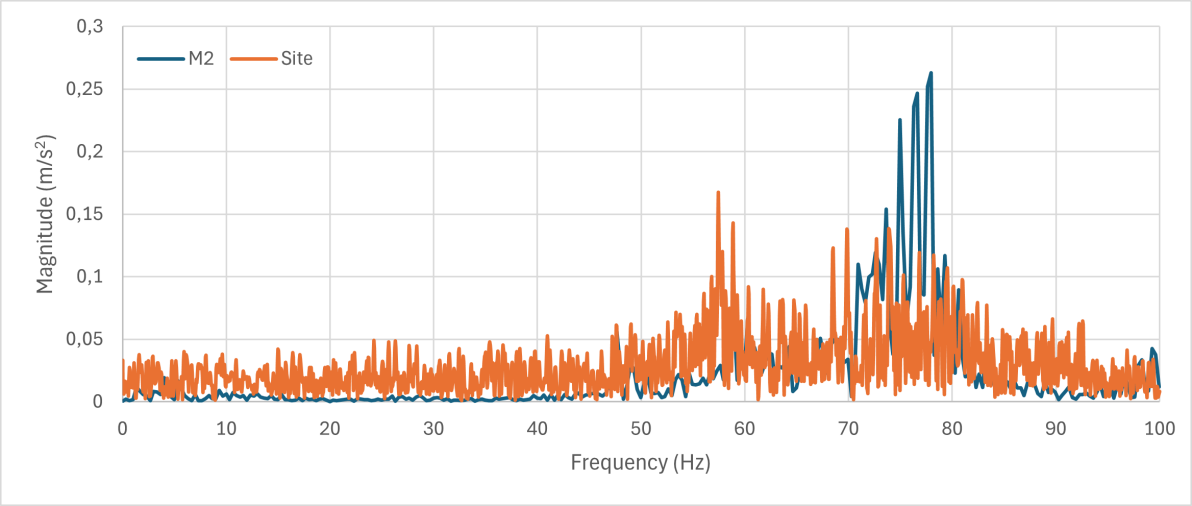

Figure 5.22: Comparison of site and M2 simulation data at MP1 in Frequency domain

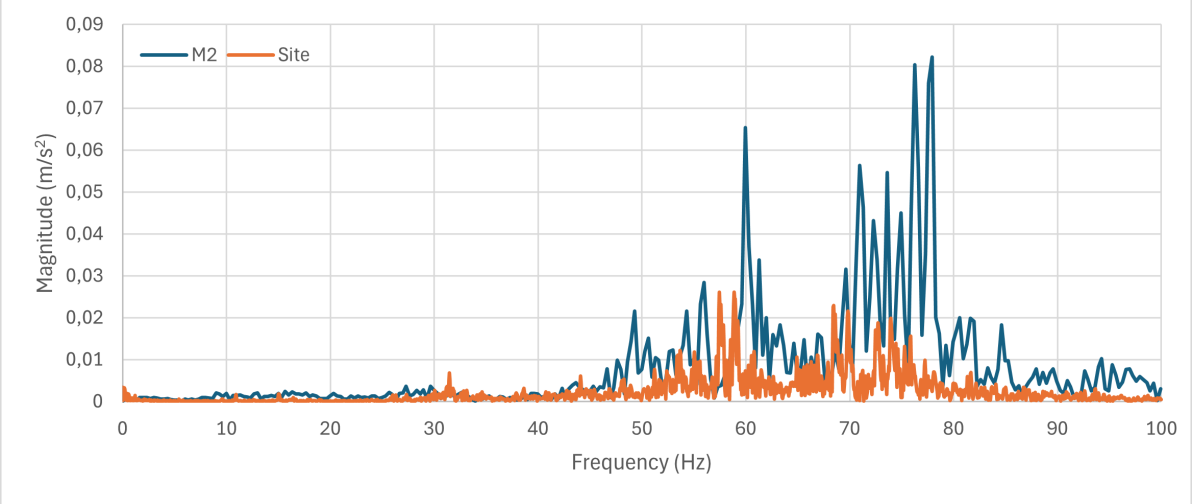

Figure 5.23: Comparison of site and M2 simulation data at MP2 in Frequency domain

In the frequency domain, it was noticed that at MP1, as expected the magnitudes of the frequency are high. However, when comparing the magnitudes at MP2 and MP3, a significant reduction in the magnitudes from the linear elastic model was observed. This shows that the non-linear model does perform better taking into account the damping on its own, without the additional addition of any Rayleigh damping parameters. The higher magnitudes can be rectified with better information on site characterisation and the consideration of other uncertainties.

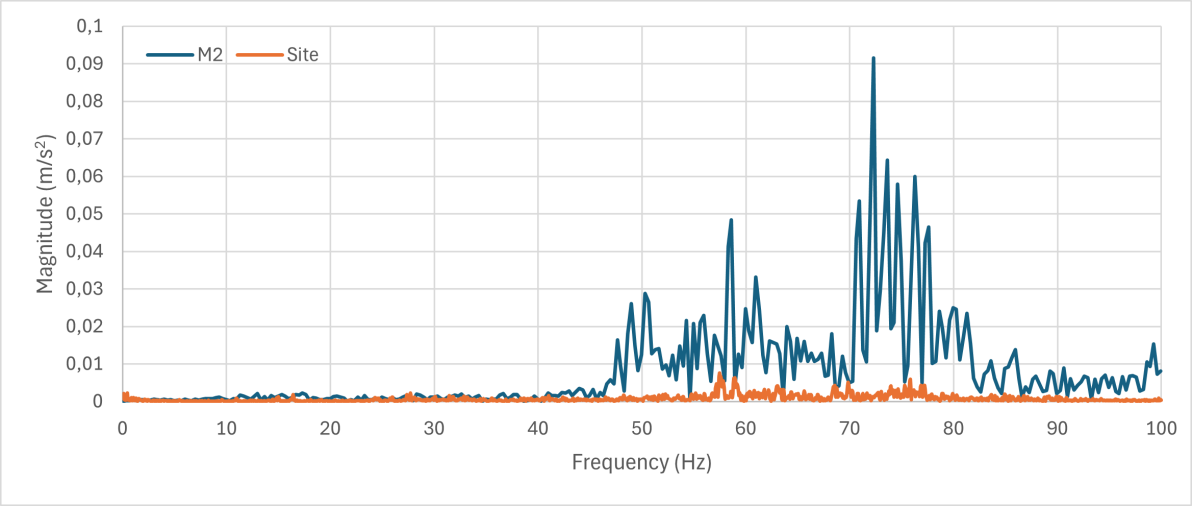

Figure 5.24: Comparison of site and M2 simulation data at MP3 in Frequency domain

5.2.3. M2 with water table fluctuations

The M2 model was then simulated, by varying the water table by 0.5 m, reducing it to -1.5 m and then later to -0.5 m to investigate its effects. All other parameters remained the same. The following graphs will show the obtained data. Figures 5.25 to figure 5.27 show the acceleration in time domain compared to the original M2 model where the water table was at -1 m.

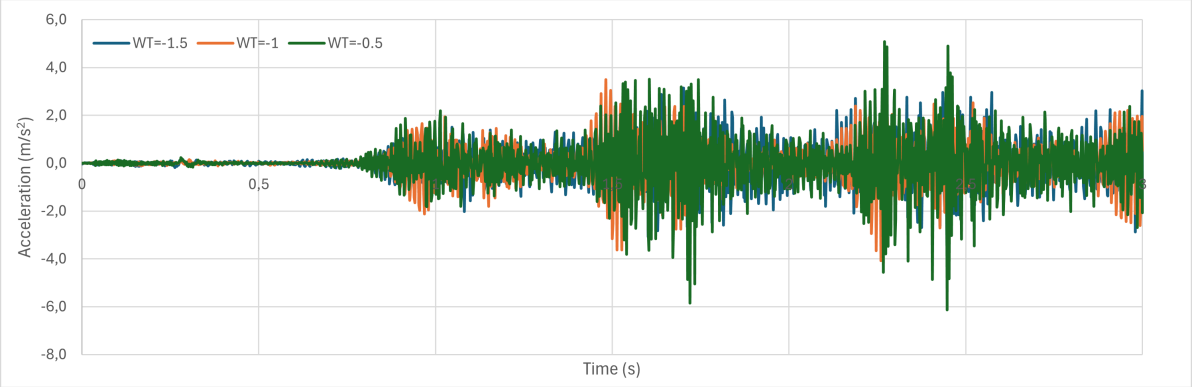

Figure 5.25: Comparison of acceleration in time domain at MP1 for M2 for water table fluctuation

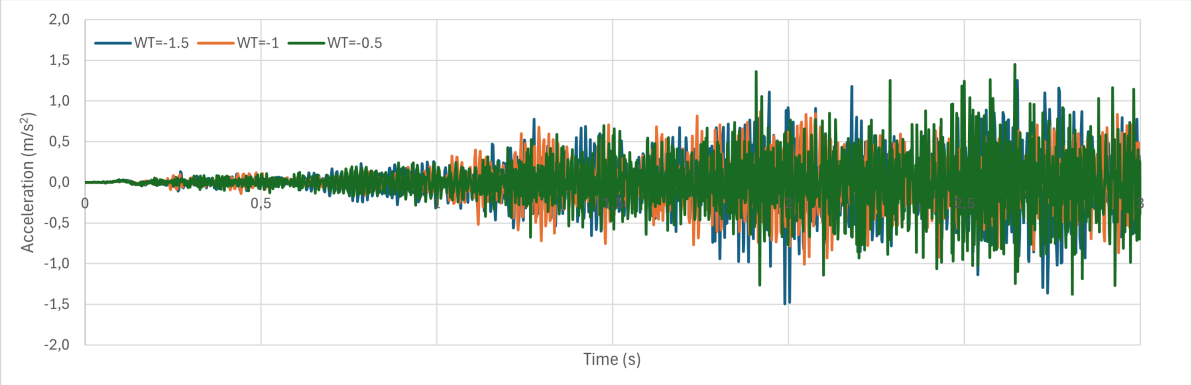

Figure 5.26: Comparison of acceleration in time domain at MP2 for M2 for water table fluctuation

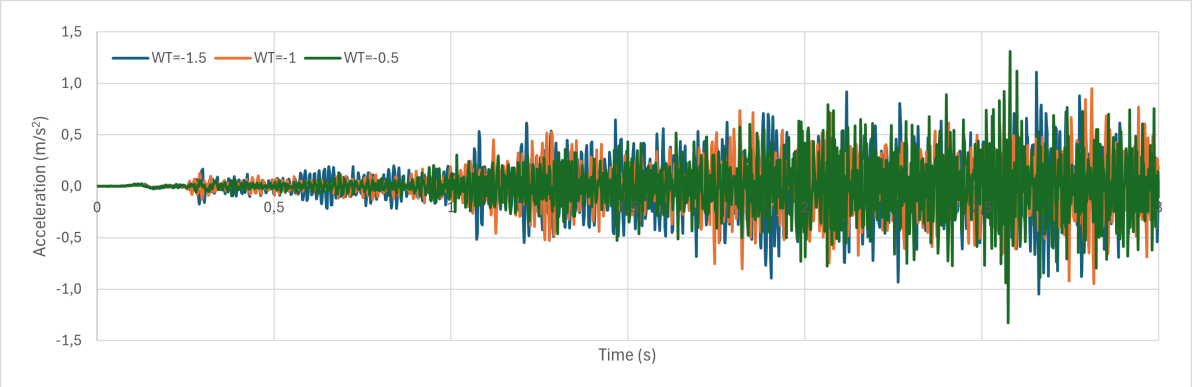

Figure 5.27: Comparison of acceleration in time domain at MP3 for M2 for water table fluctuation

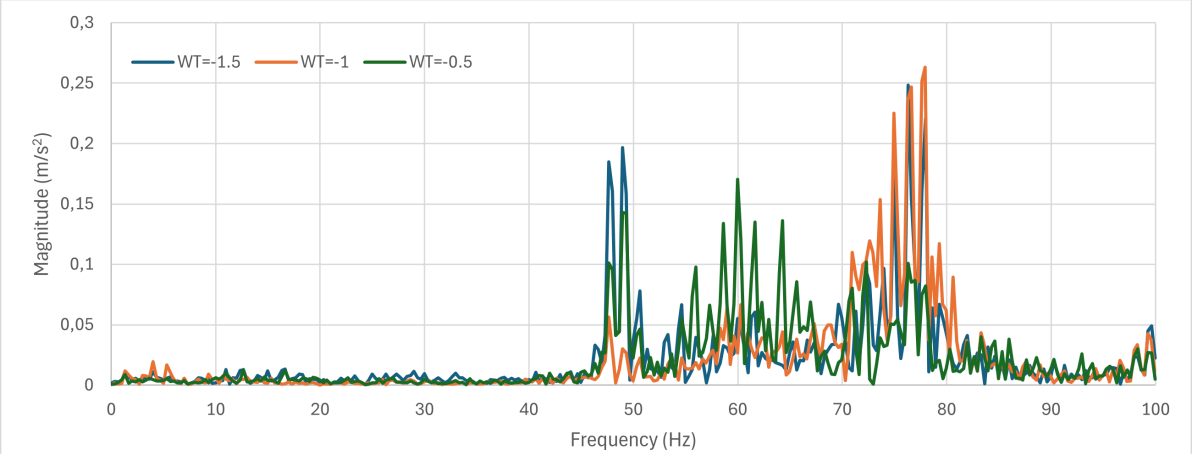

Figure 5.28: Comparison of acceleration in frequency domain at MP1 for M2 for water table fluctuation

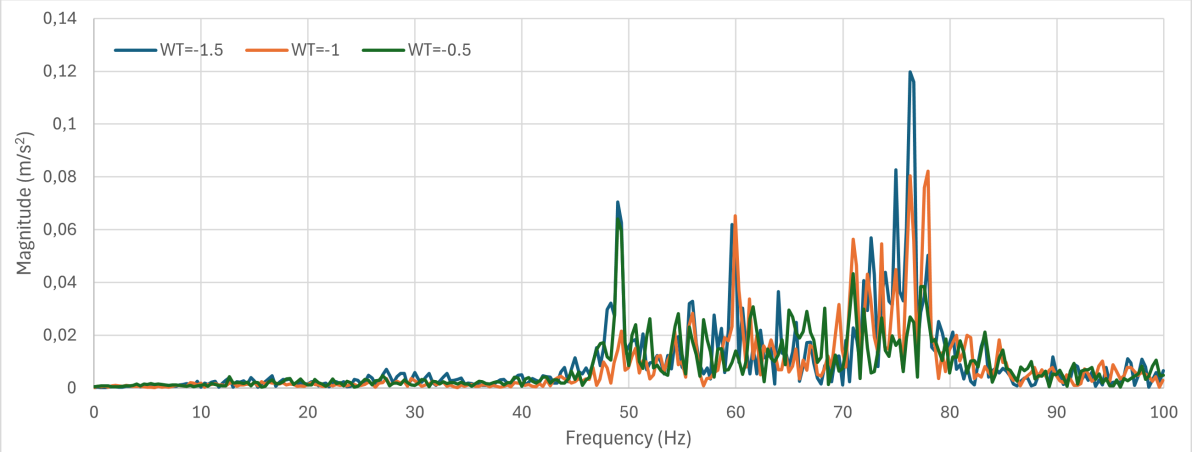

Figure 5.29: Comparison of acceleration in frequency domain at MP2 for M2 for water table fluctuation

From the data obtained from the simulations, the following were observed:

Regarding the magnitude of acceleration in time domain, much variation was not observed at any of the measurement points. The vibration spectral energy is concentrated primarily in the 50–80 Hz range, which is well correlated with the findings in the field that railway-induced ground vibrations typically exhibit prominent frequencies between about 10 and 80 Hz, de-

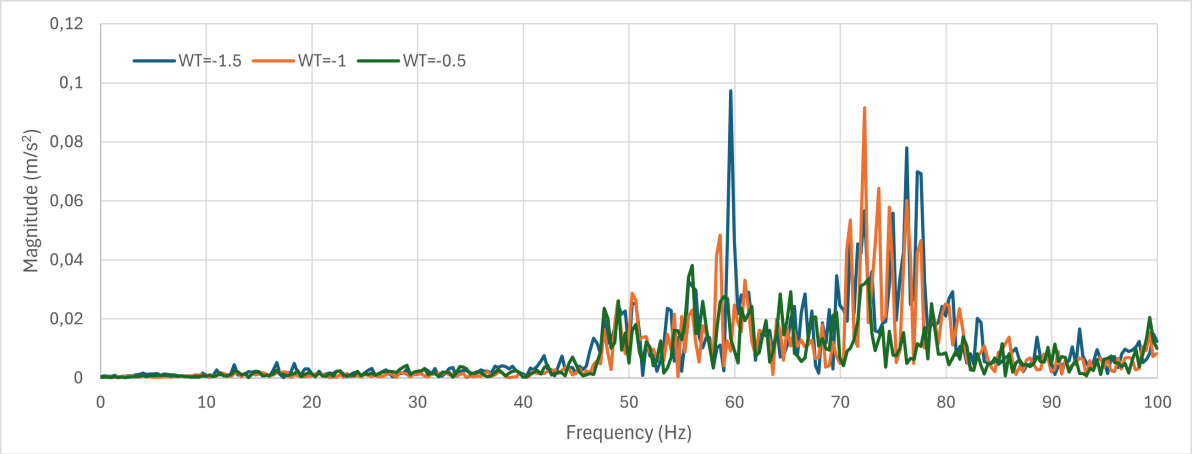

Figure 5.30: Comparison of acceleration in frequency domain at MP3 for M2 for water table fluctuation

pending on rail-wheel interaction, train speed, and track/soil characteristics.

The case where the water table was 1.5 m below the surface (WT = -1.5) tend to show higher spectral amplitudes at certain frequencies, notably at specific resonance peaks (around 60–80 Hz). This behaviour is linked to soil stiffness: as the soil above the WT is less saturated, it acts stiffer, enabling more efficient transmission of certain frequency components and resulting in sharper, more pronounced peaks.

At WT = -0.5 m, spectral peaks are generally lower and more damped, a reflection of increased damping in saturated soils, which tends to suppress higher frequency components due to viscous energy dissipation. This pattern is further supported by studies using poroelastic and time-frequency domain models, which show that increased soil saturation amplifies lower frequency response but damps sharp high-frequency transients.

When focussing on the point closer to the track (e.g., 3 m), the acceleration spectra show higher peak magnitudes and distinct resonance frequencies. As distance increases (up to 16.7 m), overall spectral magnitudes decrease, and the frequency content becomes broader and less sharply peaked, highlighting the attenuation and scattering effect with propagation through the ground. The intensity of higher frequencies reduced as the water table began to rise from -1.5 m to -0.5 m.

5.2.4. Non-Linear Model (M3)

In model M3, the rail, railpad, and fasteners, and the sleepers were the only components modelled with a linear elastic material model. All other components of the embankment, the ballast and subballast and the soil layers beneath the embankment were modelled with HSsmall material model.

	α	β
Sleeper	1.257	0.000030

Table 5.4: Damping parameters for the non-linear model (M3)

The acceleration results in the time domain are presented in Figure 5.31 for MP1, Figure 5.32 for MP2 and Figure 5.33 for MP3 comparing it with the site results. The acceleration results in frequency domain are presented in Figure 5.34 for MP1, Figure 5.35 for MP2 and Figure 5.36 for MP3 comparing it with the site results. It was observed that the acceleration was

overestimated at MP1 and at MP3 but underestimated at MP2. In the frequency domain for MP1, the FFT of the simulation data gave values less than the site, this can be due to similar reasons as mentioned before, which are the assumptions and approximations used in the modelling. The FFT of MP2 had peaks in the expected frequency range. As observed before, the magnitudes at MP3 is over-estimated, and a slight amplification was observed. This may be due to the frequency being close to the resonance frequency of the system.

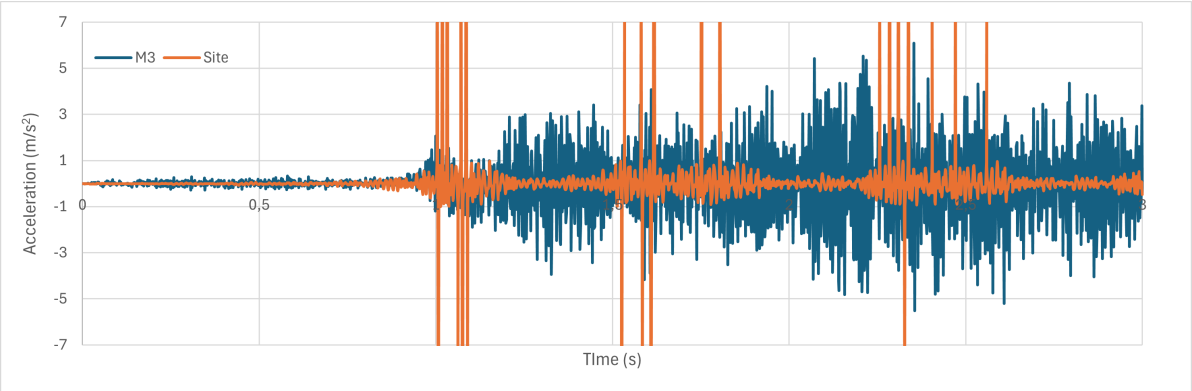

Figure 5.31: Comparison of site and M3 simulation data at MP1 in time domain

[h!]

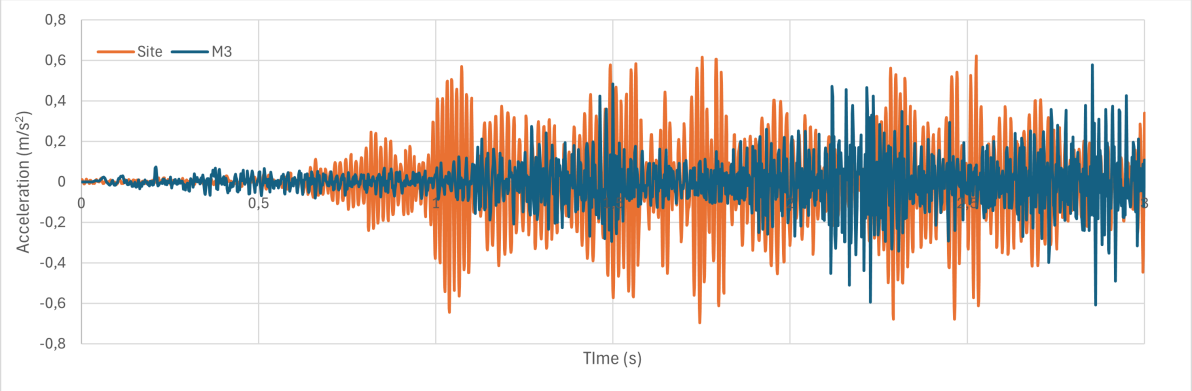

Figure 5.32: Comparison of site and M3 simulation data at MP2 in time domain

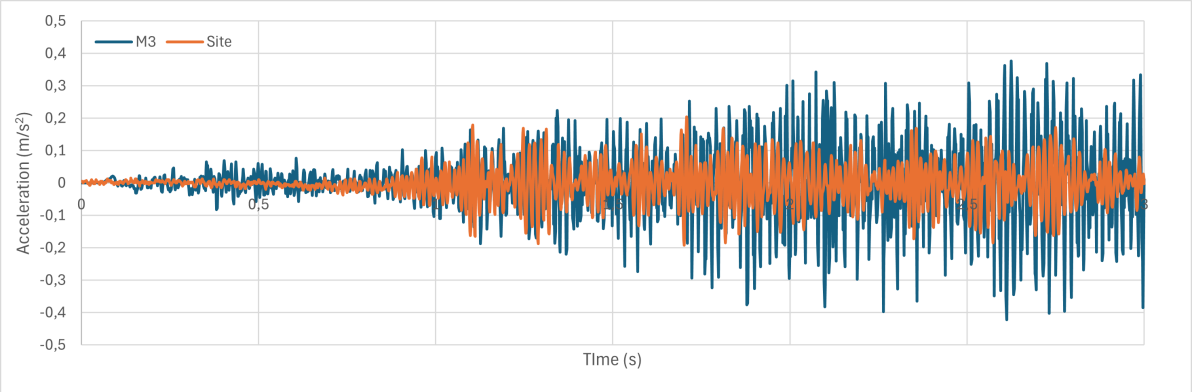

Figure 5.33: Comparison of site and M3 simulation data at MP3 in time domain

The results in the frequency domain gave more information about the simulation. It is noticed that the intensity was overestimated at both measurement points but they were closer to

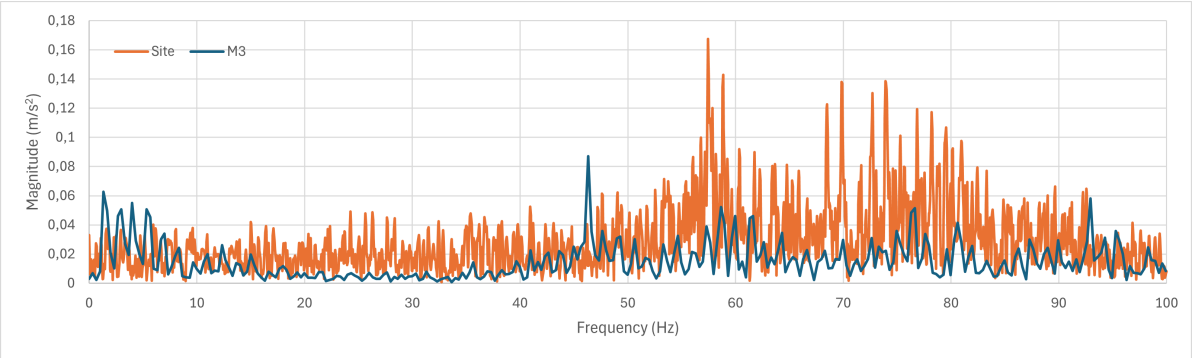

Figure 5.34: Comparison of site and M3 simulation data at MP1 in Frequency domain

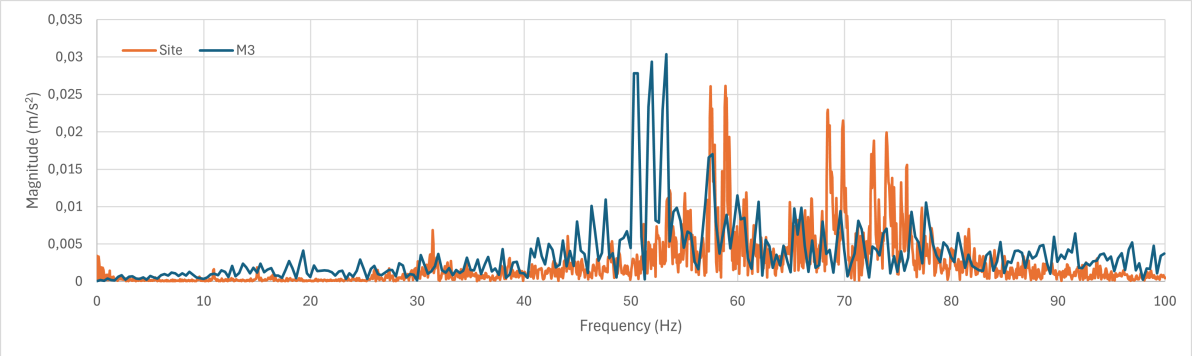

Figure 5.35: Comparison of site and M3 simulation data at MP2 in Frequency domain

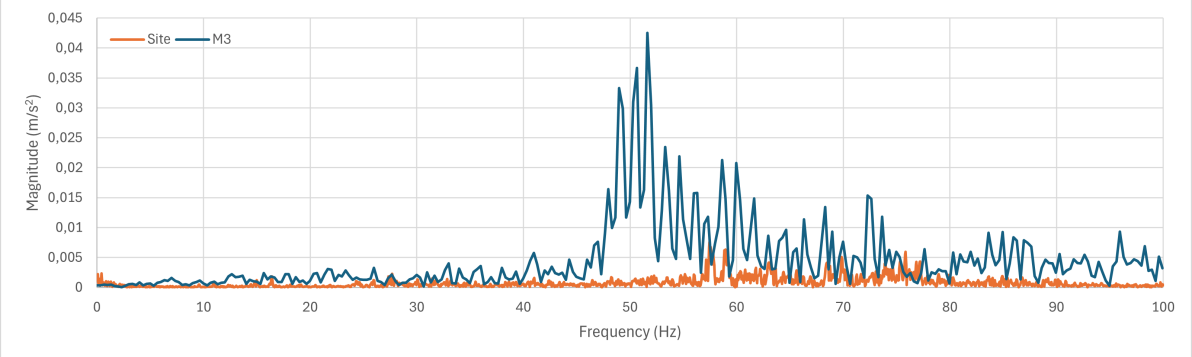

Figure 5.36: Comparison of site and M3 simulation data at MP3 in Frequency domain

the site data, when compared to models M1 and M2. A shift in the dominant frequency was observed at MP2 and the magnitudes were underestimated at higher frequencies when compared to the site data. This can be due to the assumptions and variation in the exact layering and other parameters. However, the model M3 performed better when compared to the other when comparing the values of acceleration in frequency domain.

5.2.5. M3 and water table fluctuations

To investigate the influence of groundwater conditions on vibration propagation, acceleration time histories were analysed for varying water table depths: −1.5 m, −1.0 m, −0.5 m and 0 m. Figures 5.39 to 5.41 present the acceleration responses in the time domain for each water table case. The results indicate how changes in the phreatic surface may alter the dynamic response of the track-ground system.

Subsequently, the corresponding frequency domain representations are shown in Figures 5.42 to 5.45. These plots provide further insight into the frequency content of the acceleration signals under different groundwater conditions.

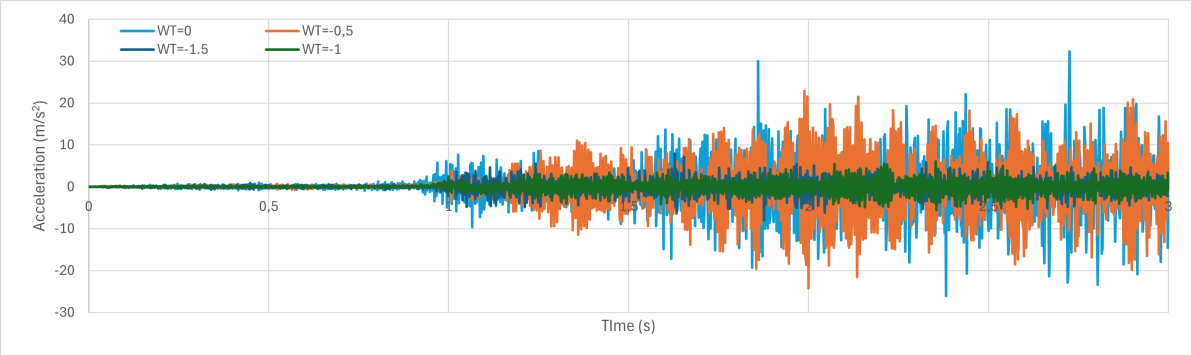

Figure 5.37: Comparison of M3 simulation data at MP1 in time domain for varying water table

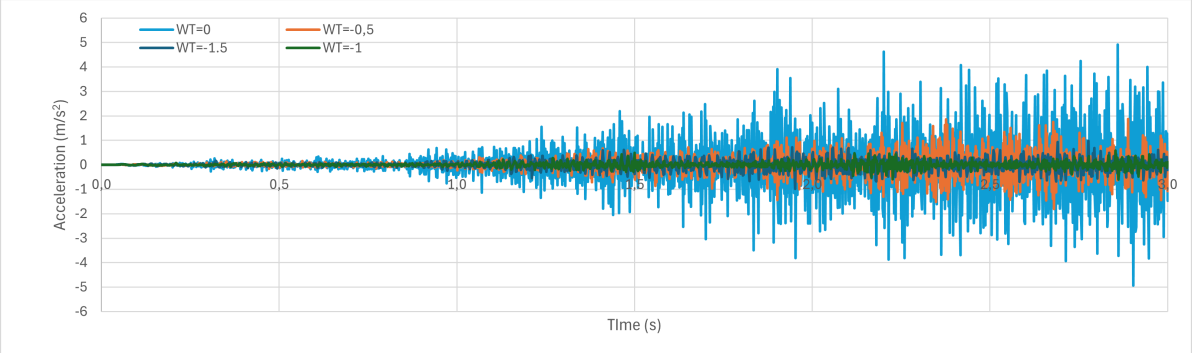

Figure 5.38: Comparison of M3 simulation data at MP2 in time domain for varying water table

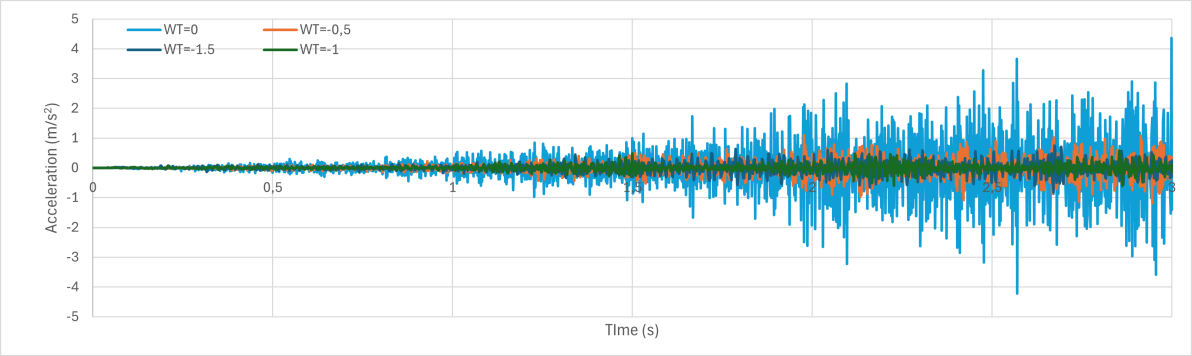

Figure 5.39: Comparison of M3 simulation data at MP3 in time domain for varying water table

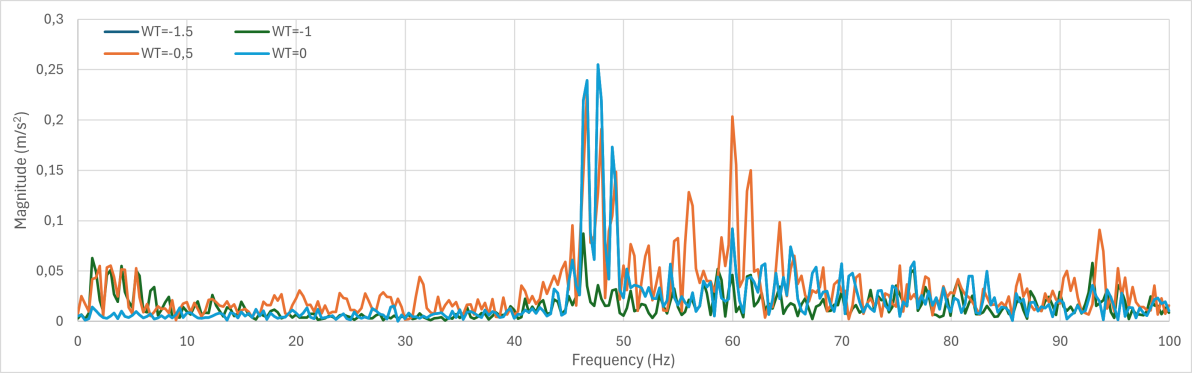

Figure 5.40: Comparison of M3 simulation data at MP1 in frequency domain for varying water table

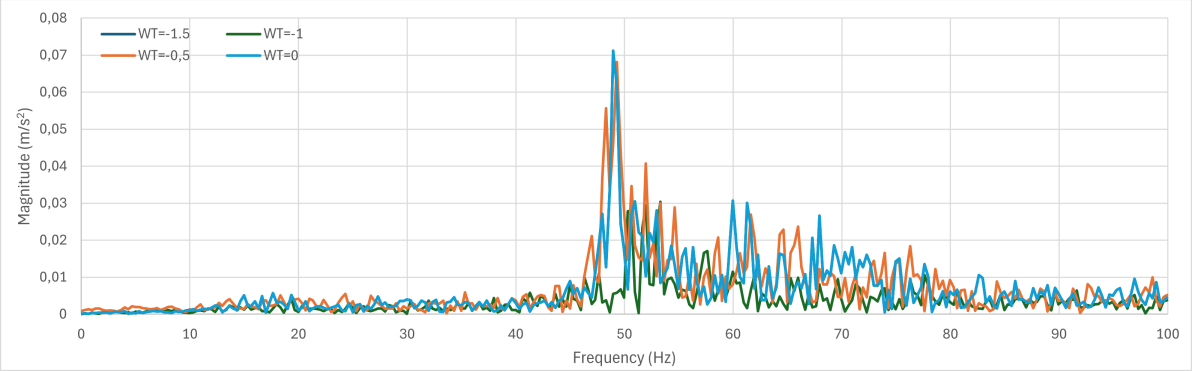

Figure 5.41: Comparison of M3 simulation data at MP2 in frequency domain for varying water table

The elevation of the water table has a profound and complex effect on the magnitude and character of transmitted vibrations, though there are some differing findings depending on the specific context and type of dynamic load. Also, the damping effect of water table rise may not increase as expected if the sand is very coarse-grained, as capillarity and viscosity effects are reduced, or if soil structure changes (like collapse or liquefaction zones) dominate energy loss mechanisms rather than simple viscous damping. Such complexity is highlighted in field and laboratory reports indicating that site-specific soil and hydrodynamic conditions can overrule general trends.

Findings on Amplitude and Frequency: Some studies suggest that rising groundwater levels typically reduce displacement amplitudes and increase natural frequencies [65]. Similarly, analysis of metro-induced vibrations indicates that as the level of the water water table in-

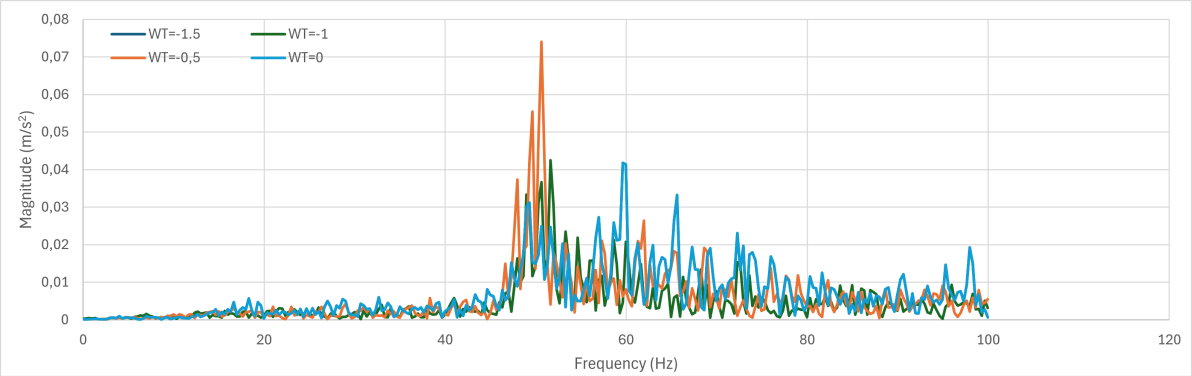

Figure 5.42: Comparison of M3 simulation data at MP3 in frequency domain for varying water table

creases, the intensity of ground motion decreases [40]. One study on dynamic compaction also found that peak acceleration of soil decreases abruptly when the tamper impacts water, suggesting energy dissipation. However, recent research directly supports the observations from this work, that amplitude of vibration increases as the water table rises, particularly for a machine-foundation-soil system [33]. This rise in the water table in sand may amplify induced vibrations. Additionally, in studies of train-induced ground settlement, soil deformation increased with rising water level [56]. But the fully non-linear models consistently predict higher acceleration peaks and larger deformations than linear or hybrid (linear + non-linear) models—especially under strong or repeated loading such as trains. For example, a research [46] demonstrated that rail displacements from a non-linear model were up to 20–30% greater than those from a linear model due to plastic strain and shear modulus degradation in the soil near the load. The time-history plots, especially at shallow water table (WL = -0.5 m), exhibit significantly larger amplitude excursions compared to deeper water level. This matches the predictions of fully non-linear models, where large strains in saturated/soft soils lead to enhanced non-linear effects and dynamic amplification, especially close to the track.

Critical Speed Shifts and Resonance Critical velocity (when train speed approaches the speed of Rayleigh waves) is lower in fully non-linear models. Non-linear behaviour means that as train speed increases, dynamic amplification and soil deformation accelerate much faster than in linear models, both in amplitude and depth. Fully non-linear analyses show that dynamic amplification becomes highly sensitive to small changes in input speed or load—track deflections can easily exceed those estimated from linear/hybrid models, with possible safety and serviceability issues if not properly considered. In the linear-nonlinear model (M2) results, while non-linearity is visible, full non-linearity would show even larger, often asymmetric, acceleration peaks and potentially more sustained high-magnitude responses [46] [21].

Frequency Content, Damping, and Attenuation: Non-linear soil models display frequency shift, increased waveform asymmetry, and greater damping at high strain levels. High-amplitude, low-frequency components are more pronounced in fully non-linear models, while high-frequency content may be less due to increased material damping from large strains.

Water Table and Soil Saturation Effects: Saturated soils (shallow water level) amplify non-linearity even further. Non-linear models show that, for the same input, very shallow water tables can lead to much greater strains and plastic effects than linear/hybrid models predict, making them crucial for accurate risk and mitigation assessment. The dominance of the orange trace (WL = -0.5 m) in the results is consistent with the recent findings from fully non-linear predictions, but a fully non-linear run would likely give even larger peak accelerations

and more significant decay differences between traces for different water table depths.

5.2.6. M3 with Self weight only

In the linear model, an additional dynamic load (expressed as a certain percentage of the primary load) was introduced during the loading phase to achieve the desired simulation outcomes. The physical scenario involves a moving load, representing train wheels traversing rails supported by sleepers spaced at regular intervals. Theoretically, the dynamic effects should naturally arise from the movement of the load itself, and the necessity for an extra dynamic load remains an unresolved question in the context of the linear model.

In contrast, for the fully nonlinear model, simulations were conducted with varying levels of additional dynamic load: 5%, 3%, and 0%. The objective was to assess the influence of these variations on vibration transmission. The results demonstrated in time domain in Figures 5.43 to figure 5.45 and Figures 5.46 to figure 5.48 shows that altering or omitting the additional dynamic load produced no significant changes in the measured accelerations, both in the time and frequency domains. The acceleration magnitudes remained largely consistent across all cases.

Specifically:

- M3: Model with 5% dynamic load
- M3A: Model with 0% dynamic load
- M3B: Model with 3% dynamic load

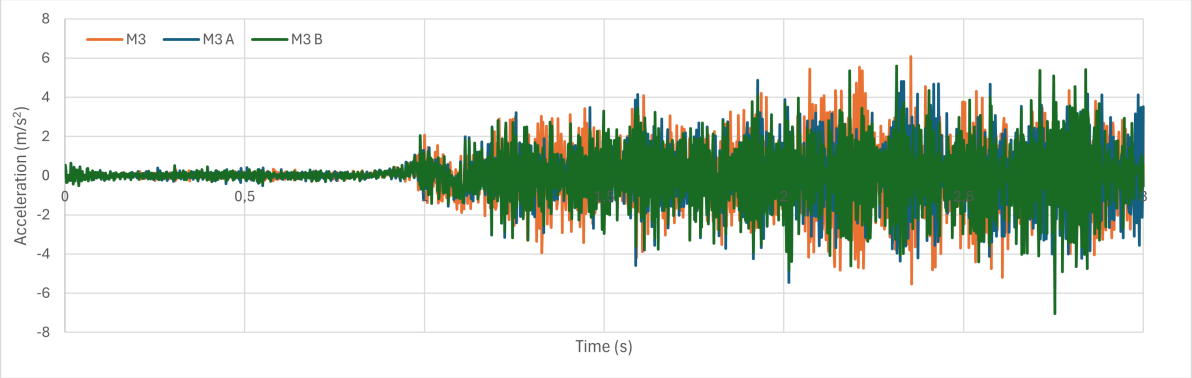

Figure 5.43: Comparison of M3, M3-A and M3-B simulations at MP1 in time domain

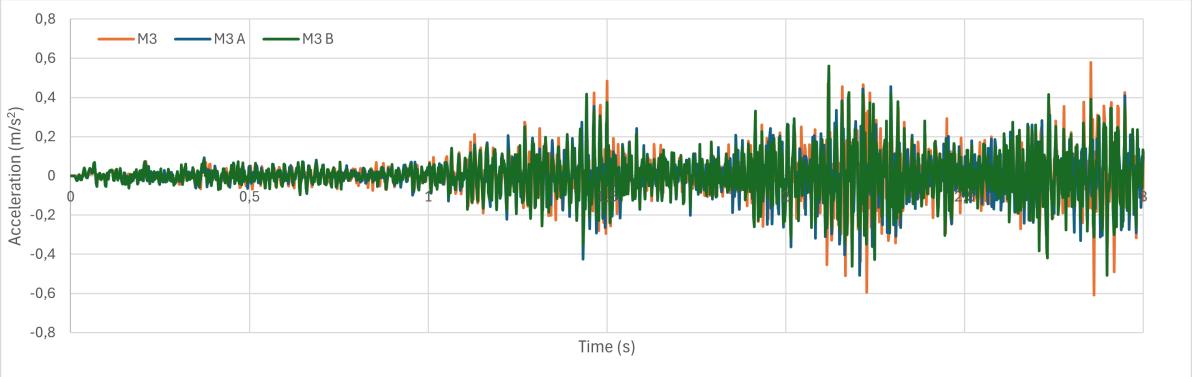

Figure 5.44: Comparison of M3, M3-A and M3-B simulations at MP3 in time domain

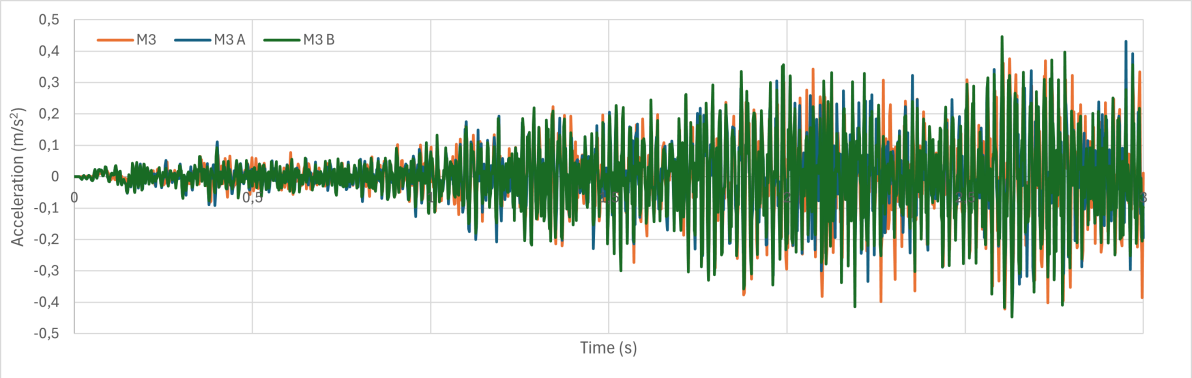

Figure 5.45: Comparison of M3, M3-A and M3-B simulations at MP3 in time domain

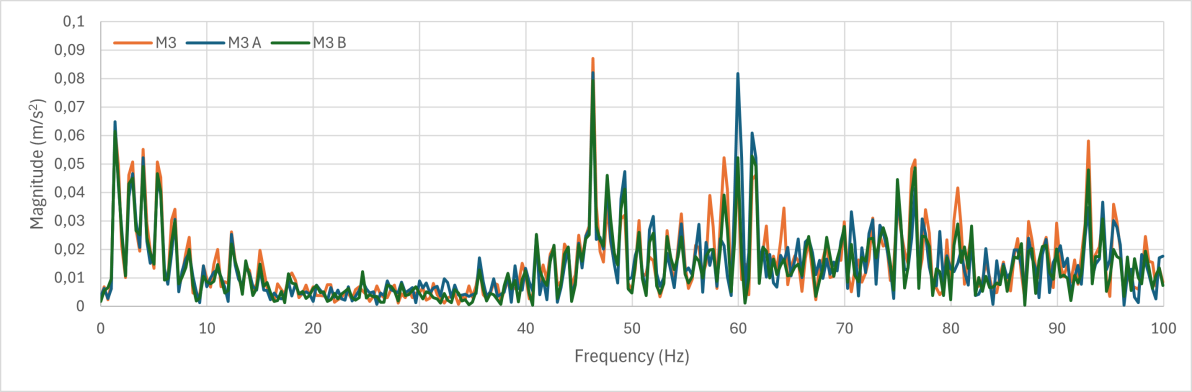

Figure 5.46: Comparison of M3, M3-A and M3-B simulations at MP1 in frequency domain

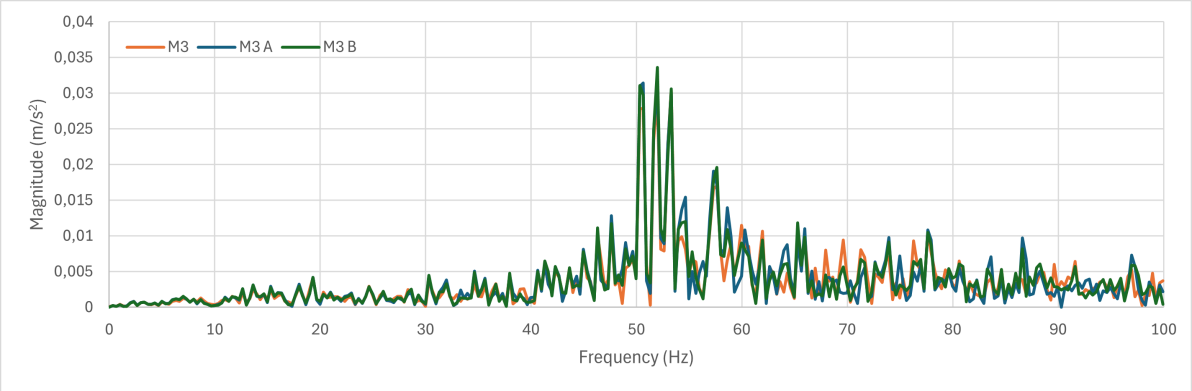

Figure 5.47: Comparison of M3, M3-A and M3-B simulations at MP2 in frequency domain

Linear Models and the Need for Additional Dynamic Load

Linear elastic models are often chosen for their computational efficiency, as they are ”much less demanding on computer resources [25] than a non-linear one”. However, this comes with inherent simplifications:

- **Approximation of Dynamic Effects:**Linear models may not fully capture the complex, time-varying dynamic forces induced by a moving train, which arise from wheel-rail interaction, rail unevenness, and variations in support stiffness. While a moving load inherently generates a time-varying response at a fixed point, a simplified linear model might

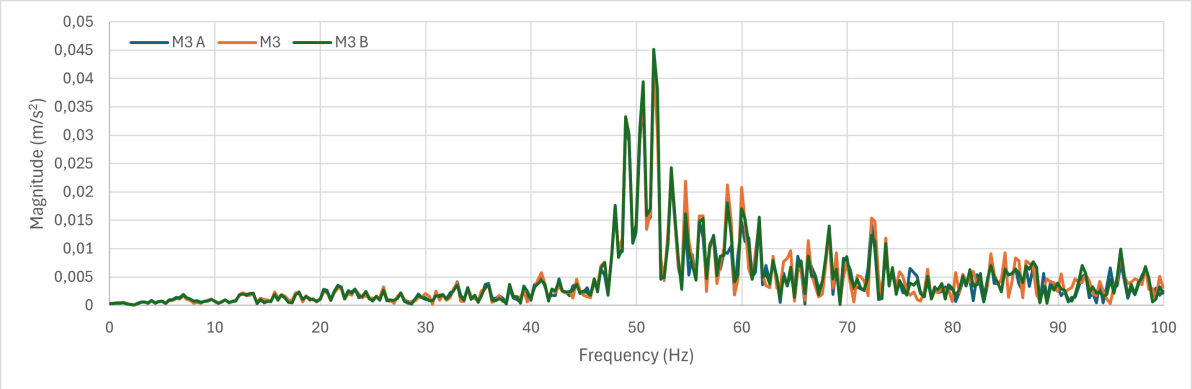

Figure 5.48: Comparison of M3, M3-A and M3-B simulations at MP3 in frequency domain

struggle to translate this motion into the full spectrum of dynamic ground response.

- **Compensating for Non-linearity:**Actual soil behaviour under train loads is often non-linear, especially at high speeds or when large shear strains occur. Since linear elastic models cannot inherently simulate non-linear phenomena like stiffness degradation or hysteretic damping, an ”additional dynamic load—expressed as a certain percentage of the primary load” might be introduced during the loading phase. This is an ad hoc adjustment designed to artificially inject dynamic energy or approximate non-linear effects that the model’s constitutive laws cannot otherwise generate (e.g., iterative reduction of shear modulus as an approximation for large shear strains in linear elastic analyses). Such an approach is used to ”achieve the desired simulation outcomes” in a simplified context.

Fully Non-linear Models and Insensitivity to Additional Dynamic Load

In contrast, fully non-linear models, particularly those formulated in the time domain, are better equipped to simulate the ”real behaviour of railway systems”. These models can inherently account for the complex dynamic interactions and non-linear soil properties, making an artificially added dynamic load less critical, or even redundant:

- **Intrinsic Dynamic Simulation:** Non-linear models (e.g., Hardening-Soil with small-strain stiffness (HSsmall)) are designed to capture complex dynamic responses, including ”hysteretic damping in cyclic loading” and the ”plastic behaviour” of soils. This means the model naturally generates dynamic effects through its sophisticated representation of material behaviour and interaction, reducing the need for external percentage-based adjustments.
- **Capturing Complex Excitation Mechanisms:** The dynamic component of train loads originates from actual train-track interactions, wheel/rail unevenness, and spatial variations in track stiffness. A non-linear model, by accurately simulating these underlying physical processes (including non-linear wheel-rail contact), will naturally generate the associated dynamic vibrations without requiring a separate ”additional dynamic load” to be explicitly specified.
- **Experimental Observations:**In the fully non-linear model, varying the additional dynamic load (5%, 3%, 0%) produced ”no significant changes in the measured accelerations, both in the time and frequency domains”. This observation aligns with the principle that if a non-linear model accurately captures the fundamental dynamic interactions and material properties, such an explicitly added ”additional dynamic load” becomes

less influential. The intrinsic dynamic response generated by the model's physics likely overwhelms or makes negligible the impact of this additional arbitrary percentage.

5.2.7. Comparison of the Site, M1 and M3 data in frequency domain.

The results from the simulations in frequency domain were compared with the site data to see how they perform.

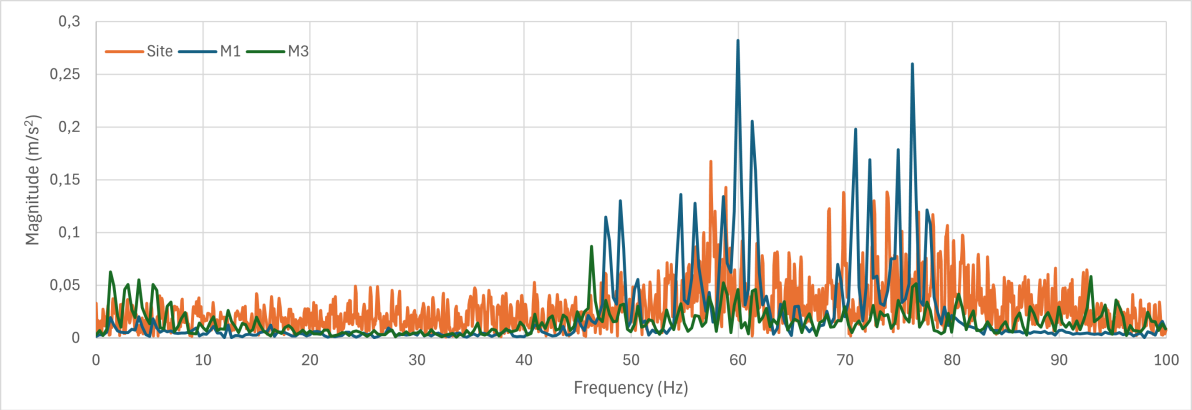

Figure 5.49: Comparison of site, M1 and M3 simulation data at MP1 in frequency domain

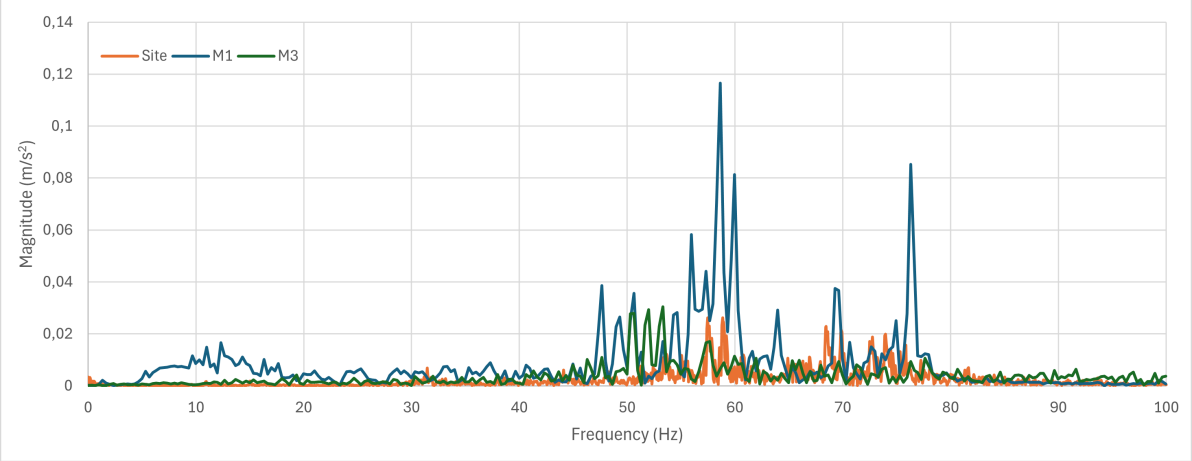

Figure 5.50: Comparison of site, M1 and M3 simulation data at MP2 in frequency domain

For all three distances, the linear model (M1) typically predicts the highest vibration magnitudes at certain frequencies, especially apparent around 50–70 Hz, while the nonlinear model (M3) and the site measurements show lower and smoother profiles. This is consistent with literature, where the nonlinear soil response tends to provide higher damping and energy dissipation, reducing peak amplitudes relative to linear models.

At 16.7m, the site measurements increase in overall energy, suggesting surface wave propagation and potential amplification due to soil conditions and water-table effects. The damping characteristics of the models need to be investigated in detail, as it did not show expected performance farther from the line of loading. The site data has a very low value of acceleration in frequency domain at 16.7 m but the simulation overestimated it by a lot. Vibrations generally attenuate with distance, but non-linear soils (M3) and real site soil (Site) show a gentler decline or even secondary amplification zones, which matches observations from both field and numerical studies where water table variations and layered soil effects cause complex

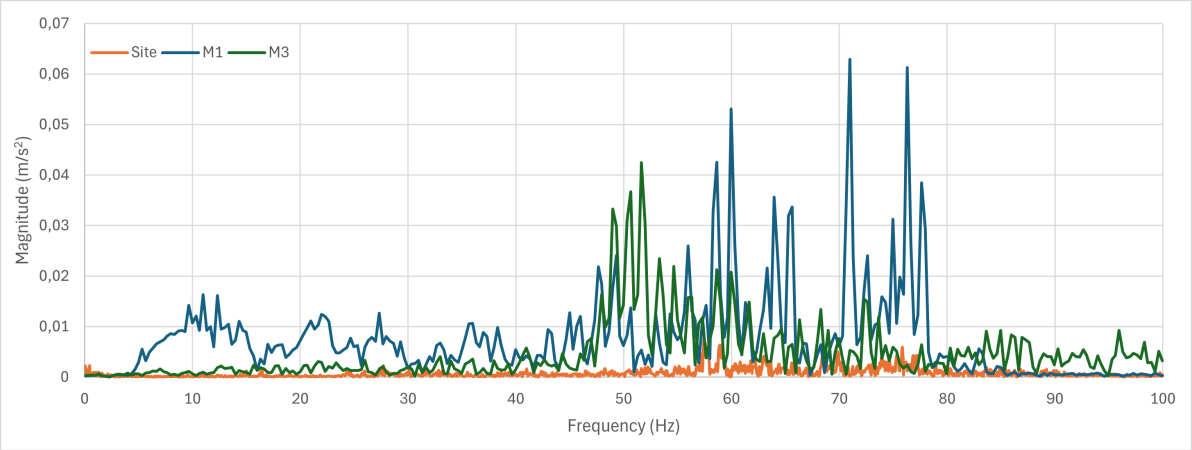

Figure 5.51: Comparison of site, M1 and M3 simulation data at MP3 in frequency domain

propagation and sometimes local amplification. Linear models tend to over-predict vibration amplitudes and under-represent damping effects. Nonlinear models (and field/site data) show more realistic, lower peak amplitudes, and increased damping—the effect is amplified at locations with high water tables and soft soils. Some frequencies show local amplification (site resonances), emphasizing the need for site-specific modelling and the limitations of purely linear or idealized models. Nonlinear and field-informed models better capture such phenomena.

Understanding the frequency content and attenuation of railway-induced vibrations supports targeted design of vibration isolation measures, like elastic track mats, barriers, or isolation piles, which are tuned to observed frequency ranges.

6

Conclusion

The focus of this research was on the study of vibrations from railways, by implementing the moving load method, modelling the cross section with a linear and non-linear model, to eventually study the effect of fluctuating water table on the transfer of vibrations.

- The moving load method in the FEM software was found to provide a better representation of train wheel movement on a rail compared to the triangular pulses method, as it simulates continuous contact even between nodes. An additional dynamic load of 5% of the axle load was found to yield good simulation results only in linear models.
- Linear elastic models (M1) performed satisfactorily for initial studies, showing patterns similar to site measurements, but generally overestimated acceleration magnitudes compared to real-world data, especially at distances further from the rail. This indicates that while useful, linear models with Rayleigh damping were insufficient to fully capture real-life conditions due to approximations and site uncertainties.
- Incorporating non-linear material models, specifically the Hardening Soil model with small-strain stiffness (HSsmall), showed better agreement with site data compared to purely linear models. This highlights the importance of using non-linear models for more accurate representation of soil behaviour and damping characteristics, even without additional Rayleigh damping parameters in the soil layers.
- The effect of water table fluctuations on vibration transfer was investigated, and while varying the water table in the M2 model showed no significant variation in acceleration magnitudes in the time domain, the intensity of higher frequencies reduced as the water table rose from -1.5 m to -0.5 m. Literature suggests complex and sometimes contradictory effects, but often points to reduced soil stiffness and potential for amplified vibrations near resonance when the water table rises.
- The observations from fully non-linear model (M3) of this research supported recent literature, indicated that the amplitude of vibration increased as the water table rose. However, this needs an in depth study to understand the phenomena in detail.
- Simulations with the fully non-linear model (M3), where most components except rails, railpads, fasteners, and sleepers used HSsmall, demonstrated that altering or omitting the additional dynamic load (5%, 3%, or 0%) produced no significant changes in measured accelerations. This suggests that non-linear models inherently capture dynamic effects, making external percentage-based adjustments less critical.

- The study acknowledges significant assumptions and simplifications (e.g., no surrounding buildings, isotropic soil, sharp soil layer boundaries, unknown utilities) that contribute to discrepancies between simulation results and real-world data. Despite higher computational demands, it is advised to incorporate non-linearity for results that better mimic soil behaviour.

6.1. Limitations

Based on the study, the following are the shortcomings of this work:

- The model was constructed with numerous assumptions, which contributed to discrepancies between simulation results and real-world data. The model did not account for any buildings in the surroundings. The presence of utility lines beneath the surface, which play an important role in vibration dispersion and frequency content, was not considered. The soil in the model was assumed to be isotropic, whereas in reality, soil is an anisotropic material. The gradual shifts in soil layers and types were represented as sharp boundaries, affecting the results.
- Despite introducing Rayleigh damping into the linear model, it was not sufficient for the model to closely resemble site data, indicating its limitations in capturing real-life damping characteristics. Rayleigh damping's frequency-dependent nature can lead to a loss of accuracy outside the chosen optimal frequency range, potentially underestimating low frequencies and over-attenuating high frequencies.
- Implementing non-linear models and 3D dynamic simulations requires significantly higher computational power and time, with simulations potentially taking hours or days. This often necessitates compromises in model size and mesh refinement outside the immediate region of interest.
- The study acknowledged the presence of unexpected peaks in frequency from the simulation data that need further investigation.
- The raw measurement data from the site had unusual peaks at MP1, potentially due to vehicular effects like a flat wheel or other site-specific irregularities. These ”high peaks” were disregarded for detailed investigation, focusing instead on MP2 and MP3.
- While the effect of water table fluctuations was investigated, the model M2 showed no significant variation in acceleration magnitudes in the time domain despite literature suggesting complex and sometimes contradictory effects. This aspect needs more detailed study.

6.2. Further research scope

This topic is immensely huge and a small portion of it was covered in this thesis. Further research opportunities with respect to this topic remains vast and are promising, a few of them are mentioned below.

- The careful investigation of unexpected peaks in frequency from the simulations need to be studied.
- The rise in acceleration magnitudes with the increase in water level in the non-linear model needs to be investigated in detail.
- It is necessary to develop a method to incorporate non-linearity in soil layers at the site more accurately.

- Sensitivity analysis of the embankment layers will help to understand the mitigating of the transfer of vibrations through the soil.

References

[1] S. Acharyaa and R.C. Tiwarib. “Ground Response Analysis for Train-Induced Vibration”. In: *Transportation Infrastructure Geotechnology* (2023).

[2] Z.A. Alkaissi. “Three Dimensional Finite Element Model of Railway Ballasted Track System under Dynamic Train Loading”. In: *Construction Technologies and Architecture* 8 (2023), pp. 11–21.

[3] S. Alzabeebee. “Calibration of a finite element model to predict the dynamic response of a railway track bed subjected to low-and high-speed moving train loads”. In: *Transportation Infrastructure Geotechnology* 10.3 (2023), pp. 504–520.

[4] ArcelorMittal Rails. *European Standards: Rail UIC54 54E1*. Accessed: 09/07/2025. URL: https://rails.arcelormittal.com/profiles/transport-rails/european-standards/rail-uic54-54e1/.

[5] Lutz Auersch. “Ground vibration due to railway traffic—The calculation of the effects of moving static loads and their experimental verification”. In: *Journal of Sound and Vibration* 293.3-5 (2006), pp. 599–610.

[6] M. Bahrekazemi. “Train-induced ground vibration and its prediction”. Doctoral dissertation. Byggvetenskap, 2004.

[7] C. Bayındır. “Effects of ground water table and ground inclination on train induced groundborne vibrations”. In: *TWMS Journal of Applied and Engineering Mathematics* 9.4 (2019), pp. 735–746.

[8] Bentley Systems. *PLAXIS 3D 2024.2 Scientific Manual 3D*. Bentley, 2024.

[9] R. B. J. Brinkgreve, Erjona Engin, and Harun Kürşat Engin. “Validation of empirical formulas to derive model parameters for sands”. In: *Numerical Methods in Geotechnical Engineering* 137 (2010), p. 142.

[10] *BS 6472-1: Guide to Evaluation of Human Exposure to Vibration in Buildings - Part 1: Vibration Sources Other than Blasting*. British Standards Institution (BSI), 2008. URL: https://www.thenbs.com/PublicationIndex/documents/details?Pub=BSI&DocID=286767.

[11] Building Research Foundation (SBR). *SBR Vibration Directive B: Practical Applications for Measuring and Evaluating Vibrations in the Netherlands*. 2017. URL: https://sbr-trillingsmeter.nl/en/practical-applications/.

[12] T.L. Christiansen. “A Comparison of Railway Load Models for Geotechnical Analysis”. MA thesis. NTNU, 2018.

[13] DP Connolly et al. “Benchmarking railway vibrations–Track, vehicle, ground and building effects”. In: *Construction and Building Materials* 92 (2015), pp. 64–81.

[14] *DIN 4150-2: Structural Vibration - Part 2: Human Exposure to Vibration in Buildings*. German Institute for Standardization (DIN), 1999. URL: https://www.dincodes.com/product/din-4150-2/.

[15] *DIN 4150-3: Structural Vibration - Part 3: Effects of Vibration on Structures*. German Institute for Standardization (DIN), 1999. URL: https://www.dincodes.com/product/din-4150-3-2/.

[16] K. Dong et al. “Non-linear soil behavior on freight vs passenger lines”. In: *Computers in Railways XVI*. Vol. 181. Leeds, July 2018, pp. 507–516.

[17] K. Dong et al. “Non-linear soil behaviour on high speed rail lines”. In: *Computers and Geotechnics* 112 (2019), pp. 302–318.

[18] Federal Transit Administration (FTA). *Transit Noise and Vibration Impact Assessment Manual*. FTA-VA-90-1003-06. U.S. Department of Transportation. 2006. URL: https://www.transit.dot.gov/sites/fta.dot.gov/files/docs/FTA_Noise_and_Vibration_Manual.pdf.

[19] S. J. Feng et al. “Effects of water table on ground-borne vibration screening effectiveness by using open trenches”. In: *Soil Dynamics and Earthquake Engineering* 131 (2020), p. 106031.

[20] J. Fernández Ruiz et al. “Study of ground vibrations induced by railway traffic in a 3D FEM model formulated in the time domain: experimental validation”. In: *Structure and Infrastructure Engineering* 13.5 (2017), pp. 652–664.

[21] J. Fernández-Ruiz et al. “Influence of non-linear soil properties on railway critical speed”. In: *Construction and Building Materials* 335 (2022), p. 127485.

[22] Government of the Netherlands. *Dutch Policy Rules of Track Vibration (Bts)*. 2024. URL: https://www.government.nl/binaries/government/documenten/reports/2024/02/09/road-traffic-signs-and-regulations-in-the-netherlands/Road+Traffic+Signs+and+Regulations+in+the+Netherlands.pdf.

[23] T.G. Gutowski and C.L. Dym. “Propagation of ground vibration: a review”. In: *Journal of Sound and Vibration* 49.2 (1976), pp. 179–193.

[24] M.A. Hadi and S. Alzabeebee. “Development of a finite element model to study the settlement of ballasted railway tracks subjected to two adjacent moving trains”. In: *Transportation Infrastructure Geotechnology* 10.5 (2023), pp. 733–748.

[25] L. Hall. “Simulations and analyses of train-induced ground vibrations in finite element models”. In: *Soil Dynamics and Earthquake Engineering* 23.5 (2003), pp. 403–413.

[26] C.E. Hanson, D.A. Towers, and L.D. Meister. *High-speed ground transportation noise and vibration impact assessment*. Tech. rep. HMMH Report 293630-4. U.S. Department of Transportation, Federal Railroad Administration, Office of Railroad Development, Oct. 2005.

[27] C.E. Hanson, D.A. Towers, and L.D. Meister. *Transit noise and vibration impact assessment*. Tech. rep. FTA-VA-90-1003-06. U.S. Department of Transportation, Federal Transit Administration, Office of Planning and Environment, May 2006.

[28] Saeed Hosseinzadeh et al. “Prediction of Light Rail Transit Vibrations and Vibration-Reducing Measures”. In: *International Conference on Transportation Geotechnics*. Singapore: Springer Nature Singapore, 2024, pp. 281–289.

[29] G. Kouroussis, D.P. Connolly, and O. Verlinden. “Railway-induced ground vibrations–a review of vehicle effects”. In: *International Journal of Rail Transportation* 2.2 (2014), pp. 69–110.

[30] E.A. Kunicka. “Concrete slab beneath ballast bed - An Abatement Measure For Railway Induced Vibration”. Master’s thesis. Delft University of Technology, Faculty of Civil Engineering & Geosciences, 2019.

[31] M.K.A. Mohd Lazi, M.A. Adnan, and N. Sulaiman. “Empirical Model of Ground-Borne Vibration Induced by Freight Railway Traffic”. In: *Pertanika Journal of Science & Technology* 29.3 (2021).

[32] P. W. Mayne. “In-situ Test Calibrations for Evaluating Soil Parameters”. In: 3 (2007), pp. 1601–1652.

[33] M. Miranda Cremaschi et al. “Experimental evaluation of the effect of soil water fluctuations in the dynamic behavior of machines”. In: *SN Applied Sciences* 3.5 (2021), p. 530.

[34] *NS 8176: Vibration and Shock - Measurement of Vibration in Buildings from Land-based Transport and Guidance to Evaluation of its Effects on Human Beings*. Norwegian Standards (NS), 2017. URL: https://online.standard.no/en/ns-8176-2017.

[35] M. Oregui. *Vertical railway track dynamics: From measurements to numerical modelling: Characteristic frequencies and rail-railpad-sleeper interaction*. 2015.

[36] Nicola Pontani et al. “A numerical assessment of variable saturation of the upper layers on the ground borne vibrations from underground trains: A case history”. In: *Transportation Geotechnics* 40 (2023), p. 100981. DOI: 10.1016/j.trgeo.2023.100981.

[37] K M Ramil. “Analysis of Vibration by Rail Traffic Using PLAXIS 3D”. In: *International Research Journal of Engineering and Technology (IRJET)* 8.2 (2021), pp. 321–324. URL: https://irjcfm.irjet.net/archives/V8/i2/IRJET-V8I2321.pdf.

[38] Peter K. Robertson and K. L. Cabal. *Guide to Cone Penetration Testing for Geotechnical Engineering*. Signal Hill, CA: Gregg Drilling & Testing, 2015.

[39] Jesús Fernández Ruiz and Luis Medina Rodríguez. “Application of an advanced soil constitutive model to the study of railway vibrations in tunnels through 2D numerical models: a real case in Madrid (Spain)”. In: *Revista de la Construcción. Journal of Construction* 14.3 (2015), pp. 53–61.

[40] Javad Sadeghi et al. “Effect of water table level on metro-induced vibrations received by adjacent historical buildings”. In: *Soil Dynamics and Earthquake Engineering* 163 (2022), p. 107553.

[41] F. Samb et al. “Railway traffic vibration impact analysis on surrounding buildings by FEM—case study: TER (regional express train) Dakar—AIBD”. In: *Geomaterials* 9.1 (2019), p. 17.

[42] M. Schevenels, G. Degrandec, and G. Lombaert. “The influence of the depth of the ground water table on free field road traffic-induced vibrations”. In: *International Journal for Numerical and Analytical Methods in Geomechanics* 28.5 (2004), pp. 395–419. DOI: 10.1002/nag.349.

[43] M. Shahraki et al. “3D modelling of train induced moving loads on an embankment”. In: *Plaxis Bulletin* 36 (2014), pp. 10–15.

[44] X. Sheng. “A review on modelling ground vibrations generated by underground trains”. In: *International Journal of Rail Transportation* 7.4 (2019), pp. 241–261.

[45] X. Sheng, C.J.C. Jones, and D.J. Thompson. “Modelling ground vibration from railways using wavenumber finite-and boundary-element methods”. In: *Proceedings of the Royal Society A: Mathematical, Physical and Engineering Sciences* 461.2059 (2005), pp. 2043–2070.

[46] Jou-Yi SHIH, David J. THOMPSON, and Antonis ZERVOS. “The influence of soil nonlinear properties on the track/ground vibration induced by trains running on soft ground”. In: *Transportation Geotechnics* 11 (2017), pp. 1–16.

[47] D. V. Singh and Y. Seth. “3D modelling of ground surface vibration induced by underground train movement”. In: *Procedia Engineering* 173 (2017), pp. 1580–1586.

[48] M.G. Smith et al. “On the Influence of Freight Trains on Humans: A Laboratory Investigation of the Impact of Nocturnal Low Frequency Vibration and Noise on Sleep and Heart Rate”. In: *PloS One* 8.2 (2013), e55829. DOI: 10.1371/journal.pone.0055829.

[49] *SS 4604861: Vibration and Shock - Guidelines for Measurement and Evaluation of Vibration in Buildings*. Swedish Standards Institute (SIS), 1999. URL: https://www.sis.se/en/produkter/environment-health-protection-safety/vibration-and-shock-with-respect-to-human-beings/ss4604861/.

[50] Martijn Stoof. “Dutch double-decker train at Amsterdam station”. In: (). URL: https://www.pexels.com/photo/dutch-double-decker-train-at-amsterdam-station-32128685/.

[51] J. Sun, X. Ge, and P. Li. “Vibration mechanism and energy transfer analysis of dynamic compaction method on ground with high groundwater level”. In: *International Journal of Geomechanics* 23.11 (2023), p. 04023200.

[52] Bentley Systems. *PLAXIS 3D 2024.2 Material Models Manual 3D*. Bentley, 2024.

[53] Bentley Systems. *PLAXIS 3D 2024.2 Reference Manual 3D*. Bentley, 2024.

[54] D.J. Thompson, G. Kouroussis, and E. Ntotsios. “Modelling, simulation and evaluation of ground vibration caused by rail vehicles”. In: *Vehicle System Dynamics* 57.7 (2019), pp. 936–983.

[55] D.J. Thompson, G. Kouroussis, and E. Ntotsios. “Modelling, simulation and evaluation of ground vibration caused by rail vehicles”. In: *Vehicle System Dynamics* 57.7 (2019), pp. 936–983.

[56] K.Y. Tiong, F.N.L. Ling, and Z.A. Talib. “Effect of train vibration on settlement of soil: A numerical analysis”. In: *AIP Conference Proceedings*. Vol. 1892. 1. AIP Publishing, 2017.

[57] UIC - Sustainable Development Department. *Railway Induced Vibration - State of the Art Report*. 1st ed. Available in English, downloadable format. Publication date: November 14, 2017. Paris, France: International Union of Railways (UIC), 2017, p. 82. ISBN: 978-2-7461-2663-3. URL: https://shop.uic.org/en/other-reports/9172-railway-induced-vibration-state-of-the-art-report.html.

[58] A. van Uitert et al. “Studying Railway Vibration Projects with a Focus on Environmental Aspects”. In: *Advances in Transportation Geotechnics IV: Proceedings of the 4th International Conference on Transportation Geotechnics Volume 2*. Springer International Publishing, 2022, pp. 155–168.

[59] Agnes van Uitert et al. “A practical perspective on railway-induced ground-borne noise and vibrations”. In: *Global Railway Review* (Feb. 2020). URL: https://www.globalrailwayreview.com/article/93781/practical-perspective-ground-borne-noise-vibrations/.

[60] B.J. Van Dyk et al. “Evaluation of dynamic and impact wheel load factors and their application in design processes”. In: *Proceedings of the Institution of Mechanical Engineers, Part F: Journal of Rail and Rapid Transit* 231.1 (2017), pp. 33–43.

[61] H. Verbraken, G. Lombaert, and G. Degrande. “Experimental and numerical determination of transfer functions along railway tracks”. In: *Proceedings of the 9th National Congress on Theoretical and Applied Mechanics, Brussels*. National Congress on Theoretical and Applied Mechanics. May 2012, pp. 9–10.

[62] H. Verbraken et al. “Numerical and empirical prediction methods for railway induced vibrations in buildings”. In: *Proceedings of the 8th International Conference on Structural Dynamics, EURODYN 2011*. European Association for Structural Dynamics. 2011, pp. 727–734.

[63] Stefan Verdenius, Sjoerd Hengeveld, and Johan Maljaars. “New fatigue load models for assessing railway bridges in Europe”. In: *Engineering Structures* 284 (2023), p. 115914.

[64] Bernard R. Wair, Jason T. DeJong, and Thomas Shantz. *Guidelines for Estimation of Shear Wave Velocity Profiles*. Pacific Earthquake Engineering Research Center, 2012.

[65] Yexin Wan et al. “Analytical analysis on the influence of groundwater level variation on seismic ground motion under plane wave incidence”. In: *Computers and Geotechnics* 183 (2025), p. 107212.

[66] F. Yarmohammadi, K. Ziotopoulou, and K. Lontzetidis. “Effect of Train-Induced Ground Vibrations on Liquefiable Soils”. In: *International Conference on Transportation Geotechnics*. Singapore: Springer Nature Singapore, Oct. 2024, pp. 83–90.

A

Appendix

A.1. Cross section of rail

The dimensions of the rail were taken from commercial industries. The rail represented here is taken from ArcelorMittal [4].

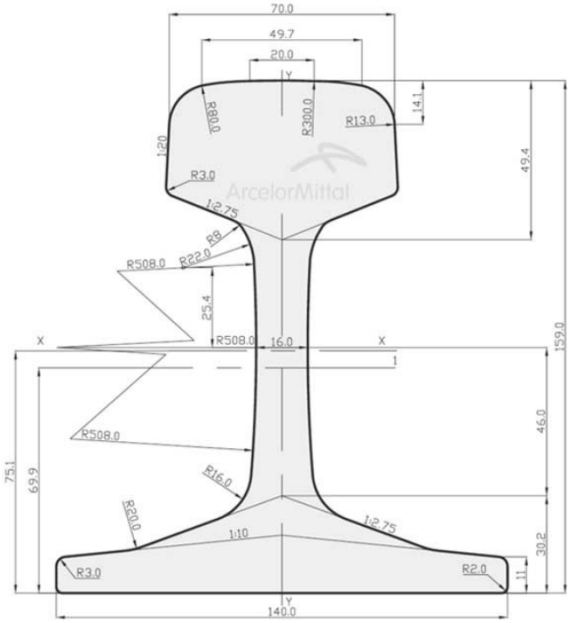

Figure A.1: Rail UIC54 and its properties (ArcelorMittal)

B

Appendix

B.1. Reference Model

The reference model was analysed with the same parameters and time steps as done in the reference thesis and the results are as follows. Figure B.1 shows the the acceleration time graph obtained from the simulation and a Fast Fourier Transform (FFT) was performed on it to obtain the results in the frequency domain, which is presented in Figure B.2.

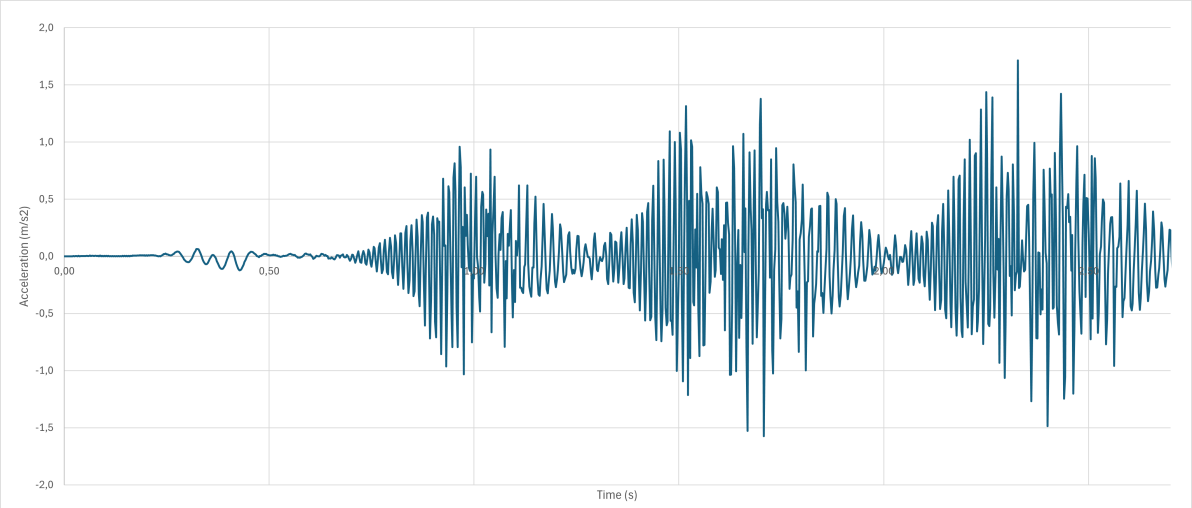

Figure B.1: Acceleration time graph from the Reference model

From the graph it is also seen that the acceleration values range between -2m/s^2 and 2m/s^2 at most. This is in alignment with the expected values of acceleration vales at this distance and in comparison with the data obtained from the site. The figure B.2 shows the FFT of the reference model. The dominant frequencies are seen in between 45Hz and 60Hz and 75Hz and 80Hz.

B.2. Calculation of Reflection Coefficient

The equation for reflection coefficient (R) is as in equation B.1 where Z is calculated as per B.2

$$R = \frac{Z_2 - Z_1}{Z_2 + Z_1} \tag{B.1}$$

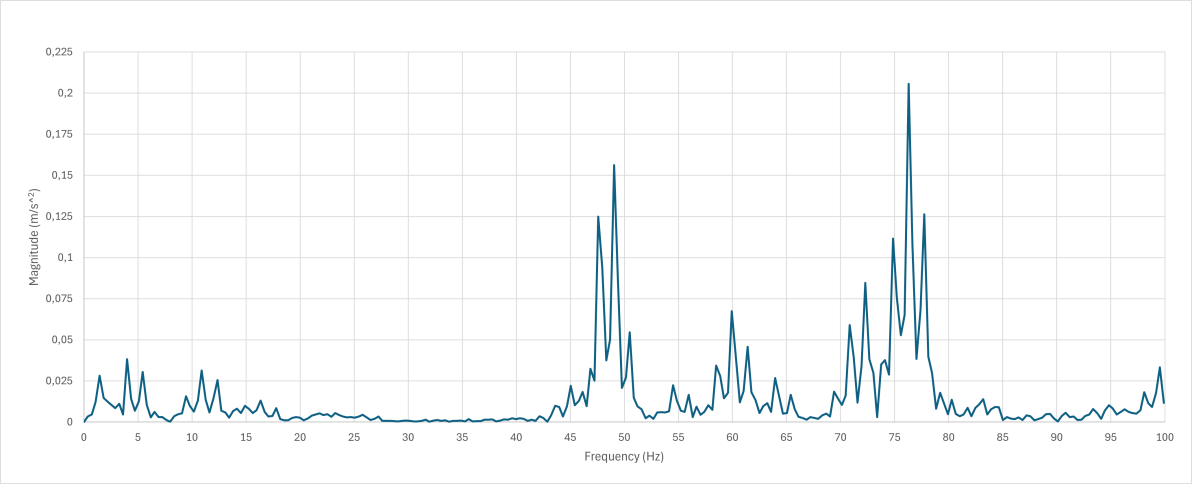

Figure B.2: FFT of the reference model

$$Z = \rho \times V \tag{B.2}$$

The density and the shear wave velocity of the layers at the bottom are as in table B.1. The shear wave velocity is calculated as per [9].

Layer	Density (kg/m^3)	Shear Wave Velocity (m/s)	Impedance Z (kg/m^{2}s)
3	1,732.93	195	337,921
4	1,834.86	201	368,807

Table B.1: Density and Shear Wave velocity of Layer 3 and 4

Substituting the impedance values in equation B.1 gives the reflection coefficient, R to be;

$$R = \frac{368.8 - 337.9}{368.8 + 337.9} = 0.44 \tag{B.3}$$

B.3. Correlations used in finding parameters for HSsmall model

Compared to the linear elastic material model which uses the Young's modulus and the poissons ratio, the HS Small model contains four different stiffness parameters, each of them quantifying the reference stiffness in a particular stress path for a given reference stress level, p^{ref}. For a detailed description of the HSsmall model and the meaning of its parameters, reference is made to Benz (2007) and Brinkgreve et al. (2008).

$$E_{50}^{\text{ref}} = \frac{60000\,RD}{100} \quad [\text{kN/m}^2] \tag{B.4}$$

$$E_{\text{oed}}^{\text{ref}} = \frac{60000\,RD}{100} \quad [\text{kN/m}^2] \tag{B.5}$$

$$E_{\text{ur}}^{\text{ref}} = \frac{180000\,RD}{100} \quad [\text{kN/m}^2] \tag{B.6}$$

$$G_0^{\text{ref}} = 60000 + \frac{68000\,RD}{100} \quad [\text{kN/m}^2] \tag{B.7}$$

where, E_{50}^{ref} is the Secant stiffness in standard drained triaxial test, $E_{\text{oed}}^{\text{ref}}$ Tangent stiffness for primary oedometer loading $E_{\text{ur}}^{\text{ref}}$ is the modulus of unloading/reloading, G_0^{ref} Reference shear modulus at very small strains and RD is the relative density of the material.

C

Appendix

C.1. Measurement Point 1

The graph below shows the raw data obtained from the site with the magnitudes of acceleration in time. It is observed that the magnitude of acceleration is usually high reaching upto $20m/s^2$. This unusual peaks can be attributed to the uncertainties at the location.

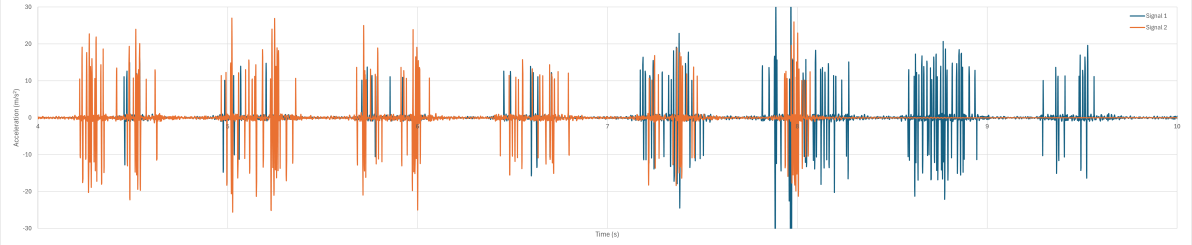

Figure C.1: Acceleration at MP1 in time domain

C.2. Comparing the Linear model (M1-A) and Site

The linear model was initially modelled as per the validated reference model, which had the self weight of the train and a percentage of additional dynamic load added with the sleeper passing frequency of 60 Hz which corresponds to the sleeper spacing of 0.6 m and the train speed of 130 kmph. The additional dynamic load was seemed to be necessary when the model used a linear material model to model the soil and embankment. To verify this, a simulation (M1-A) was performed with only the self-weight of the train and no additional dynamic load added. The results of the simulation and its comparison with the site data and the model M1's data is presented and compared.

The following graphs will present the obtained acceleration data in time domain. Figure C.2 to figure C.4 presents the variation of magnitudes of acceleration among the measurement points. As expected the magnitude of acceleration reduces as distance from the rail increases, but the magnitude of acceleration observed is quite lower than what is seen at site. Figure **??** to figure **??** presents the data in frequency domain after a Fourier Fast Transform was performed on the data in time domain.

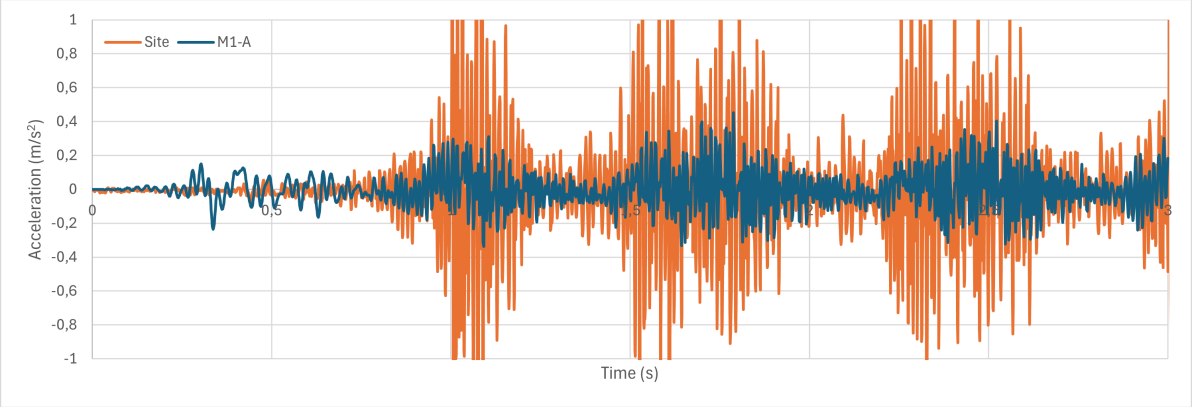

Figure C.2: Comparison of acceleration in time domain at MP1 for site and M1-A

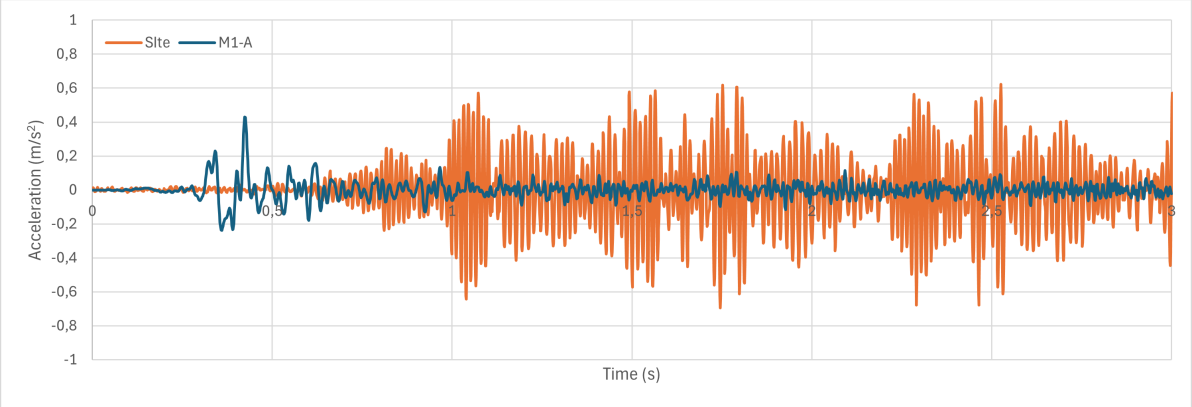

Figure C.3: Comparison of acceleration in time domain at MP2 for site and M1-A

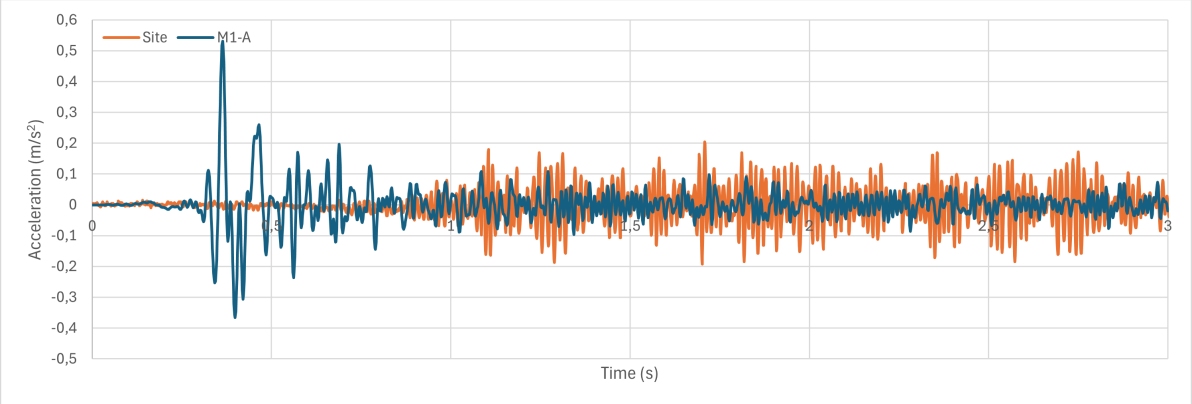

Figure C.4: Comparison of acceleration in time domain at MP3 for site and M1-A

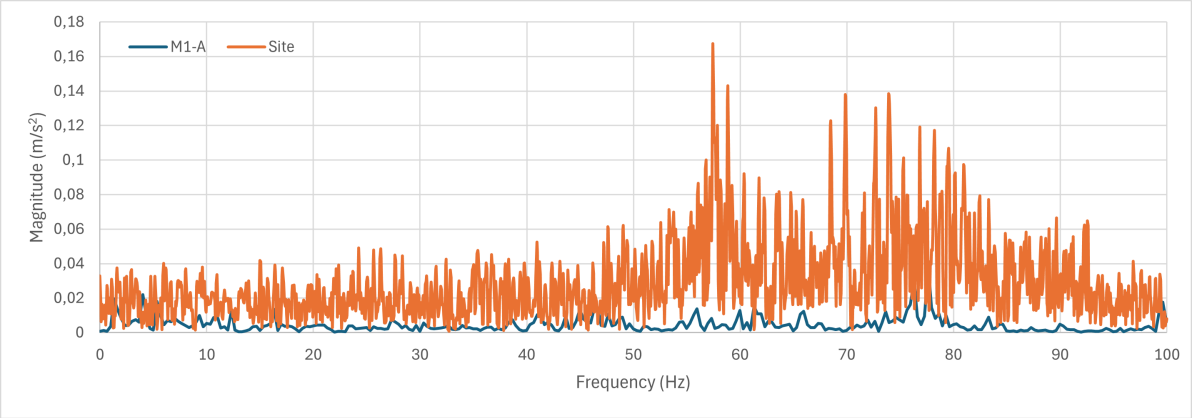

Figure C.5: Comparison of acceleration in frequency domain at MP1 for site and M1-A

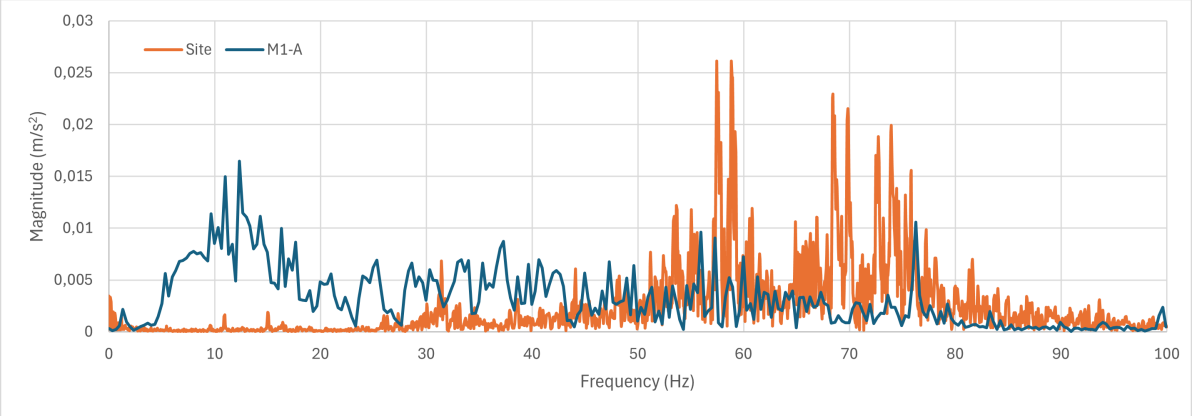

Figure C.6: Comparison of acceleration in frequency domain at MP2 for site and M1-A

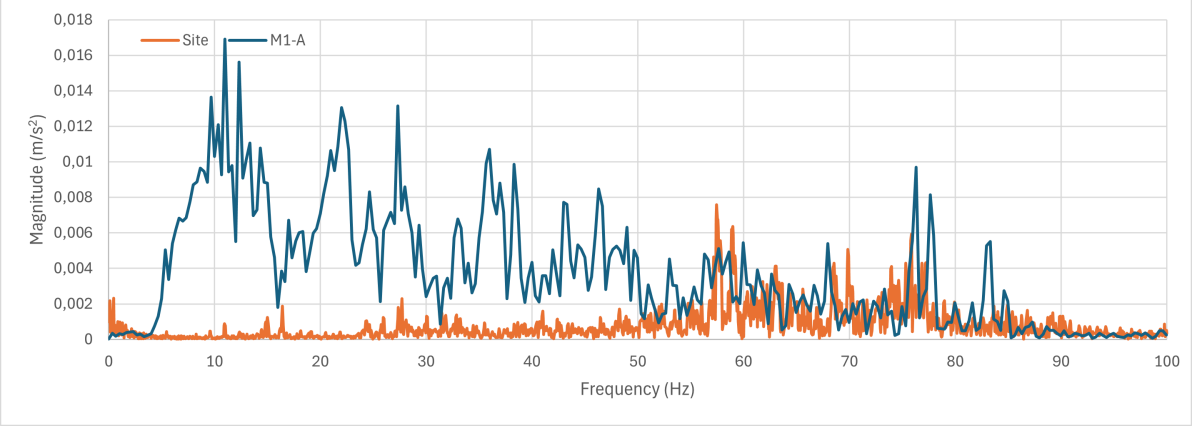

Figure C.7: Comparison of acceleration in frequency domain at MP2 for site and M1-A

C.3. Comparing the Linear model M1-A and M1

As mentioned in the previous section, the model M1-A was modelled with only the self-weight of the train and no additional dynamic load added. The model M1 as mentioned in 5.2.1 is modelled and the simulation is run with the self weight of the train and an additional percentage of dynamic load on the rail.

The results from the M1-A model simulation will be presented below. Figure C.8 to figure C.10 presents the acceleration data in time domain and figure C.11 to figure C.13 presents the acceleration data in frequency domain.

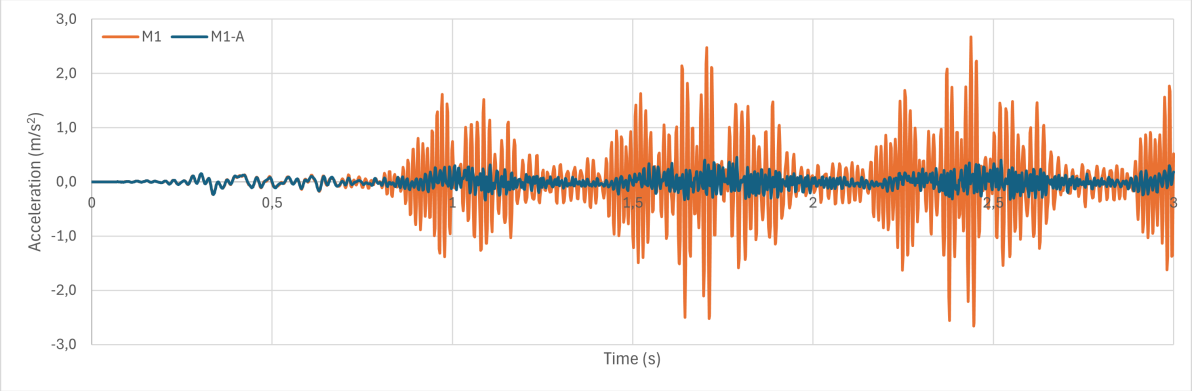

Figure C.8: Comparison of acceleration in time domain at MP1 for M1 and M1-A

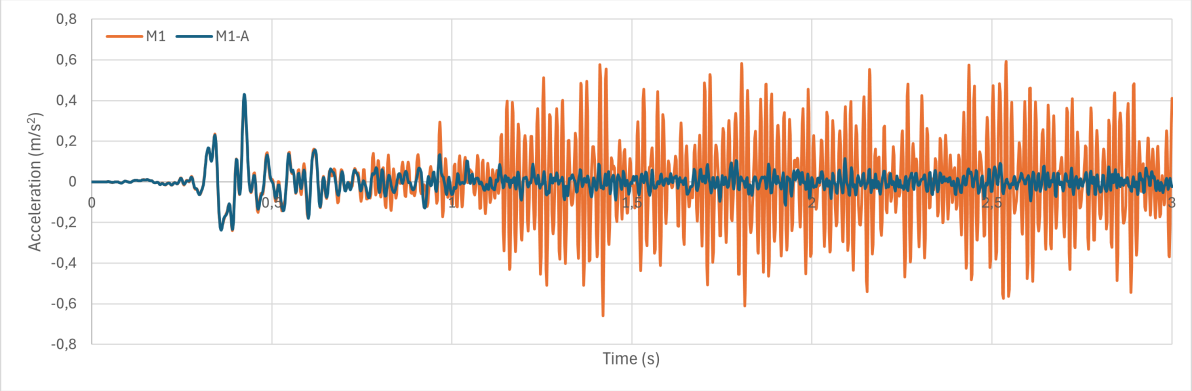

Figure C.9: Comparison of acceleration in time domain at MP2 for M1 and M1-A

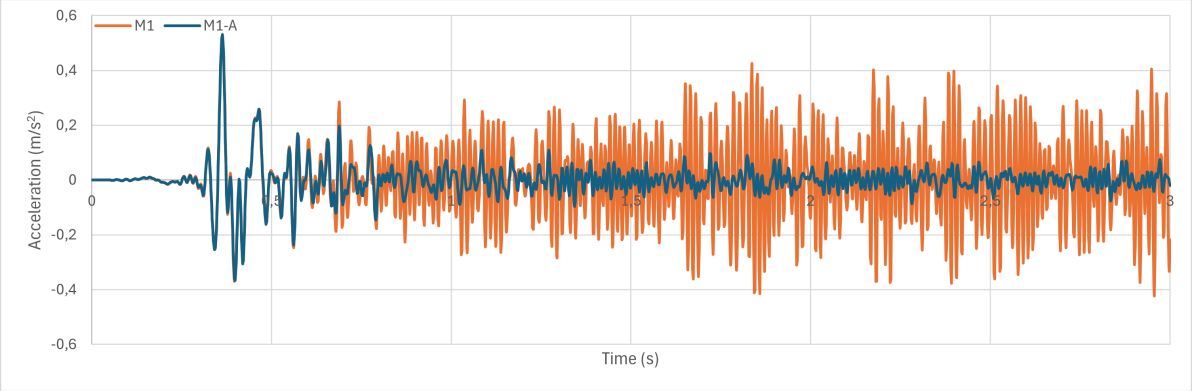

Figure C.10: Comparison of acceleration in time domain at MP3 for M1 and M1-A

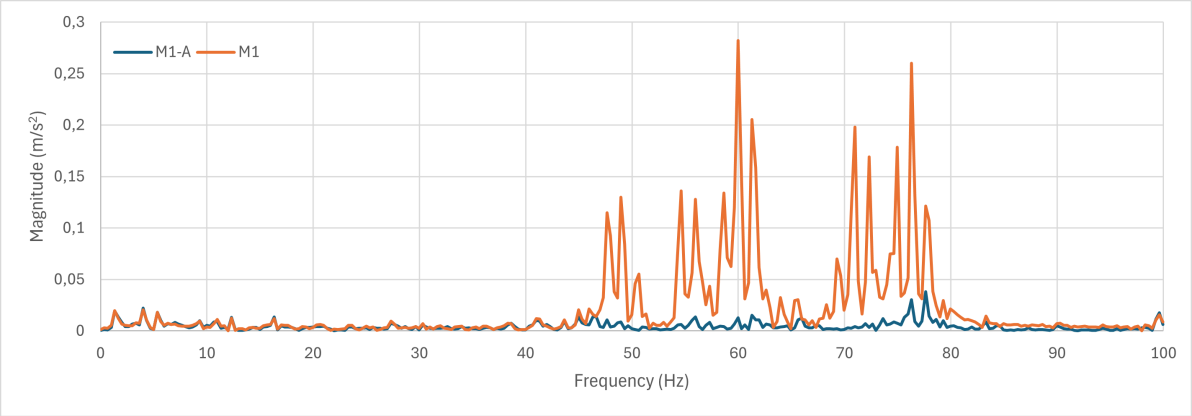

Figure C.11: Comparison of acceleration in frequency domain at MP1 for M1 and M1-A

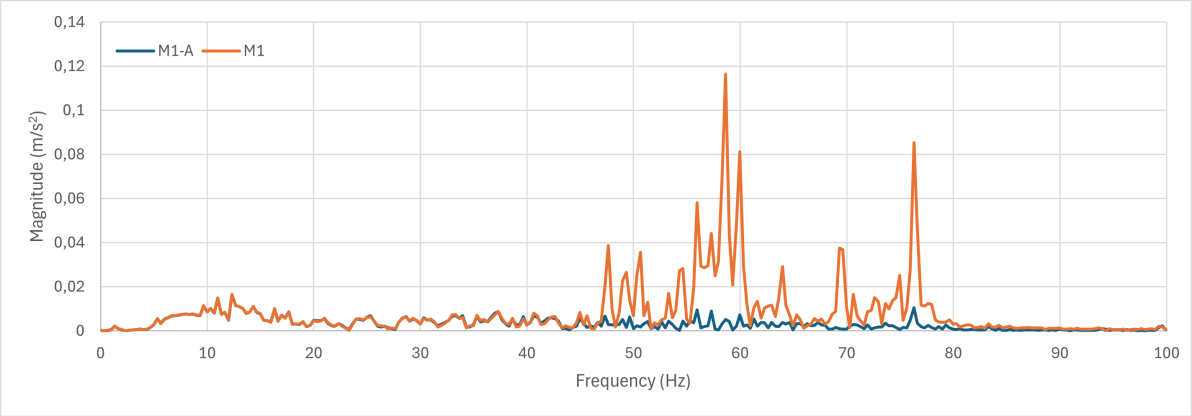

Figure C.12: Comparison of acceleration in frequency domain at MP2 for M1 and M1-A

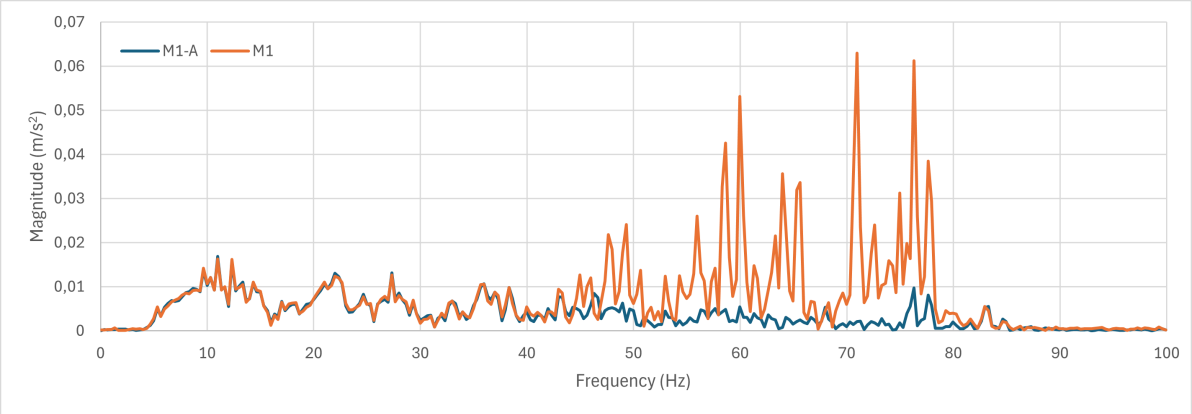

Figure C.13: Comparison of acceleration in frequency domain at MP3 for M1 and M1-A

C.4. Comparing the Non-Linear model loading

Initially, all the models were loaded such that the self weight of the train and an additional dynamic load was added and the simulation was run. The question whether PLAXIS takes into account, the dynamic characteristics was in doubt. So in order to investigate that, a simulation with just the self weight of the train was run and the following results were obtained. The model M3-A with only the self weight was analysed and compared with the non-linear model M3 with the delft weight and the dynamic load in the loading. Figures C.14 to C.16 are

the acceleration data in time domain for the simulation M3-A in comparison with non-linear model M3. And figure C.17 to figure C.19 are the acceleration data in frequency domain for the simulation M3-A in comparison with non-linear model M3.

From these graphs, it was observed that the omission of the extra dynamic load did not bring in any significant change to the results in the time and frequency domain. There were only slight differences seen when the results were compared.

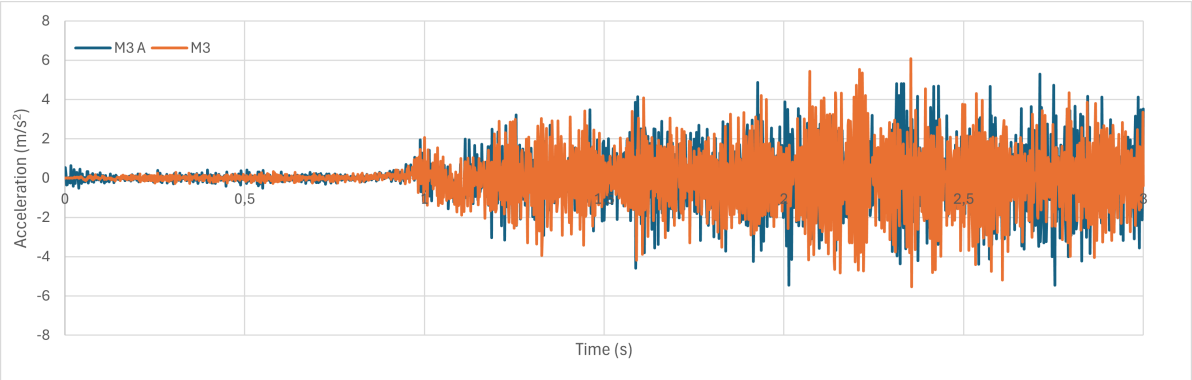

Figure C.14: Comparison of acceleration in time domain at MP1 for M3 and M3-A

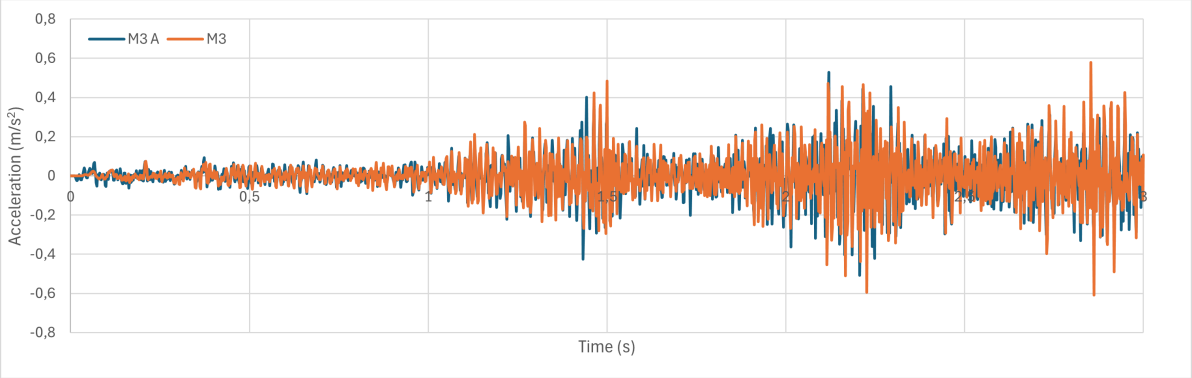

Figure C.15: Comparison of acceleration in time domain at MP2 for M3 and M3-A

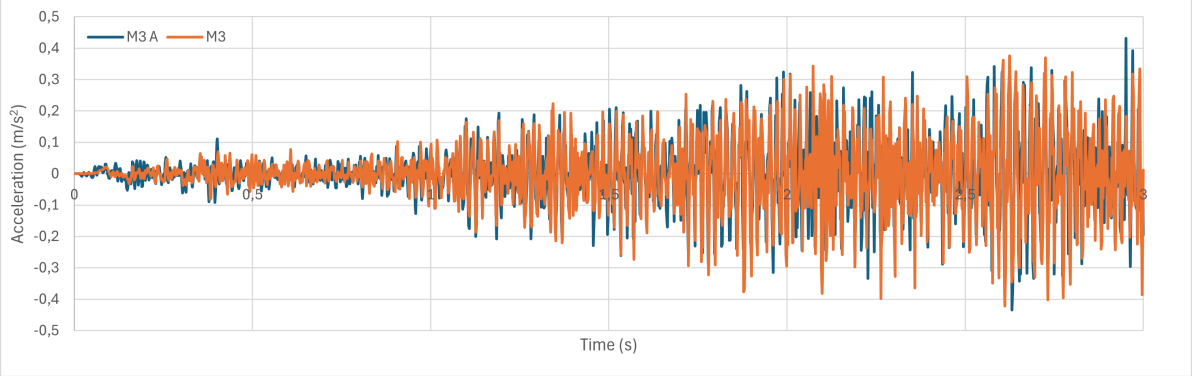

Figure C.16: Comparison of acceleration in time domain at MP3 for M3 and M3-A

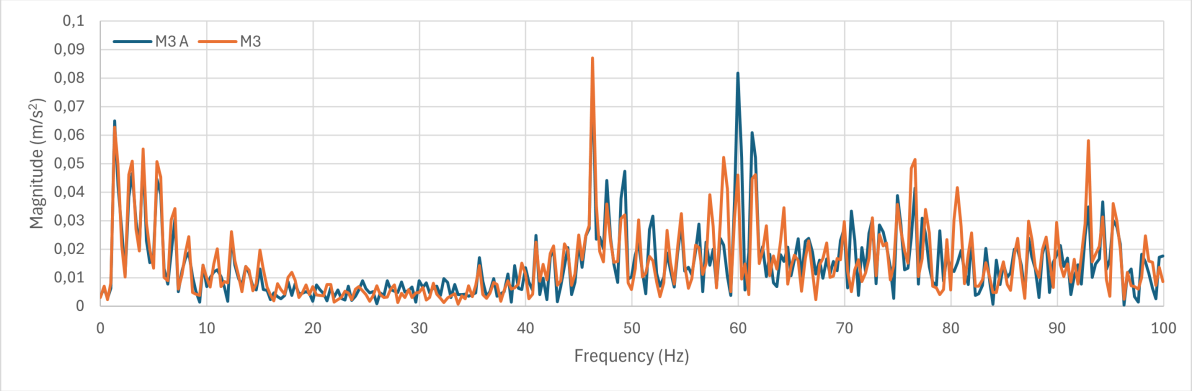

Figure C.17: Comparison of acceleration in frequency domain at MP1 for M3 and M3-A

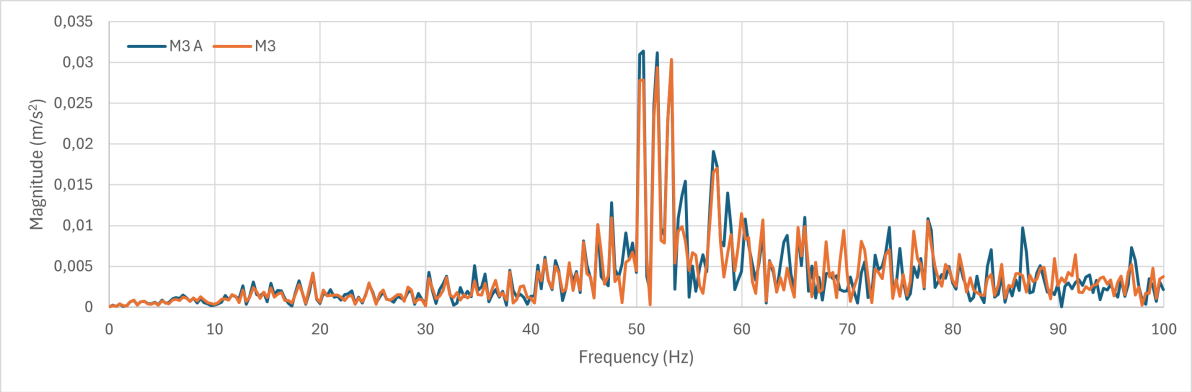

Figure C.18: Comparison of acceleration in frequency domain at MP2 for M3 and M3-A

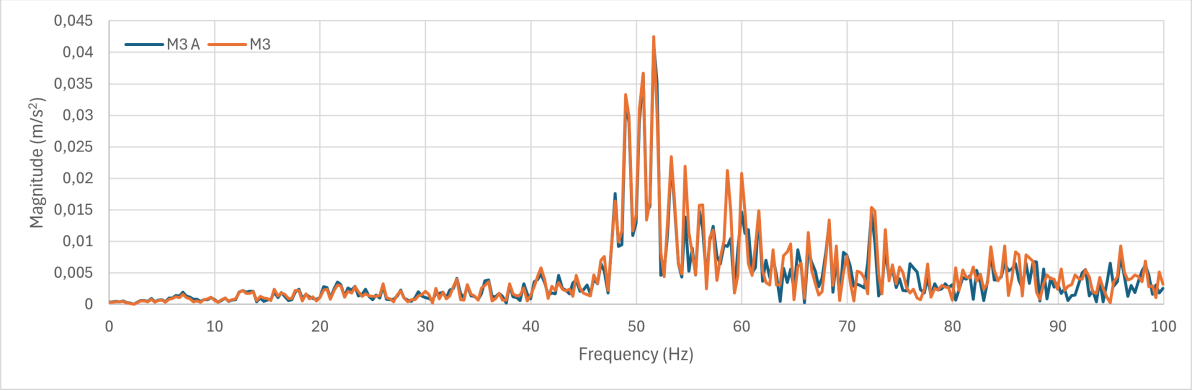

Figure C.19: Comparison of acceleration in frequency domain at MP3 for M3 and M3-A